Structural Approach to the HuR Function

Aproximación Estructural a la Función de HuR

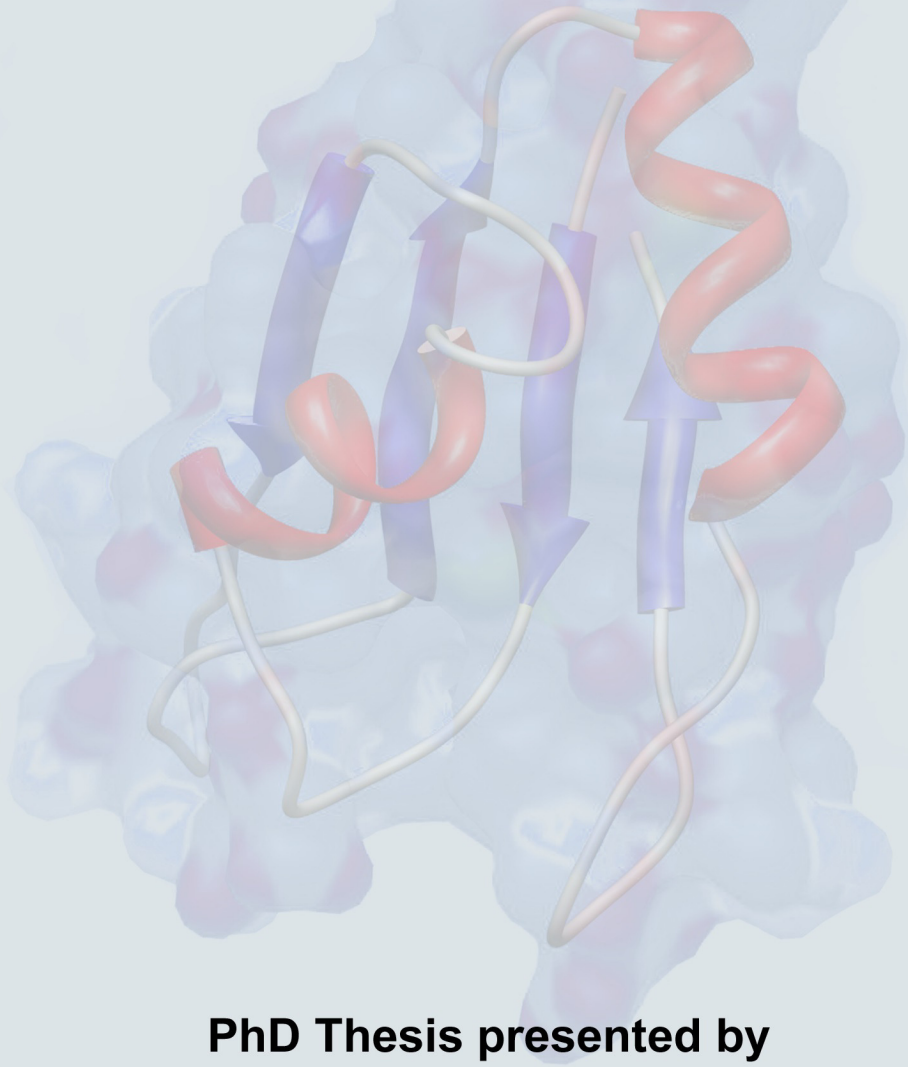

PhD Thesis presented by
Rafael Manfred Scheiba
Seville, 2013

Consejo Superior de Investigaciones Científicas
Universidad de Sevilla

Instituto de Bioquimica Vegetal y Fotosintesis
cicCartuja

Structural Approach to the HuR Function

Aproximación Estructural a la Función de HuR

Memoria presentada por el licenciado D. Rafael Manfred Scheiba para optar al grado de Doctor en Ciencias Biológicas

Sevilla, 2013

Directora

Irene Díaz-Moreno, PhD

Profesora Titular de Universidad

cicCartuja centro de investigaciones científicas isla de la cartuja

Consejo Superior de Investigaciones Científicas
Junta de Andalucía
Universidad de Sevilla

Acknowledgments

I thank Dr. Irene Díaz-Moreno, Dr. Antonio Díaz-Quintana and Prof. Miguel Ángel de la Rosa for accepting me in their team, for their motivation and informative discussions, as well as for offering me the possibility to carry out this work at the cicCartuja, Seville.

I am grateful to Dr. Francisco J. Blanco, Dr. María Luz Martínez-Chantar, Dr. Luis Alfonso Martínez-Cruz and Dr. Adriana Rojas Cardona for their pleasant coordinated guidance and helpful discussions at the CIC bioGUNE, Bilbao.

I am indebted to Dr. Manuel Angulo (CITIUS, Sevilla) and Dr. Tammo Diercks (CIC bioGUNE, Bilbao) for their professional help and advice on NMR experiments.

My acknowledgments also go to Dr. M. Gorospe (NIH, Baltimore, USA) and Dr. J. A. Steitz (Yale University, New Haven, USA) for providing us the HuR vectors.

I thank the laboratory teams of the Structural Biology and Metabolomics Units at CIC bioGUNE for their help, especially Dr. Alain Ibáñez de Opakua for NMR data processing, Iker Oyenarte for crystallization experiments, Dr. Nieves Embade and Dr. David Fernández for cell culture.

My gratitude goes to the working group members of laboratories 1 and 5 of the “Instituto de Bioquímica Vegetal y Fotosíntesis (IBVF)” at cicCartuja. Everyone contributed its part to the work - those who stayed and those who left. It was a great pleasure for me to have all them accompanying me along the way, so helping me to see the things from many different points of view.

This work has been supported by:

the Andalusian Government (P07-CVI-2896),

the Spanish Research Council (JAEpre08-00375)

and the European Social Fonds (ESF 2007-2013).

The six months stay at the CIC bioGUNE was supported by a fellowship from the Spanish Scientific Council (2011ESTCSIC–6934).

Dedicated to my parents.

“No book can ever be finished. While working on it we learn just enough to find it immature the moment we turn away from it.”

Karl R. Popper, 1950

(The Open Society and Its Enemies,
Preface to the Second Edition)

Index

Tables and Figures Index

Figures

Tables

Abbreviations

Abbreviations

40S and 60S	small and large subunits of the ribosome
ADAR2	Adenosine Deaminase Acting on RNA-2
APRIL	Acidic Protein Rich In Leucine
AREs	Adenylate and Uridylate enRiched Elements
Ars2	Arsenate resistance protein 2
ATP	Adenosine Tri Phosphate
AU	Analytical Ultracentrifugation
AUF1	AU-rich binding Factor 1
AU-rich	Adenylate and Uridylate enriched
CCR4	Cysteine-cysteinyl Chemokine Receptor 4
Cdk5	Cyclin-dependent kinase 5
c-fos	cellular fos
CGRP	Calcitonin/calcitonin Gene-Related Peptide
Chk2	Checkpoint kinase 2
c-myc	cellular myc
COX	CycloOXigenase
CR	Coding Region
CRM1	Chromosomal Region Maintenance Protein 1
CSD	Cold Shock Domain
CspA	Cold shock protein A

CUG-BP2	CUG-Binding Protein 2
DAN	Deoxyribonucleoside-Activated Nucleotidase
Dcp1-3	Decapping enzyme 1-3
DcpS	Scavenger mRNA Decapping enzyme
DEAD/DEAH	RNA helicase DEAD/ DEAH box
DNA	DesoxyriboNucleic Acid
Dnd1	Dead end protein 1
DRBD	Double-stranded RNA Binding Domain
dsRBD	double-stranded RNA Binding Domain
Drosha	ribonuclease type III, drosha
ds	double-stranded
Edc1	Enhancer of decapping enzyme 1
ELAV	Embryonic Lethal Abnormal Vision
FBP	FUSE Binding Protein
FIR	FBP-Interacting Repressor
FL	Full Length
FMR1	Fragile X Mental Retardation transcript 1
FXR	Fragile X Related protein,
GAP-43	Growth-Associated Protein-43
HIV1	Human Immunodeficiency Virus type I
hnRNA	heterogeneous nuclear RNA
hnRNP	heterogeneous nuclear RiboNucleoProtein

HNS	HuR Nucleocytoplasmic Shuttling sequence
Hrp1	Heterogeneous nuclear ribonucleoprotein 1
Hu protein	Human antigen protein
K_A	Association constant
K_D	Dissociation constant
KH	K-Homology domain
KSRP	KH-type Splicing Regulatory Protein
LB	*Luria Bertani*
LSm	Sm-Like proteins
m^7GDP	7 methylGuanosine DiPhosphate
m^7GTP	7 methylGuanosine TriPhosphate
MALDI	Matrix Assisted Laser Desorption/Ionization
Me^{2+}	divalent Metal cation
Mg^{2+}	Magnesium Ion
miRNA	microRNA
mRNA	messenger RNA
NFκB	Nuclear Factor kappa B
NF1	NeuroFibromatosis type 1
PABP	PolyAdenylate-Binding Protein
PAGE	Poly Acrylamide Gel Electrophoresis
PAIP2	Poly(A)-binding protein-Interacting Protein 2
PAN	Pab1p-dependent poly(A) Nuclease

PARN	Poly(A)-specific RNase
PAZ	Piwi/Argonaute/Zwille domain
PIWI	P-element Induced WImpy testis
PH	Pleckstrin
PKC	Protein Kinase C
PNPase	PolyNucleotide Phosphorylase
poly(A)	multiple Adenosine monophosphates
pp32	phosphoprotein 32
pre-mRNA	RNA precursors
qRRM	quasi-RNA Recognition Motif
RBD	RNA Binding Domain
RBP	RNA Binding Protein
REV	REgulator of Virion expression
RGG	Arg-Gly-Gly box
RISC	RNA Induced Silencing Complex
RNA	RiboNucleic Acid
RNAse	RiboNucleAse
RNP	RiboNucleoProtein complex
RppH	RNA pyrophosphoHydrolase
RRM	RNA Recognition Motif
SDS	Sodium Dodecyl Sulfate
SF1-5	Super Family 1-5

siRNA	small interfering RNA
SIRT1	stress protein SIr2-Related protein Type 1
snRNP	small nuclear RiboNucleoprotein Particles
SR proteins	Serine/aRginine-rich proteins
ss	single-stranded
TAR	TrAnsactivation response RNA sequences
TAT	Trans-AcTivator
TEV	Tobacco Etch Virus
TIA-1	T-cell-restricted Intracellular Antigen 1
TIAR	TIA-1 Related protein
TFIIIA	5S gene-specific Transcription initiation Factor
T_m	Melting point
TNF	Tumor Necrosis Factor
TRN	TRaNsportin
TTP	Tris-TetraProline
U2B''	U2 snRNP-specific B'' protein
UNR	Upstream of N-Ras
U-rich	Uracile enriched
UTR	UnTranslated Regions
UV	UltraViolett
WT	*Wild-Type*

xRRM	atypical RRM in and unique to genuine La and LARP7 proteins
ZnF	Zinc Finger

Resumen

Resumen

En esta tesis se presenta un análisis estructural de la proteína de unión a ARN HuR y, en particular, se profundiza en el análisis con su estructura modular y a su regulación post-traducional mediante fosforilación.

Los resultados obtenidos revelan que los dominios N-terminales RRM1 y RRM2 de HuR funcionan como una unidad, según se deduce de los datos de la estabilidad térmica con las construcciones de uno y dos dominios.

Los mutantes S88D, S100D y S158D que mimetizan fosforilación, diseñados sobre la construcción RRM12, muestran cambios despreciables en la estructura secundaria respecto a la proteína silvestre. La T_m del mutante S100D no cambia respecto a la de la proteína silvestre, mientras que el mutante S88D es más estable y la especie S158D se desestabiliza ligeramente debido a la mutación que mimetiza la fosforilación. En cuanto a las propiedades de unión a ARN, las especies RRM12 S88D y RRM12 S100D mostraron K_Ds parecidas a la proteína silvestre, mientras que el mutante S158D presenta una afinidad 4 veces mayor que el silvestre por la secuencia de ARN 5´-AUUUUUAUUUU-3´ del *c*-fos.

El dominio C-terminal de HuR (RRM3) se comporta en disolución de forma independiente a la unidad RRM12. Se ha desarrollado, por primera vez, una estrategia innovadora basada en detergentes para solubilizar el módulo RRM3. Los modelos calculados para la proteína silvestre y el mutante fosfomimético S318D basados en restricciones de RMN y generados con el servidor CS23D, reflejan la topologia canónica de los dominios RRM ($\beta_1\alpha_1\beta_2\beta_3\alpha_2\beta_4$). En el sitio de unión a ARN de RRM3 se encuentran las dos hebras β centrales β_1 y β_3, aunque también se puede extender a toda la lámina β.

Además, la proteína silvestre RRM3 parece unirse al oligonucleótido 5´-UUUUU-3´ con una afinidad mayor que al 5´-AUUUA-3´. La presencia de un residuo cargado negativamente en la posición 318 dificulta el reconocimiento por el ARN.

La región comprendida entre el Trp261 y la Thr271 de HuR RRM3 alberga residuos responsables de la dimerización, tanto en presencia como en ausencia de ARN. De hecho, la sustitución del Trp por Glu en el mutante W261E RRM3 desplaza el equilibrio monómero/dímero característico de la proteina HuR RRM3 silvestre hacia la forma monomérica.

Los resultados de esta tesis han dado lugar a la publicación de un artículo en una revista de alto impacto y a otro enviado:

1. Scheiba RM, Aroca A, Díaz-Moreno I (2012) HuR thermal stability is dependent on domain binding and upon phosphorylation. *Eur Biophys J* **41**:597-605

2. Scheiba RM, Ibañez Opakua A, Oyenarte I, Díaz-Quintana A, Martínez-Chantar ML, Martínez-Cruz LA, Blanco FJ and Díaz-Moreno I (2012) Shedding light on the most C-terminal RNA binding motif of HuR: its role in RNA recognition (enviado)

Summary

Summary

The thesis reports a structural approach to the RNA binding protein HuR, so providing relevant information on its modular assembly and phosphorylation.

Our experimental data demonstrate that the N-terminal domains HuR RRM1 and RRM2 work as a functional unit, as inferred from the thermal stability analysis of single- and two-domain constructs. The phosphorylation mimic mutants S88D, S100D and S158D designed on RRM12 di-domain show negligible changes in secondary structure with respect to the WT. Thus, the T_m of the S100D construct does not change with respect to WT, while S88D is stabilized and S158D is slightly destabilized upon phosphorylation mimicking. With regard to RNA binding properties, RRM12 S88D and RRM12 S100D species showed similar K_Ds to that of WT, whereas RRM12 S158D has a 4-fold higher binding affinity to the *c*-fos RNA 5′-AUUUUUAUUUU-3′.

The C-terminal HuR RRM3 tumbles independently from the RRM12 unit. A challenging detergent-based strategy to get HuR RRM3 solubilized has been developed for the first time. Structural models for RRM3 WT and its phosphomimetic mutant RRM3 S318D based on NMR restraints with the CS23D server show the canonical RRM topology ($\beta_1\alpha_1\beta_2\beta_3\alpha_2\beta_4$). The RNA binding site of RRM3 comprises the two central β strands (β_1 and β_3), although it can be eventually expanded to the whole β-sheet. Additionally, WT protein seems to bind 5′-UUUUU-3′ with a higher affinity than 5′-AUUUA-3′ based on NMR chemical-shift perturbations. Negatively-charged residue at position 318 impairs the RNA recognition.

The stretch from Trp261 to Thr271 of HuR RRM3 hosts residues responsible for protein dimerization even in absence of RNA. In fact, the Trp-by-Glu substitution shifts the monomer/dimer

equilibrium characteristic of HuR RRM3 WT towards the monomeric form of HuR RRM3 W261E mutant.

The thesis resulted in one publication in a high impact journal and another one submitted:

1. Scheiba RM, Aroca A, Díaz-Moreno I (2012) HuR thermal stability is dependent on domain binding and upon phosphorylation. *Eur Biophys J* **41**:597-605

2. Scheiba RM, Ibañez Opakua A, Oyenarte I, Díaz-Quintana A, Martínez-Chantar ML, Martínez-Cruz LA, Blanco FJ and Díaz-Moreno I (2012) Shedding light on the most C-terminal RNA binding motif of HuR: its role in RNA recognition (submitted)

Introduction

1.1 Messenger RNA Processing in the Eukaryotic Cell

The information flow for the expression of genes in an organism is directed from a DNA sequence to RNA and protein, according to the central "dogma" of molecular biology (Crick, 1958 and 1970). Translation from the messenger RNA (mRNA) to protein takes place in the cytoplasm at the ribosomes, whereas transcription of DNA to RNA by polymerase II is localized in the cell nucleus. There, the pre-mRNAs are co-transcriptionally modified by 5´ end capping, splicing, 3´ end cleavage and polyadenylation (for a review see Hirose *et al.*, 2000).

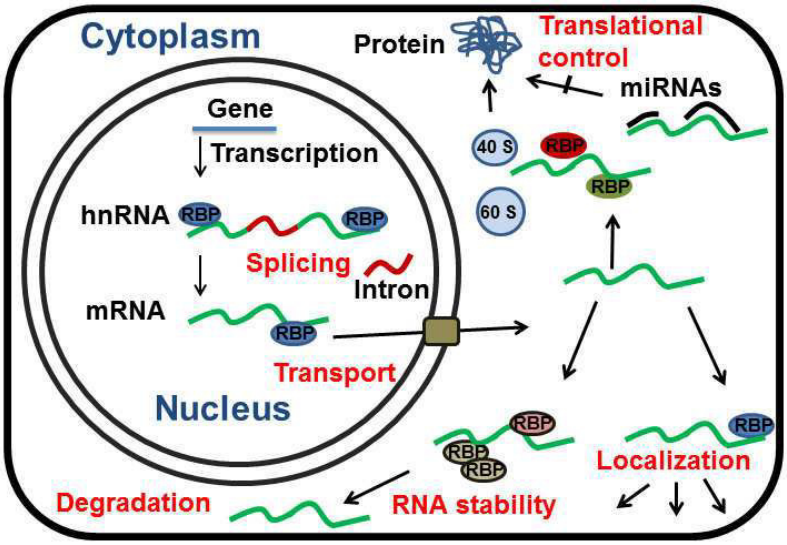

Figure 1.1: Simplified transcription and translation processes within the eukaryotic cell. Abbreviations: RBP: RNA binding protein, hnRNA: heterogeneous nuclear RNA, 40S, 60S: small (40S) and large (60S) subunits of the ribosome, miRNA: microRNA. Figure is adapted from Janga *et al*., 2011.

Transcription and translation events are highly complex processes and have a variety of regulation modes. From the

beginning of transcription, the pre-mRNAs with introns (so-called heterogeneous nuclear RNAs, hnRNAs) and mRNAs never appear isolated in the cell, but accompanied by RNA binding proteins (RBPs, see chapter 1.2, RNA Binding Proteins), which are responsible for stabilization or degradation of these RNAs. Then, the mRNA is translocated from the nucleus to the cytoplasm, still bound by proteins, crossing the nuclear pore complex. By binding to RNAs, RBPs and RNA form a RiboNucleoProtein complex (RNP), which prevents uncontrolled mRNA degradation and also regulates mRNA processing.

The last step of information flow from DNA to protein is the transport of mRNAs from the cell nucleus to the cytoplasm, where protein synthesis takes place at the ribosomes (for a simplified overview see Figure 1.1).

MicroRNAs (miRNAs) play an additional role for the regulation of gene expression. These small RNAs (about 22 nucleotides in length) appear in viruses, plants and animals and represent nearly 1% of the genome of humans, *Drosophila* and *Caenorhapditis* (Bartel *et al.*, 2004; Bushati *et al.*, 2007). miRNAs repress mRNA translation by binding to 3´ UnTranslated Regions (3´ UTRs) of mRNAs. Like other genes, miRNAs are transcribed by Polymerase II, then precursor RNAs are cleaved by the Drosha RNAse III (Lee *et al.*, 2003) and transported to the cytoplasm (Yi *et al.*, 2003; Lund *et al.*, 2004), where they are processed by the Dicer enzyme (Lee *et al.*, 2003).

1.2 mRNA Stabilization and mRNA Decay

The thesis deals with the RNA Binding Protein (RBP) HuR that is involved in mRNA stabilization, while other RBPs promote a degradation of mRNAs. The mRNA processing is essential to understand the role of RBPs in the biological context.

1.2.1 Role of AREs for mRNA Stability

Many mRNAs contain Adenylate and Uridylate enRiched Elements (AREs or AU-rich elements) within their 3´ or 5´ UnTranslated Regions (UTRs; for a review, see Barreau *et al.*, 2005). By comparing RNA sequences, a total of 5%-8% of human genes contain AREs (Bakheet *et al.*, 2001 and 2003). These genes code for cell growth factors, interleukins, interferons, TNFα and proto-oncogenes (Bakheet *et al.*, 2001). AREs regulate the stability of mRNAs coding for proteins that are implicated in processes like cell differentiation, cell growth, inflammation, immune responses or cancer (Chen and Shyu, 1995; Barreau *et al.*, 2005).

There are three different classes of AREs (Chen and Shyu, 1995):

a) Class I: AREs with a multiple repetition of AUUUA sequences.

b) Class II: AREs with two or more overlapping nonamers, containing AUUUA sequences.

c) Class III: AREs with U-rich regions, lacking AUUUA sequences.

Several RBPs interact with AREs promoting either a stabilization or degradation of the mRNAs. Certain RBPs recognize AU-rich elements at specific sequences, such as for example HuB (Levine *et al.*, 1993), HuD (Szabo *et al.*, 1991) or HuR (Ma *et al.*, 1996; Chen *et al.*, 2002; Myer *et al.*, 1997; Lopez de Silanes *et al.*, 2004). Accompanied by these stabilizing RBPs the RNAs are protected against decay, since the degrading machinery cannot access the UTRs. In this case a degradation of the mRNAs is prevented. On the other hand, a rapid degradation of mRNA can be effected by binding to AREs. Some RBPs together with the AU-rich elements

interact with the exosome (Chen *et al.*, 2001), whereas distinct reactions for different RBPs were observed. Binding of AREs to KH-type Splicing Regulatory Protein (KSRP) and Tris-TetraProline (TTP) results in a rapid degradation of mRNA, whereas HuR and AU-rich binding Factor 1 (AUF1) have stabilizing effects and prevent degradation (Chen *et al.*, 2001). These examples demonstrate the multiple ways in how far AREs and RBPs regulate stabilization and degradation of mRNAs and expression levels of these genes.

There exist two publicly available web server databases for investigation of AREs under the directions:

http://rna.tbi.univie.ac.at/AREsite. (Gruber *et al.*, 2010)

http://brp.kfshrc.edu.sa/ARED/ (Bakheet *et al.*, 2001 and 2003)

1.2.2 RNA Degradation

RNA degradation depends on *trans*-regulatory factors (proteins) and *cis*-regulatory elements (mRNA sequences) and occurs in three different ways: 3´ exonucleases degrade the transcripts beginning from 3´ site, 5´ exonucleases hydrolyze the RNAs beginning from the 5´ site, whereas endonucleases can cleave RNA molecules internally (Garneau *et al.*, 2007; Houseley and Tollervey, 2009).

Usually, the Pab1p-dependent Poly(A) Nuclease (PAN2-PAN3) complex performs a 3´ deadenylation of mRNA at the beginning of degradation. This shortens the polyadenylic tail to a length of about 80 nucleotides (Brown *et al.*, 1996; Yamashita *et al.*, 2005). Additionally, a deadenylation-independent mRNA decay occurs in the cell. Thus, the proteins Rps28 (Badis *et al.*, 2004) and the Enhancer of decapping protein (Edc1; Muhlrad and Parker, 2005) decap and degrade RNAs without previous deadenylation. In the deadenylation-dependent pathway the PAN2-PAN3 complex and the Cysteine-cysteinyl Chemokine Receptor 4-NOT (CCR4-NOT; Tucker *et al.*, 2001; Yamashita *et al.*, 2005) are involved in decapping. Another important protein taking part in deadenylation is the Poly(A)-specific RNase (PARN, previously called Deoxyribonucleoside-Activated Nucleotidase, DAN), as shown by experiments with *Xenopus*

laevis oocytes (Korner *et al.*, 1998) and other Eukaryotes (Dehlin *et al.*, 2000; Gao *et al.*, 2000; Chiba *et al.*, 2004; Milone *et al.*, 2004; Reverdatto *et al.*, 2004; Opyrchal *et al.*, 2005).

1.2.2.1 RNA Degradation in 5´ to 3´ Direction

mRNA degradation by exonucleases acting in 5´ to 3´ direction considered the major mRNA degradation pathway (Chen *et al.*, 2001). This type of degradation depends on the 7 methylguanosine triphosphate (m^7GTP)-cap at the 5´ ends of mRNAs. The cap protects the nucleic acids from 5´ to 3´ exonucleases. Additionally, the Decapping enzyme (Dcp1 and Dcp2) complex is involved in this process (Beelmann *et al.*, 1996; Lykke-Andersen, 2002; Steiger *et al.*, 2003; van Dijk *et al.*, 2002; Wang *et al.*, 2002) and other factors are needed, as Sm-like proteins (LSm1-7 complex; Tharun *et al.*, 2000 and 2001), LSm14 or RAP55 (Yang *et al.*, 2006) and the enhancer of decapping enzyme 3 - Edc3p or Lsm16 (Kshirsagar and Parker, 2006). When decapped, the RNA is fragmented into two RNA stretches: one ending with a 5´ monophosphate and the other with the m^7GDP rest. The monophosphate does not protect the RNA from exonuclease degradation anymore, so the transcripts are continuously degraded by the exoribonuclease Xrn1 (Stevens and Maupin, 1986). In bacteria, the process is similar but the 5´ end is modified by a triphosphate rest instead of the 5´ cap. After catalysis to a monophosphate by the RNA pyrophosphoHydrolase (RppH; Deana *et al.*, 2008), the degradation can take place.

1.2.2.2 RNA Degradation in 3´ to 5´ Direction – the Exosome

The alternative mRNA degradation pathway in 3´ to 5´ direction is carried out by the exosome, consisting of 9 to 11 proteins acting as a 3´ to 5´ exonuclease. The complex varies in numbers of subunits, depending on the organism and localization of the complex (Liu *et al.*, 2006). The human exosome is highly similar to the yeast exosome (Chen *et al.*, 2001), but differs in enzymatic activites of some complexes (Liu *et al.*, 2006) and has also homolog proteins in bacteria, which have Pleckstrin Homology (PH) and PolyNucleotide Phosphorylase (PNPase) domains (Symmons *et al.*, 2002; Lorentzen *et al.*, 2005; Liu *et al.*, 2006). In bacteria, the complex is

called degradosome, but the functions are the same: degradation of mRNA in 3´ to 5´ direction.

Before degradation occurs by the exosome, the Trf4-Air1/Air2-Mtr4 polyadenylation complex (TRAMP; Lacava *et al.*, 2005) marks the RNA targets with a poly(A) tail. When the RNAs are degraded, the remaining methylated cap is hydrolyzed by the scavenger mRNA decapping enzyme (DcpS; Liu *et al.*, 2002).

1.2.3 RNA Stabilization

Although the most frequently described consequence of RBP binding to AREs is the degradation of the mRNA targets, some RBPs have a stabilizing function upon binding to AREs. Besides the extensively studied mRNA stabilizing Hu proteins (see chapter 1.3 - Hu proteins), only few more proteins are known to stabilize mRNAs, such as CUG-Binding Protein 2 (CUG-BP2), Nucleolin, TINO, Poly(A)-binding protein-Interacting Protein 2 (PAIP2) and AUF1, which has both stabilizing and destabilizing functions (Barreau *et al.*, 2005). The well studied Hu family member HuR binds to more than 50 RNA targets related to disease (Srikantan and Gorospe, 2012). The mayority of these RNAs are stabilized. Thereby, degradation processes (see chapter 1.2.2 – RNA degradation) as well as interaction of mRNA with miRNAs or other RBPs are prevented.

1.3 RNA Binding Proteins

From the beginning of transcription, RNAs are always accompanied by RNA Binding Proteins (RBPs). RBPs are constituted by different types of small (30 to 100 amino acids in length) RNA Binding Domains (RBDs), which bind specifically to nucleic acid sequences and have diverse functions in the processing of the RNAs. In this context, the nucleic acids are described as the *cis*-regulatory elements and proteins as *trans*-regulatory factors. Dreyfuss and coworkers (Dreyfuss *et al.*, 2002) reviewed the various functions in which RBPs are involved, such as transcriptional regulation (Tomonaga *et al.*, 1995; Michelotti *et al.*, 1996; Du *et al.*, 1998; Miau *et al.*, 1998), telomere length maintenance (Ishikawa *et al.*, 1993; La Branche et al, 1998; Eversole *et al.*, 2000; Fiset *et al.*, 2001), immunoglobulin gene recombination (Dempsey *et al.*, 1999), splicing (van der Houven van Oordt

et al., 2000; Mayeda *et al.*, 1992; Caceres *et al.*, 1994, Yang *et al.*, 1994; Min *et al.*, 1995; Chan *et al.*, 1997; Chabot *et al.*, 1997; Ashiya *et al.*, 1997; Chou *et al.*, 1999; Del Gatto-Konczak *et al.*, 1999; Chen *et al.*, 1999; Mourelatos *et al.*, 2001) pre-ribosomal RNA processing (Russel *et al.*, 1992) and 3' end processing (Kessler *et al.*, 1997; Moreira *et al.*, 1998; Minvielle-Sebastia *et al.,* 1998, Bagga *et al.*, 1998). In the same review (Dreyfuss *et al.,* 2002) is also reported that, besides these nuclear actions, RBPs have also functions in the cytosol and are involved in mRNA transport between nucleus and cytoplasm (Lee *et al.*, 1996; Liu *et al.*, 1995; Izzauralde et al, 1997; Gallouzi *et al.*, 2001a). Further, RBPs play roles in mRNA localization (Hoek *et al.*, 1998; Matunis *et al.*, 1994; Cote *et al.*, 1999; Mouland *et al.*, 2001; Carson *et al.*, 2001) translation (Habelhah *et al.*, 2001; Ostareck *et al.*, 1997; Collier *et al.*, 1998; Silvera *et al.*, 1999; Ostareck *et al.*, 2001) and mRNA stability (Kiledjian *et al.*, 1995 and 1997, Rajagopalan *et al.*, 1998; Chkhheidze *et al.*, 1998; Shih *et al.*, 1999; Loflin *et al.*, 1999; Xu *et al.*, 2001). Different RBPs are able to interact specifically with either single-stranded RNA (ssRNA, as for example the RRM) or double-stranded RNA (dsRNA, as the double-stranded RBD), as also with small interfering RNA (siRNA, as PIWI and PAZ domains) and even bind to DNA (as zinc finger domains). The modular assembly and auxiliary domains in combination with linkers of different lengths determine the binding mechanisms and functions of the protein (for reviews see Lunde *et al.*, 2007; Glisovic *et al.*, 2008).

Combination of RBDs results in a big variety of RNPs with different RNA sequence specificities (Lunde *et al.*, 2007). Furthermore, the length of a linker between RBDs is important for the protein-RNA interaction. A long linker (about 50-60 residues; Lunde *et al.*, 2007) allows the RBDs to interact with RNA targets, which are separated on the same RNA strand. Also, it allows binding to various differently structured RNA molecules, as it is the case for the Adenosine Deaminase Acting on RNA-2 protein (ADAR2) that can bind dsRNA on differently structured transcripts (Stefl *et al.*, 2006). A short linker between RBDs, on the other hand, yields a high specificity to distinct RNA sequences, since the RBDs interact with RNA stretches with close proximity to each other. This is the case for the HuD protein (see chapter 1.4 – Hu proteins), whose N-terminal RRMs - RRM1 and RRM2 - work as a tandem domain, with a 3_{10}-helix linker (Wang and Tanaka Hall, 2001).

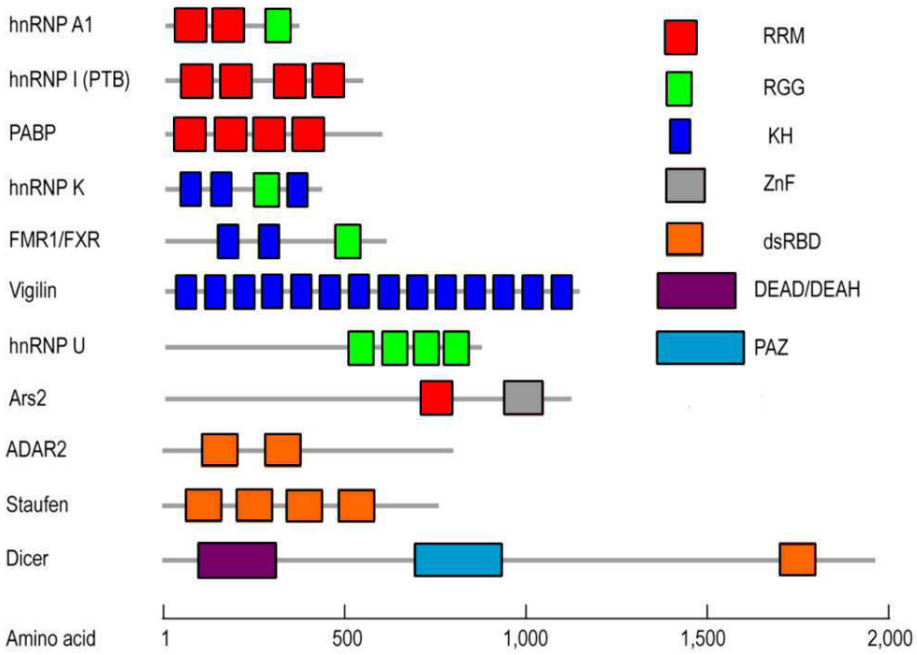

Figure 1.2: RBPs and their composition in RBDs.
The size of the RBPs can be estimated by the scale of amino acids at the bottom. Abbreviations: hnRNP: heterogeneous nuclear RiboNucleoProtein, PABP: PolyAdenylate-Binding Protein, FMR1: Fragile X Mental Retardation transcript 1, FXR: Fragile X Related protein, Ars2: Arsenate resistance protein 2, ADAR2: Adenosine Deaminase Acting on RNA-2, RRM: RNA Recognition Motif, RGG: Arg-Gly-Gly box, KH: K-Homology domain, ZnF: Zinc Finger, dsRBD: double stranded RNA-Binding Domain, DEAD/DEAH: RNA helicase DEAD/ DEAH box, PAZ: Piwi/Argonaute/Zwille domain. The figure is adapted from Glisovic *et al.*, 2008.

The length of linkers differ from four amino acids (Bj6 protein) to 122 amino acids (snRNP U1A protein) and can have a strong influence on the RNA binding characteristics, affecting sequences and affinities (Shamoo *et al.*, 1995; Finger *et al.*, 2004; Lunde *et al.*, 2007). When binding to RNA, a flexible disordered linker can change to an ordered structure, as reported for the Heterogeneous nuclear ribonucleoprotein 1 (Hrp1; Perez-Cañadillas, 2006). A short linker increases the affinity of RNA binding by additional RNA contacts with the linker. On the other hand, long flexible linkers are predicted to be less involved in RNA binding (Lunde *et al.*, 2007). For example, the 82 residue linker of nucleolin does not contact RNA. Thus, RNA binding is restricted to the RBDs (Stefl *et al.*, 2006).

In addition, protein-protein-interactions in RBPs occur frequently. On one hand, RNA binding proteins can dimerize, such as reported for HuR

(Benoit *et al.*, 2010) and the p19 protein (Vargason *et al.*, 2003; Ye *et al.*, 2003). This dimer formation modulates the protein-RNA interface, resulting in different binding characteristics of the protein.

On the other hand, protein-protein interactions are involved in protein shuttling between compartments. For instance, HuR protein has a 60 amino acid HuR Nucleocytoplasmic Shuttling sequence (HNS) (Fan and Steitz, 1998a) between the two C-terminal RRMs. This region is responsible for the shuttling of the protein from the nucleus to the cytoplasm and *vice versa*. This mechanism is coupled to protein binding of transportins (TRN) 1 and 2 (Gallouzi *et al.*, 2001a; Guttinger *et al.*, 2004; Rebane *et al.*, 2004) or in association with pp32 and the Acidic Protein Rich In Leucine (APRIL) by the Chromosomal Region Maintenance Protein 1 (CRM1; Gallouzi *et al.*, 2001b; Brennan *et al.*, 2000). Other proteins known to interact with HuR are SETalpha, SETbeta and Importin α (Wang *et al.*, 2004). Further examples for binding of RBPs to different kind of proteins are well reported by Lunde *et al.*, 2007 with important outcomes in mRNA fate.

RBPs have been extensively explored at the structural level with the pioneer techniques x-ray crystallography and Nuclear Magnetic Resonance (NMR), although slightly more crystallographic structures (26 in total; Daubner *et al.*, 2013) have been published in comparison with NMR solution structures (23 in total). Despite the fact that the atomic resolution of crystallographic structures gives more structural details about RNA bound protein, NMR is able to give information about dynamics and binding affinities that makes it an advantageous tool for analysis of RBPs (Cukier and Ramos, 2011).

On the following, the most important RBDs are presented (for reviews see Dreyfuss et al., 2002; Lunde *et al.*, 2007; Glisovic *et al.*, 2008, Elliott and Ladomery, 2011)

1.3.1 The RRM Domain

The RNA Recognition Motif (RRM, also known as RBD or RNP; for reviews see Maris *et al.*, 2005, Clery *et al.*, 2008; Muto *et al.*, 2012) is the most common RBD and the best characterized one. It is found in viruses, bacteria and eukaryotes (Maris *et al.*, 2005). About 1-2% of human genes

contain sequences coding for RRMs, often in multiple copies in the same gene (Venter *et al.*, 2001; Maris *et al.*, 2005). The domain is built up by about 90 amino acids, forming the secondary topology of $\beta_1\alpha_1\beta_2\beta_3\alpha_2\beta_4$ (Nagai *et al.*, 1995).

In most RRMs, RNA binding takes place at the highly conserved RiboNucleoProtein1 (RNP1; Adam, 1986; Swanson *et al.*, 1987; Oubridge *et al.*, 1994) and RNP2 motifs (Dreyfuss *et al.*, 1988) at the inner β_1 and β_3 strands of the protein, which are constituted by 8 amino acids for the RNP1 motif (Lys/Arg-Gly-Phe/Tyr-Gly/Ala-Phe/Tyr-Val/Ile/Leu-X-Phe/Tyr) and 6 amino acids for the RNP2 (Ile/Val/Leu-Phe/Tyr-Ile/Val/Leu-X-Asn-Leu) motif. Four residues of these RNPs interact with RNA at distinct positions (Birney *et al.*, 1993; Maris *et al.*, 2005). Position 1 of RNP1 contacts the RNA phosphodiester backbone by a salt bridge, while stacking interactions between aromatic residues and RNA bases are found at position 3 and 5 of RNP1 and position 2 of RNP2. However, not always all the four contacts contribute together to RNA binding (Ding *et al.*, 1999; Maris *et al.*, 2005).

An isolated RRM is able to recognize RNA stretches ranging from two (RRM2 of nucleolin; Allain *et al.*, 2000; Johansson *et al.*, 2004) to eight RNA bases (RRM1 of U2 snRNP-specific B protein, U2B''; Price *et al.*, 1998). Interestingly, some exceptional cases of RNA binding by RRMs have been described (Muto and Yokoyama, 2012). Instead of binding to RNA at the inner β_1 and β_3 strands, some RRMs bind RNA in a non-classical manner, such as the quasi-RNA recognition motif (qRRMs; Dominguez *et al.*, 2010) of hnRNP F, xRRM of p65 (Singh *et al.*, 2013) or the bacterial RNA helicase YxiN (Wang *et al.*, 2006). For these proteins also α-helices and loops are implicated in the RNA binding.

The RRM domain is involved in many posttranscriptional processes, as pre-mRNA processing, splicing, mRNA stability, RNA editing, RNA export and pre-mRNA complex formation, translation and degradation. In addition to RNA association, RRM domains are also known to interact with other proteins (Gallouzi *et al.*, 2001a; Maris *et al.*, 2005; Cho *et al.,* 2010). Well-studied examples of RRM binding proteins constituted by RRM domains are the proteins hnRNP A1 (Ding *et al.*, 1999), Hu proteins (Hinman and Lou, 2008) or Sex-lethal protein (Handa *et al.*, 1999).

1.3.2 The K-homology Domain

The K-Homology (KH) domain binds to both single-stranded RNA (ssRNA) and ssDNA (Backe *et al.*, 2005; Beuth *et al.*, 2005; Braddock *et al.*, 2002a and b; Du *et al.*, 2005; Lewis *et al.*, 2000; Liu *et al.*, 2001). It is ubiquitous in Eukaryotes, Eubacteria and Archaea (Siomi *et al.*, 1993). The typical KH domain consists of 70 amino acids and forms two different types of topologies: Type 1 has a $\beta_1\alpha_1\alpha_2\beta_2\beta_3\alpha_3$ constitution, whereas Type 2 is arranged according to the $\alpha_1\beta_1\beta_2\alpha_2\alpha_3\beta_3$ topology. This domain is able to bind four nucleotides in a cleft formed by the GXXG loop joining the neighboring helices, the strands β_2 (Type 1) or β_3 (Type 2) and the variable loop between $\beta_2\beta_3$ (Type 1) and $\beta_2\alpha_2$ (Type 2). The interaction between nucleic acids and protein is performed by hydrogen bonds and electrostatic interactions.

1.3.3 The Double-Stranded RBD Domain

The double-stranded RNA Binding Domain (dsRBD or DRBD) is constituted by 70 to 90 amino acids and has the topology $\alpha_1\beta_1\beta_2\beta_3\alpha_2$. In contrast to other RBDs, this motif binds to double-stranded RNA (dsRNA). The interaction is not sequence dependent and involves two successive minor RNA grooves and the intervening major groove of the dsRNA helix. Thus, binding of dsRBDs to dsRNAs depends on the structure of the nucleic acids. Binding is performed by hydrogen bonds between the 2´-OH groups of the RNA phosphates and the protein backbone (Ryter and Schultz, 1998).

1.3.4 Zinc Finger Domains

The Zinc Finger (ZnF) domains are known as classical DNA binding motifs, but they are also able to in interact with RNAs (Carballo *et al.*, 1998; Picard *et al.*, 1979). These domains consist of ca. 30 residues with a $\beta_1\beta_2\alpha_1$ topology. The different kinds of metal coordination result in three types of ZnFs: Cys Cys His His (CCHH), CCCH and CCHC arrangements. ZnF proteins often comprise several ZnF domains, as shown for the 5 S gene-specific Transcription initiation Factor (TFIIIA; Clemens *et al.*, 1993; Searles *et al.*, 2000), which is constituted by nine ZnF domains with different RNA or DNA binding preferences. The binding mechanism depends on the structure of

the nucleic acid. For instance, TFIIIA ZnFs 4 and 6 are associated with two RNA loops by the α-helix of the protein (Clemens *et al.*, 1993). Zif268 is a typical example for a protein with CCHH domains and its DNA binding is known from the crystal structure (Pavletich *et al.*, 1991; Wolfe *et al.*, 2000). Here the major groove of DNA is involved in binding to an α-helix by hydrogen bonds. TIS11d is an example of a CCCH-type ZnF protein (Hudson *et al.*, 2004) which binds to Adenine and Uridine Rich Elements (AREs) in 3´ UnTranslated Regions (UTRs) of RNA molecules. The interaction between RNA and TIS11d is based on hydrogen bonds. An example for the CCHC-type of ZnF domains is the Human Immunodeficiency Virus type I (HIV-1) nucleocapsid protein (De Guzman *et al.*, 1998; D´Souza *et al.*, 2004), which follows the same mechanism for RNA binding as the CCCH-type ZnF proteins.

1.3.5 Cold Shock Domains

Cold Shock Domains (CSD) were primarily identified in bacteria, for example the Cold shock protein A (CspA) from *E. coli,* which is expressed in upon temperature changes from 37 ˚C to 10 ˚C (Jones *et al.*, 1987). From the structural point of view, this small domain is built up by 70 amino acids arranged exclusively in five β strands forming two β-sheets. The protein-nucleic acid binding mechanism is similar to that of RRM domains: aromatic residues form stacking contacts with RNA bases and positively charged amino acids maintain contacts with phosphates from RNA and DNA. CSDs are also found in eukaryotes, such as the “Upstream of N-Ras” (UNR) protein (Chang *et al.*, 2004) and the Y-box protein (Sommerville and Ladomery, 1996a and b; Matsumoto and Wolffe, 1998). UNR has a repetition of five CSDs, the Y-box protein contains one CSD and is accompanied by additional sequences. These domains have additional functions related to RNA binding, multimerization and phosphorylation, making the eukaryotic proteins behave as multifunctional proteins. On the contrary, bacterial CSDs are less specialized with a main function as chaperones, synchronizing transcription and translation events.

1.3.6 PIWI Domain

P-element Induced Wimpy testis (PIWI) domains are involved in the processing of mRNAs and small interfering RNAs (siRNAs). PIWI topology consists of a 5-stranded β-sheet with α–helices at the periphery. The PIWI domain appears in the Argonaute protein and has an endonuclease cleavage function through binding to the 5' end of RNA (Ma *et al.*, 2005; Yuan *et al.*, 2005; Song *et al.*, 2004; Parker *et al.*, 2004 and 2005). Argonaute protein (Song *et al.*, 2004), along with Dicer (Macrae *et al.*, 2006), is involved in RNA degradation and RNA silencing pathways by forming an RNA Induced Silencing Complex (RISC; Hammond *et al.*, 2000; Bartel *et al.*, 2004).

1.3.7 PAZ Domain

PIWI Argonaute and Zwille (PAZ) domains bind non-coding micro RNAs (miRNAs) and small interfering RNAs (siRNAs). The PAZ domain comprises 110 amino acids with an $\alpha_1\beta_1$ arrangement and siRNAs bind to a hydrophobic pocket by 2 nucleotide overhangs. Stacking interactions and hydrogen bonds stabilize the complex (Ma *et al.*, 2004). Examples for proteins containing PAZ domains are Argonaute (Song *et al.*, 2004) and Dicer proteins (Macrae *et al.*, 2006) which are involved in RNA silencing pathways like the PIWI domains by forming RISC that degrades RNAs by interaction with siRNAs (Hammond *et al.*, 2000; Bartel *et al.*, 2004).

1.3.8 Arginine Rich Domains

Arginine Rich Domains are known as gene expression regulators. They were first discovered in bacteria and viruses, such as the TAT (Trans-AcTivator) domain in Human Immunodeficiency Virus type I (HIV-1; Garcia *et al.*, 1988; Frankel *et al.*, 1989; Subramanian *et al.*, 1991) and the REgulator of Virion expression (REV) domain from the same virus (Heaphy *et al.*, 1990). TAT has a conserved 14 amino acid sequence, rich in arginine and lysine residues, which is involved in binding to the TrAnsactivation Response RNA sequences (TAR) and regulates the gene expression (Dingwall *et al.*, 1989; Weeks *et al.*, 1990). Actually, TAT binds specifically to the stem-loop structured TAR RNA by a single arginine (Calnan *et al.*, 1991). Positively charged arginine residues also appear in Arg-Gly-Gly (RGG) boxes

and Serine/aRginine-rich (SR) proteins. SR proteins function as splicing factors and regulators (for a review see Fu, 1995) and they are combined with RRM domains, whereas RGG boxes (Kiledjian and Dreyfuss, 1992) not only bind to RNA, but also function in protein interactions with ribosomal proteins (Bouvet *et al.*, 1998).

1.3.9 RNA Helicases

RNA Helicases recognize RNA to unwind the dsRNA, thus allowing its process. Additional functions of RNA Helicases are related to splicing, RNA export, translation, RNA turnover, mitochondrial RNA metabolism and small RNA processing (for review, see Bleichert and Baserga, 2007). Helicases are further divided into five superfamilies (SFI to SF5; Gorbalenya and Koone, 1993) constituted by other conserved motifs named DEAD box, DEAH box and Ski2-like proteins, which are common motifs for the SF2 subfamily of RNA helicases.

1.4 Hu Proteins

Hu proteins belong to a group of RBPs constituted by three RRMs (Hinman and Lou, 2008) with the family members HuR (also called HuA, Ma *et al.*, 1996), HuB (also known as Hel-N1, Levine *et al.*, 1993), HuC (Szabo *et al.*, 1991) and HuD (Szabo *et al.*, 1991). In contrast to the neuronal expression of HuC and HuD, HuB is also present in gonads while HuR is expressed ubiquitiously (Good *et al.*, 1995; Ma *et al.*, 1996). The sequences of all the members of the family of Hu proteins are highly conserved, with the highest differences at the level of the linker part between RRM2 and RRM3. Hu proteins are homologs to the *Drosophila* Embryonic Lethal Abnormal Vision (ELAV) proteins and are also classified according to the ELAV protein family. From the evolutionary point of view, HuR is the most related Hu protein to the *Drosophila* ELAV homolog. HuR is supposed to be the ancestral protein in mice, whereas the most recently evolved homologs are the neuronal specific proteins HuB and HuD (Okano *et al.*, 1997). Figure 1.3 shows a protein multiple sequence alignment of the Hu proteins.

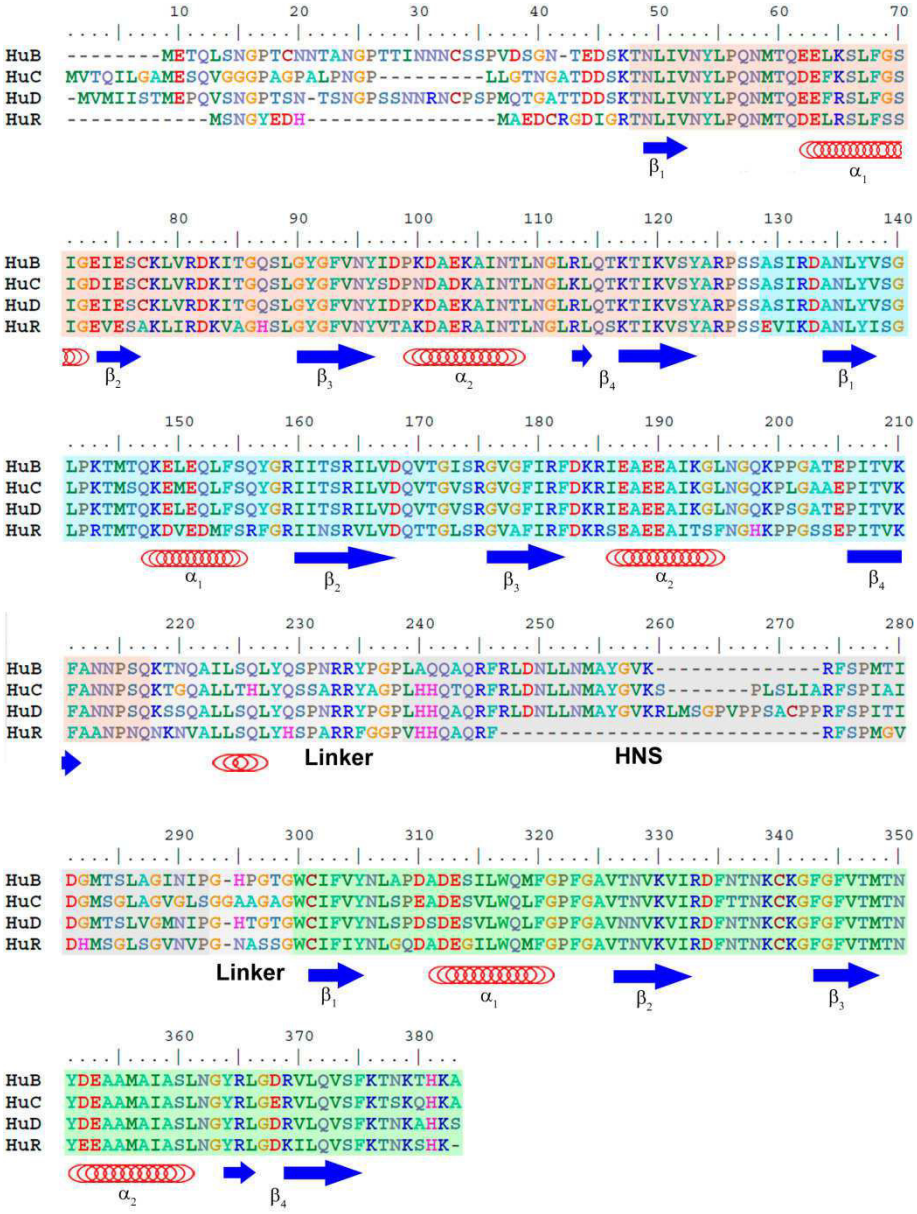

Figure 1.3: Multiple sequence alignment of Hu family proteins HuB, HuC, HuD and HuR. The alignment was built using the ClustalW server and edited by the BioEdit software. RRM1, RRM2 and RRM3 are marked in red, blue and green, respectively. HuR Nuclear Shuttling sequence (HNS) is colored in gray.Secondary elements α-helix are symbolized as red coils, β strands as blue arrows.

From the structural point of view, Hu proteins are built up by three RRMs (Adam *et al.*, 1986; Sachs *et al.*, 1986,) which show the canonical topology $\beta_1\alpha_1\beta_2\beta_3\alpha_2\beta_4$, forming a β-sheet of four antiparallel β strands packed against two α-helices (Nagai *et al.*, 1990). The most N-terminal RRM1 and RRM2 motifs work as a single unit (Wang and Tanaka Hall, 2001; Scheiba *et al.*, 2012), only separated by a 3_{10} helix. However, the third RRM domain is spaced out by a long linker, containing the HuR Nucleocytoplasmic Shuttling sequence (HNS; Fan & Steitz, 1998a). For an overview of Hu protein structures the reader is referred to section 1.4 – HuR. The HNS within the linker is responsible for the Hu protein shuttling between the nucleus and the cytoplasm and the variety of Hu functions are very dependent on the cellular compartment where the protein is (for a review see Hinman and Lou, 2008).

In the nucleus Hu proteins play two relevant functions. They are involved in the blocking of polyadenylation (Zhu *et al.*, 2007) and alternative splicing mechanisms (Zhu *et al.*, 2006 and 2008; Bellavia *et al.*, 2007. Splicing regulation was demonstrated for a set of mRNAs, such as those coding for the Calcitonin/calcitonin Gene-Related Peptide (CGRP), the NeuroFibromatosis type 1 (NF1) and the Ikaros protein, a ZnF DNA binding protein (Hinman and Lou, 2008). By integration or skipping of exons, the alternative splicing results in different protein isoforms. For instance, in the case of CGRP an inclusion or exclusion of exon 4 creates differently translated forms (Zhu *et al.*, 2006). NF1 has an analog mechanism by skipping the exon 23a (Zhu *et al.*, 2008). Such a switch is controlled by an outstanding competition between antagonistic RBPs for target-RNA binding. In this context, Hu proteins compete with the T-cell-restricted Intracellular Antigen 1 (TIA-1) and the TIA-1 Related protein (TIAR). Hu and TIA proteins recognize the same RNA targets but at different positions. For instance, Hu proteins promote a skipping of the NF1 exon 23a, whereas TIA proteins favor its inclusion (Zhu *et al.*, 2003). Furthermore, the binding of HuR to RNA prevents its association to TIA1. Lastly, Hu proteins show anti apoptotic behavior, while TIA proteins have pro-apoptotic functions (Forch and Valcarcel, 2001).

In the cytoplasm Hu proteins have the main function to stabilize mRNAs and regulate their translation by means of AREs in their 3´ UTRs (Ma

et al., 1996). In fact, cytoplasmic Hu proteins regulate the lifetime or translation of a large set of different mRNAs such as *c*-fos, *c*-myc, granulocyte macrophage colony-stimulating factor (Levine *et al.*, 1993) TNF-α (McMullen *et al*., 2003), p21, cyclin D1 (Lal *et al.*, 2004) or Growth-Associated Protein-43 (GAP-43; Bolognani *et al.*, 2006). All members belonging to the family of Embryonic Lethal Abnormal Vision (ELAV) proteins (HuB, HuC, HuD and HuR) bind to all three classes of AREs, but the proteins discriminate the targets – not all Hu proteins bind to the same RNA sequences (Hinman and Lou, 2008; Levine *et al.*, 1993; Jain *et al.*, 1997, Dean *et al.*, 2001).

1.5 HuR

Human antigen R (HuR) belongs to the Hu family of RBPs, showing the same RRM organization as explained before for Hu proteins in general.

1.5.1 HuR Functions

HuR shows all the attributes previously found for neuronal Hu proteins, despite HuR being unique in its ubiquitous expression pattern. The main function of HuR is binding to AREs in 3´ UTRs and stabilization of these mRNAs targets. This prevents mRNA degradation and enhances the protein levels of HuR targets (Brennan and Steitz, 2001; Lopez de Silanes *et al.*, 2004). HuR promotes translation by binding to mRNA targets (Kawai *et al.*, 2006) and inhibits the repressive effect of translation by miRNAs under stress conditions in cells (Bhattacharyya *et al.*, 2006). This function was shown for other RBPs, as the Dead End (Dnd1) protein (Kedde et Agami, 2008; Kundu *et al.*, 2012).

HuR is essential for the life of mice (Ghosh *et al.*, 2009) and supports a variety of functions in vertebrate organisms related to proliferation (Wang *et al.*, 2000a; Wang *et al.*, 2001), stress (Abdelmohsen *et al.*, 2007b; Mazan-Mamcarcz *et al.*, 2003; Wang *et al.*, 2000b; Gallouzi *et al.*, 2000, 2001b), apoptosis (Abdelmohsen *et al.*, 2007a, b; Mazroui *et al.*, 2008; von Roretz *et al.*, 2012), angiogenesis (Tran *et al.*, 2003), myogenesis (von Roretz *et al.*, 2011), differentiation (Figueroa *et al.*, 2003; Cherry *et al.*, 2006), senescence (Wang *et al.*, 2001; Yi *et al.*, 2010), inflammation (Katsanou *et al.*, 2005) and immune stimuli (Atasoy *et al.*, 1998; Mc Mullen

et al., 2003; Atasoy *et al.*, 2003). By stabilizing mRNAs that code for antiapoptotic proteins, HuR in general has an antiapoptotic function (Lal *et al.*, 2005; Wang *et al.*, 2000b; Mazan-Mamczarz *et al.*, 2003). However, the protein shows a promoted apoptotic behavior under stress conditions, confirmed by the dissociation of HuR from Stress protein SIr2-Related Protein Type 1 (SIRT1) RNA (Abdelmohsen *et al.*, 2007b; Mazroui *et al.*, 2008; von Roretz *et al.*, 2012).

1.5.2 Regulation of HuR

HuR is tightly regulated by posttranslational modifications. Phosphorylation, Ubiquitination, Methylation and Neddylation are described for the protein, as follows (see Figure 1.4).

Phosphorylation by different kinases changes HuR cellular localization and/or its RNA binding. Checkpoint kinase 2 (Chk2) modifies Ser88 and Ser100 and is known to increase or decrease the RNA binding, respectively (Abdelmohsen *et al.*, 2007b). Protein Kinase Cα (PKCα) phosphorylates residues Ser158 and Ser221 favoring the stability of cyclooxigenase (COX)-2 mRNA and causing the cytoplasmic localization of HuR, respectively (Doller *et al.*, 2007). PKCδ phosphorylates Ser221 and Ser318. Phosphorylation of Ser221 leads to the angiotensin II-induced export of HuR to the cytoplasm. In its turn, phosphorylation of Ser318 promotes binding of HuR to COX-2 AREs (Doller *et al.*, 2008a and b, 2010). The addition of a phosphate group at Ser242 (kinase not known) is also involved in the nuclear/cytoplasmic shuttling of the protein (Kim *et al.*, 2008). Recently, it has been reported that Cyclin-dependent kinase 5 (Cdk5) is able to phosphorylate HuR at Ser202 so as to promote mRNA displacement to the centrosome regions of the cell (Filippova *et al.*, 2012). Dephosphorylation also seems to play an important role to regulate the relocalization of HuR to the cytoplasm after infection of mammalian cells with alphaviruses (Dickson *et al.*, 2012). The methylation at Arg217 is caused by the Coactivator Associated arRginine Methyltransferase (CARM1) (Li *et al.*, 2002) and at Lys283, Lys313, and Lys326 modifications by the NEDD protein were reported (Embade *et al.*, 2012). Ubiquitination of HuR takes place at Lys182 (Abdelmohsen *et al.*, 2009).

HuR is further regulated at the transcriptional level: the promotor of HuR has a binding site for the Nuclear transcription Factor kappa B (NFκB), with the function to amplifiy the transcription (Kang *et al.*, 2008) when bound to HuR. This process was reported to take place in gastric tumors, thereby enhancing HuR levels in the cell (Yi *et al.*, 2010).

An important regulation mechanism of HuR is repressing of its translation by miRNAs. MiR-125a and MiR-519 are able to bind at HuR Coding Regions (CRs). The consequence of the repressed HuR translation is a decrease in HuR mediated gene expression. Additionally, cell proliferation and tumor growth is affected (Abdelmohsen, *et al.*, 2008 and 2010; Marasa *et al.*, 2010).

HuR also has an autoregulative function by binding to its own RNA sequences. The protein binds to an ARE bearing 3´ UTR of one of its rare mRNAs with a distal poly(A) signal (Al-Ahmadi *et al.*, 2009) and promotes the translation of HuR by an enhanced transport of its mRNA to the cytoplasm (Yi *et al.*, 2010).

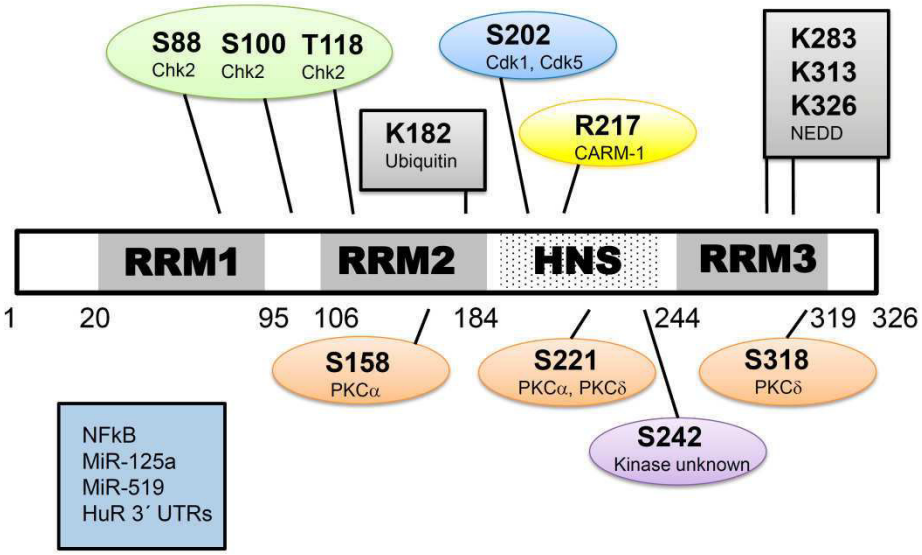

Figure 1.4: Regulation scheme of HuR. The positions of RRM1-RRM3 (marked in gray) and HNS are indicated. Phosphorylation and methylation sites with the corresponding kinases and methyltransferase, respectively, are presented in oval forms. Posttranslational modification by NEDD and ubiquitin is presented in gray boxes. Regulation of HuR at the transcriptional and translational level is presented in the blue box. For details, the reader is referred to the text. Figure is adapted from Doller *et al.*, 2008b.

1.5.3 HuR Structure

HuR belongs to the family of Hu proteins (HuR, HuB, HuC and HuD) and shows the highest sequence identity in relation to the homolog ELAV protein (Okano *et al.*, 1997). All Hu proteins are constituted by three RRMs. RRM1 and RRM2 are separated by a 3_{10} helix, whereas the third RRM domain is spaced out by a 60 residue spanning linker, containing the HuR Nucleocytoplasmic Shuttling sequence (HNS; Fan & Steitz, 1998a). The reader is referred to chapter 1.3 – Hu proteins and chapter 1.3.1 – The RRM Domain.

HuR and its homologs have the ability to multimerize (Toba and White, 2008, Benoit *et al.*, 2010, David *et al.*, 2007) and additionally to form complexes with other RBPs (David *et al.*, 2007). On one hand, HuR builds homodimers by disulfide bonds at Cys13 residue (Benoit *et al.*, 2010), on the other hand, HuR RRM3 is responsible for protein multimerization (Meisner *et al.*, 2007; Toba and White, 2008) and protein-protein interactions. Additionally, HuR RRM3 has an Adenosyl Transferase activity along with binding sites for Me^{2+} and ATP (Meisner *et al.*, 2009).

Crystallographic structures are available for HuC (RRM1: 1D8Z.pdb, RRM2: 1D9A.pdb, RRM12: 1FNX.pdb; Inoue *et al.*, 2000) and HuD (RRM12: 1FXL.pdb; Wang and Tanaka Hall, 2001). Recently the structures of HuR (RRM1: 3HI9.pdb; Benoit *et al.*, 2010; RRM12: 4ED5.pdb, 4EGL.pdb; Wang *et al.*, 2013) have been published, demonstrating the binding of RNA at the molecular level of the N–terminal RRM domains RRM1 and RRM2. Figure 1.5 shows the Richardson presentation of such structures.

HuR is a well-characterized protein *in vivo*, but little information is available at the structural level, except for the crystal structures mentioned above. Although the structures of individual and tandem RRM domains have been resolved, there is no Full Length (FL) structure reported for a protein from the Hu family. A previously crystallization report of HuR FL was published (Iyaguchy *et al.*, 2009) without further results. In particular, the structure and assembly of RRM3 in relation to RRM12 remain to be elucidated. Due to the biophysical characteristics and the low solubility of RRM3 domain, it explains the relevance of this thesis work.

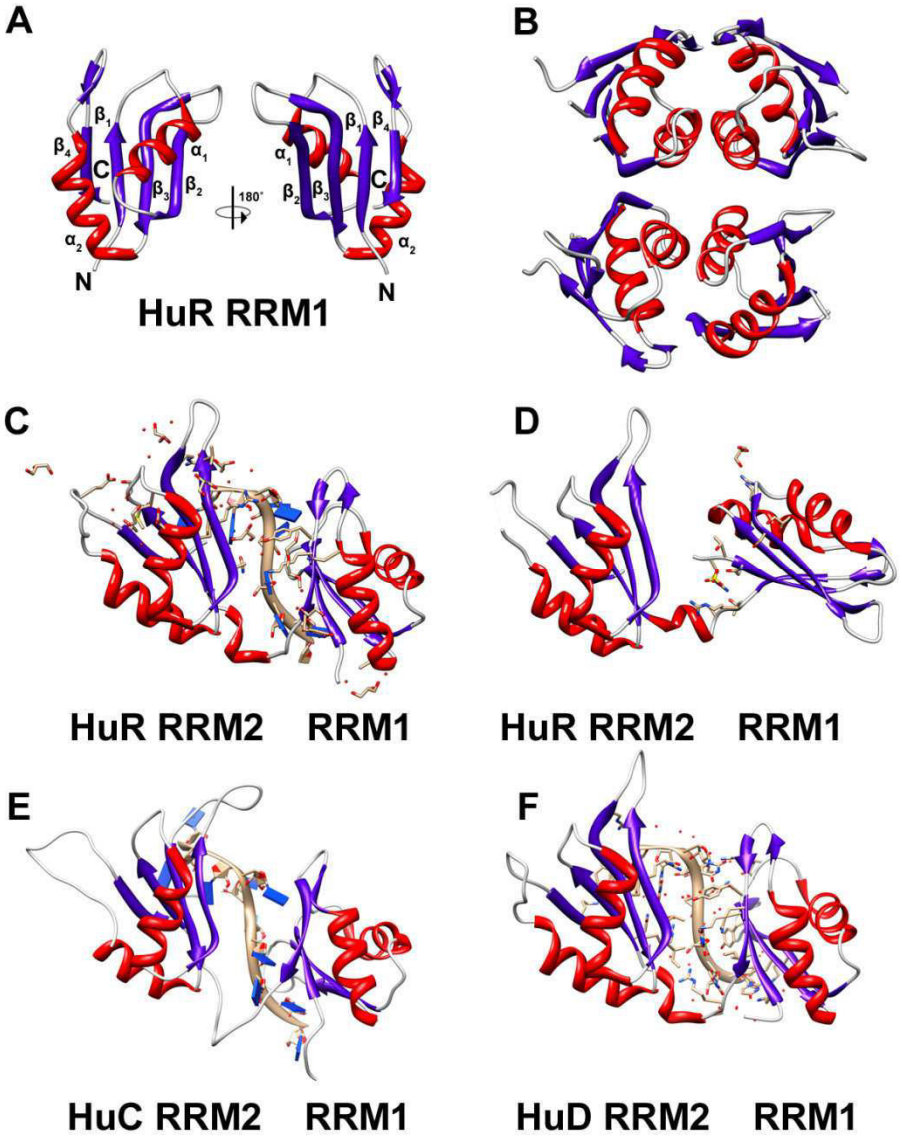

Figure 1.5: Crystallographic structures of Hu proteins. A) HuR RRM1 (3HI9.pdb), left monomer, right tetramer **B)** HuR RRM12, bound to RNA (left, 4ED5.pdb), and free (right, 4EGL.pdb) **C)** HuC RRM12, bound to RNA (1FXN.pdb) **D)** HuD RRM12 bound to RNA (1FXL.pdb).

Objectives

Objectives

This thesis work reports a biophysical characterization of the RBP HuR so as to explore its main structural features. HuR is well-characterized *in vivo*, but working mechanisms at the molecular level are still unknown. As the protein is involved in regulatory mechanisms of human pathologies, such as inflammation, cardiovascular diseases and cancer, studying in depth its biophysical and structural properties will help to understand and treat these diseases in a long term view.

The first objective is to characterize biophysically the three RRMs of HuR with respect to its modular assembly. It is proposed that each RRM has certain physical and functional properties, such as specific thermal or chemical stabilities. In this context, it is of interest how differently HuR domains behave and whether they cooperate with each other.

Second aim of this work is to perform biophysical characterization of isolated HuR RRM3 in solution by means of improving its solubility to further explore its structural features.The HuR C-terminal RRM3 domain has additional functions in comparison to the N-terminal RRM12 module, since it is known to form multimers and actively contributes to RNA modification by its adenosyl transferase activity. This domain has a low solubility due to its particular biophysical properties. Thus, a challenging protocol is necessary to increase RRM3 solubility and, further, to improve the purification of this domain. Ongoing analysis of RNA binding, interactions with the N-terminal RRM12 and multimerization events are of interest to elucidate molecular working mechanisms of HuR.

The third aim of this thesis is to investigate the effects of phosphorylation at the molecular level and its functional consequence by the design of phosphorylation mimic mutants. HuR is tightly regulated by diverse posttranslational modifications at several residues. The effects of phosphorylation of residues Ser88 (RRM1), Ser100 (in between RRM1 and RRM2), Ser158 (RRM2) and Ser318 (RRM3) are known at the cellular level. These phosphorylations alter mRNA binding and localization of the protein

in vivo. In this work, biophysical properties of RRM12 and RRM3 species have been explored through a comparison between the phospho-mimic species and the *wild-type* proteins. *In vitro* experiments get new insights into how Ser phosphorylation modulates the RNA binding properties of HuR.

Materials and Methods

Materials and Methods

2.1 Design of HuR Constructs

pGEX 5X2 vectors containing the sequences coding for HuR full-length (HuR FL) as well as individual N-terminal RRM domains RRM1 and RRM2, the two-domain construct RRM12 and the C-terminal RRM3 module, were kindly provided by Dr. M. Gorospe (National Institutes of Health, Baltimore, USA) and Dr. J. A. Steitz (Yale University, New Haven, USA). RRM1, RRM2 and RRM12 were further cloned into the pGEX-4T2 vector. pETM-11 vectors were used for HuR FL and RRM3 using EcoRI and NotI restriction sites. The gene corresponding to RRM3 domain comprises the amino acid sequence from Trp244 to Lys326. Vectors for RRM12 and HuR FL were modified as follows: the GST sequence was substituted by a 6xHis-tag using the following primers: 5´-CATCATCACCACCATCACctggttccgcgtggatccccagg-3´ (forward primer) and 5´-GTGATGGTGGTGATGATGcatgaatactgtttcctgtgtg-3´ (reverse primer) to facilitate protein purification. GST and 6xHis-tags were cleaved with thrombine or TEV protease respectively, resulting in a short additional amino acid sequence for all constructs ‘‘GSPGIPSNYEDH,’’.

Further site-directed mutagenesis was performed on the genes coding RRM modules to replace serines at positions 88, 100, and 158 of the RRM12 construct (Mutagenex, Piscataway, USA). For the RRM3 construct serine 318 was replaced by alanine or aspartate so as to mimic the phosphorylation of HuR. In addition, Trp261 was replaced by glutamic acid at RRM3 (RRM3 W261E) to study HuR oligomerization events.

2.2 Protein Expression and Purification of HuR Constructs

Recombinant HuR genes were expressed in Escherichia coli BL21-T1^{R} (SIGMA, St. Louis, USA) cells as follows: competent cells were transformed with plasmid DNA and were grown at 37 ˚C in *Luria Bertani* (LB) medium supplemented with ampicillin (50 µg/mL) for pGEX vectors or kanamycin (50 µg/mL) for pETM vectors. Gene expression was induced by addition of 1 mM isopropyl-1-thio-β-D-galactopyranoside (IPTG) once the culture reached OD_{600} of 0.6–0.8. After 5 h expression in LB medium at 30 ˚C for RRM3 and HuR FL constructs and at 37 ˚C for RRM1, RRM2 and RRM12, cells were harvested by centrifugation at 7,000 g and further resuspended in 50 mM Tris buffer (pH 8.0) for storage at -80 ˚C. Isotopically ^{15}N- and ^{13}C-labeled proteins were expressed in minimal medium (M9) supplemented either with $^{15}NH_4Cl$ or $^{15}NH_4Cl$ and ^{13}C-glucose following Marley´s protocol (Marley *et al.*, 2010).

Cells were incubated with protease inhibitors (Complete Protease Inhibitor Cocktail Tablets, 0.002% PMSF), 100 µg/mL Lysozyme and 3 mM DTT at room temperature for 15 minutes. 0.4 mg/mL DNAse was added before treating cells with an S-250 D Cell Disruptor and a fine sonifier tip (3 x 30 seconds; Branson Ultrasonic Corporation, Danbury, USA). In the particular case of RRM3 and HuR FL constructs, buffers were supplemented with 0.1% of the detergent N-Lauroylsarcosine (Sarkosyl, SIGMA, St. Louis, USA) and 800 mM NaCl to increase the solubility of both proteins during all purification steps. Then, cell material was centrifuged for 20 min at 30,000 g and the soluble fractions used for chromatography. GST fusion proteins were purified using a Glutathione Sepharose High Performance Matrix (GE Healthcare, Piscataway, USA), whereas His-tagged constructs were purified by Nickel Affinity Chromatography (Ni Sepharose^{TM} Fast Flow Matrix; GE Healthcare, Piscataway, USA). All constructs were expressed with thrombine-cleavable GST or TEV-cleavable His-tags (GE Healthcare, Piscataway, USA). To separate HuR RRM single domains from the cleaved GST protein, gel filtration chromatography (Sephadex G-75 matrix; SIGMA, St. Louis, USA) was performed. His-tags were eliminated by dialysis. In the cases of HuR FL and RRM3, the excess of salt was washed out by dialyzing the protein against the buffer devoid of NaCl. Subsequently, the buffer was

exchanged in an Amicon® centrifugation device (Merck Millipore, Massachusetts, USA) to eliminate traces of Sarkosyl. Protein concentration was determined by spectrophotometry using predicted extinction coefficients. All molecular weights of the HuR constructs used in this thesis were verified by matrix-assisted laser desorption/ionization time of flight (MALDI-TOF) spectroscopy.

2.3 Circular Dichroism Spectroscopy

All Circular Dichroism (CD) spectra were recorded in the far-ultraviolet (UV) range (190–250 nm) at 298 K in a Jasco J-815 spectropolarimeter, equipped with a Peltier temperature-control system, using a 1-mm quartz cuvette. Protein concentration was 12 µM in 10 mM sodium phosphate buffer (pH 7.3) supplemented with 0.5 mM DTT. For each sample, 20 scans were averaged for further secondary structure analysis using CDPRO software (Sreerama and Woody 2000), which includes the algorithms CONTIN, SELCON, CDSSTR and the CLSTR option to compare the protein folding with a set of similar folded proteins.

Thermal unfolding experiments were carried out in a range of temperatures from 298 to 371 K. For all these assays, the HuR species at 12 µM final concentration were dissolved in 10 mM sodium phosphate (pH 7.3) with 0.5 mM DTT. Temperature was increased at a rate of 1 K per min with an error within ± 0.1 K. Spectra were recorded at the scan rate, band width, and sensitivity of 200 nm min^{-1}, 1.0 nm, and 0.2˚, respectively. Protein unfolding was monitored by recording the CD signal at 195, 208 and 235 nm. The experimental data was fitted to a two-state native-denatured model (Privalov, 1979), using the equation of Santoro and Bolen (1988).

RNA binding was monitored by adding increasing amounts of protein to 4 µM AU 11-mer (5´-AUUUUUAUUUU-3´) RNA in 10 mM sodium phosphate (pH 7.3) 0.5 mM DTT. A temperature of 298 K was chosen to optimize the signal change upon protein binding. Each CD spectrum was the average of 10 scans. The integral of this averaged signal between 260 and 275 nm was fitted against a quadratic, 1:1 binding model (Kannt *et al.*, 1998).

2.4 Differential Scanning Fluorimetry

Thermal unfolding of HuR constructs was monitored by Differential Scanning Fluorimetry (DSF) in the presence of fluorescent SYPRO Orange dye (Invitrogen, Carlsbad, CA, USA) by using an IQ5 multicolor real-time PCR detection instrument (BioRad; Niesen *et al.*, 2007). The commercial dye [5,000x concentrate in dimethyl sulfoxide (DMSO)] was at least ten-fold diluted in 10 mM sodium phosphate buffer (pH 7.3) supplemented with 0.5 mM DTT and the HuR samples (10–40 μg protein) were added at 25 μL final volume. The thermal unfolding process was monitored between 293 K and 369 K, increasing the temperature at a rate of 1 K per min. The values for the midpoint melting temperature (T_m) were calculated from the first derivative in Origin 8.0 (Microcal Inc.) and a nonlinear curve-fitting function was used (Privalov, 1979), using the equation of Santoro and Bolen (1988).

2.5 Fluorescence Measurements

Emission spectra were monitored using a Perkin-Elmer LS-5 fluorimeter equipped with an oil-thermostated cell holder at 298 K. Excitation wavelength was 280 nm, whereas the emission spectra were recorded in a 300-400 nm range. 8 μM of RRM3 WT and RRM3 S318D in 10 mM sodium phosphate buffer (pH 7.3), 0.5 mM DTT, 0.02% NaN_3, were supplemented with increasing aliquots of Guanidine Hydrochloride (1.5–5 M) concentration for 1 h at 298 K before recording the spectra. The experiments were performed with a 1 cm quartz cuvette with slits set to 5 nm for excitation and emission. Each spectrum was the average of two scans. The background signal was subtracted from the buffer.

2.6 Analytical Ultracentrifugation

Analytical Ultracentrifugation (AU) experiments were performed at the Institute of Physical Chemistry "ROCASOLANO" (IQRF), Madrid, under supervision of Dr. Menéndez Fernández.

Sedimentation equilibrium experiments of HuR RRM3 WT domain and RRM3 W261E mutant were performed at 20 °C in an Optima XL-A

Analytical Ultracentrifuge (AU; Beckman Instruments) with an AN50-Ti rotor. 80 µL samples at 27 µM HuR RRM3 were examined in 10 mM phosphate buffer (pH 7.3), 50 mM NaCl, 3 mM DTT, 0.02% NaN_3, at three successive speeds (18,500; 22,000 and 32,000 rpm) and absorbance was measured at 280 nm at 12 and 48 h to asses that the equilibrium condition was reached. Baseline signals were determined taking a radial scan at 18,500 rpm after running the samples 8 h at 45,000 rpm. Conservation of mass in the cell was checked in all the experiments. The apparent weight-averaged molecular weights were obtained by fitting individual data sets to a sedimentation equilibrium model for single species, using the program Heteroanalysis (www.biotech.uconn.edu). The equilibrium dimerization constants, K_2, were calculated by fitting the experimental data to a monomer/dimer sedimentation equilibrium model constraining the monomer molecular mass to 14,342 Da. Sedimentation velocity experiments were performed at 45,000 rpm and 20 °C with 400-µL samples loaded into double sector cells, using the buffer and protein concentrations employed in equilibrium experiments. Radial scans at 280 nm were taken every 10 min and the sedimentation coefficient distribution was calculated by least squares boundary modelling of the sedimentation velocity data using the program SEDFIT (Schuck, 2000). The experimental coefficients were converted to standard conditions (s20,w). The partial specific volume of HuR RRM3 WT (0.728 g/L), calculated from the amino acid composition, as well as the buffer density and viscosity were determined with the SEDNTERP program (Laue *et al.*, 1992).

2.7 Nuclear Magnetic Resonance

Nuclear Magnetic Resonance (NMR) samples of HuR RRM3 WT and its RRM3 S318D mutant were prepared in 95% H_2O / 5% D_2O solutions of 10 mM sodium phosphate buffer, pH 7.3, 3 mM DTT, 0.02% NaN_3, at concentrations in a range from 130 to 175 µM. NMR spectra were recorded at 298 K on a Bruker Avance III 800 MHz spectrometer with a [^{1}H, ^{13}C, ^{15}N] triple resonance cryo-probe equipped with z gradient coil. Standard 2D and 3D NMR experiments (2D ^{15}N-HSQC, 2D ^{13}C-HSQC, 3D HNCO, 3D HNCA, 3D HN(CA)CO, 3D HNCACB, 3D HN(CO)CACB, 3D HN(CO)CA, 3D HN(CA)HA, 3D HN(COCA)HA) were used to assign backbone resonances of RRM3 domain. The spectra were processed with TopSpin NMR (Bruker) software to be

further automatically assigned by MARS server (Jung and Zweckstetter, 2004). Structural models of RRM3 WT and RRM3 S318D were created using the backbone assignment already deposited in BMRB database (entry codes are going to be published), along with the amino acid sequences, as input files for the CS23D server (Wishart *et al.*, 2008).

RNA binding of HuR RRM3 WT and RRM3 S318D was monitored by acquiring ^{15}N-HSQC spectra at a 500 MHz Bruker spectrometer provided with cryo-probe, along titrations of the 5´-AUUUA-3´ and 5´-UUUUU-3´ RNA oligonucleotides (IDT, Integrated DNA Technologies) into a sample of 50 µM ^{15}N-labeled RRM3 in 10 mM sodium phosphate buffer (pH 7.3), 3 mM DTT at RNA:protein ratios of 2:1 and 4:1. The pH value of the sample was verified after each titration step. Weighted average values of ^{15}N and ^{1}H chemical-shift perturbations ($\Delta\delta_{avg}$) of each resonance was calculated as follows: $\Delta\delta_{avg} = (([\Delta\delta_H]^2 + [\Delta\delta_N/5]^2) / 2)^{1/2}$, being $\Delta\delta_H$ and $\Delta\delta_N$ chemical-shift increments of ^{1}H and ^{15}N, respectively.

Results

Results

3.1 HuR RRM12 Domain Adopts a Canonical Topology with Negligible Changes in its Secondary Structure upon Phosphorylation

The crystallographic structure of HuR RRM1 – recently published by Benoit *et al.* (2010) – shows that the RRM folding adopts the canonical $\beta_1\alpha_1\beta_2\beta_3\alpha_2\beta_4$ topology. As shown in Figure 3.1, HuR protein consists of three RRMs.

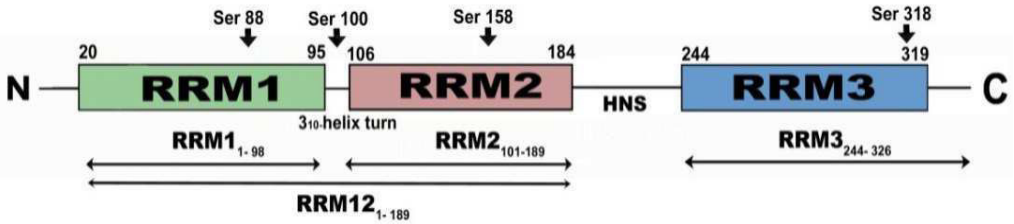

Figure. 3.1: Schematical view of HuR.

A homology model of HuR RRM12 construct was obtained using the crystallographic structure HuD RRM12 as a template (PDB entry 1FXL; Wang and Tanaka Hall, 2001). Sequence identity to the target was 75.4%, and the model represented in Figure 3.2 was built with the SWISS-MODEL server (Arnold *et al.,* 2006; Kiefer *et al.,* 2009; Peitsch, 1995) and graphically represented using Chimera software (Pettersen *et al.*, 2004).

Figure 3.2 shows the superposition of both HuR structures: the homology model of RRM12 and the crystallographic structure of RRM1. The homology based model is in good agreement with the secondary structure contents for HuR constructs.

Figure 3.3 shows the normalized far-UV CD spectra of isolated RRM1 and RRM2 domains, the tandem RRM12, and the HuR-FL protein. Notably, all HuR species show similar global secondary structures with minor differences, as summarized in Table 3.1. Whereas all constructs share similar β strand and turn contents, RRM2 differs from RRM1 and RRM12 in its higher α-helix content.

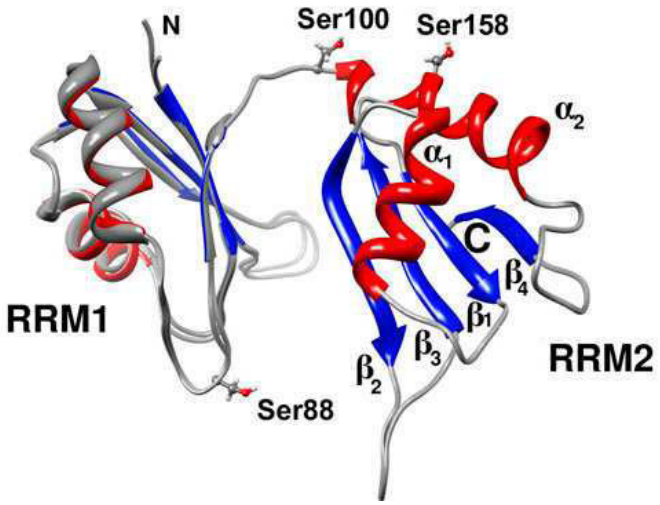

Figure. 3.2: HuR RRM12. Superposition of the crystal structure of HuR RRM1 (PDB entry 3HI9; Benoit *et al.*, 2010) and the homology model of HuR RRM12 built as described in ''Materials and Methods.'' The RMSD for backbone atoms of HuR RRM1 domain in both structures is 0.583 Å. Side-chains of serine residues to be phosphorylated are included. Quality information: The QMEAN Z-Score is 1.33.

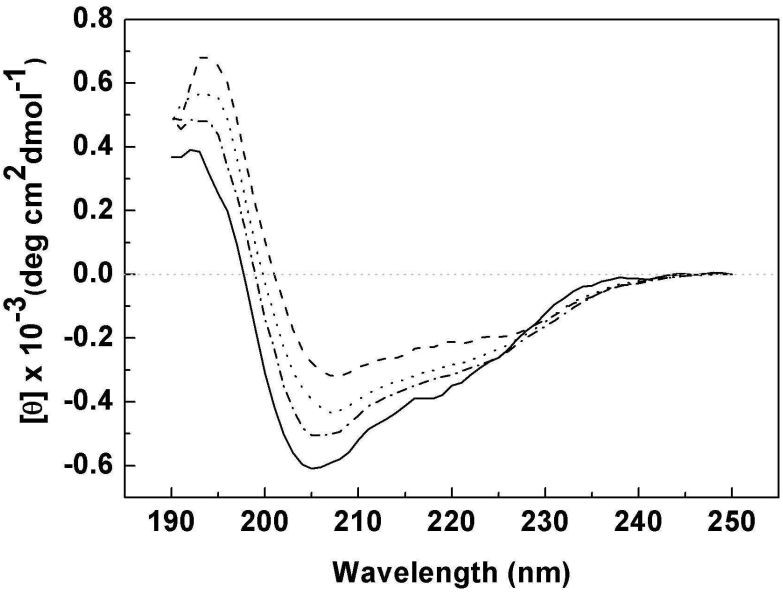

Figure 3.3: Far-UV (190–250 nm) CD spectra of different HuR N-terminal domain constructs. RRM domains are represented as follows: RRM1 by solid line, RRM2 by dashed line, RRM12 by dotted line and HuR-FL protein by dash-dotted line.

RRM12 mutants, in which Ser88, Ser100 and Ser158 have been substituted by aspartic acid residues to mimic phosphorylation events, exhibit a secondary structure similar to that of RRM12 wild-type (RRM12 WT). In addition, Ser-by-Ala control mutations show similar CD spectra (Figure 3.4; Table 3.1).

Table 3.1 Percentage of secondary structure for the different N-terminal constructs of HuR RRM domains and mutant species.

Constructs	α-helix (%)	β-strand (%)	Turn (%)	Unstructured (%)*
RRM1	6.01 ± 0.57	36.21 ± 1.25	19.49 ± 2.05	37.74 ± 3.95
RRM2	10.84 ± 0.22	34.11 ± 0.65	19.13 ± 0.90	30.81 ± 1.61
RRM12 WT	5.72 ± 0.77	39.67 ± 4.39	21.22 ± 1.80	33.03 ± 3.10
RRM12 S88D	11.03 ± 0.56	33.26 ± 2.05	19.64 ± 2.06	35.76 ± 4.75
RRM12 S88A	5.87 ± 0.44	39.00 ± 1.68	20.42 ± 1.41	34.25 ± 2.40
RRM12 S100D	5.34 ± 1.25	42.71 ± 4.30	19.25 ± 2.01	32.16 ± 3.81
RRM12 S100A	3.18 ± 0.39	40.88 ± 1.34	21.23 ± 1.15	34.78 ± 2.90
RRM12 S158D	5.14 ± 0.50	40.28 ± 1.58	20.51 ± 1.12	33.81 ± 3.17
RRM12 S158A	5.16 ± 0.34	39.79 ± 1.40	21.04 ± 1.65	33.75 ± 3.29
HuR FL	9.18 ± 1.79	34.95 ± 0.83	20.01 ± 2.39	35.23 ± 4.74

* This section refers to both disordered and flexible and ordered but nonregular structured parts of the protein.

For comparison of thermal stability data all proteins have to be in a monomeric state. Cys13 promotes a homodimer formation for the RRM12 construct (Meisner *et al.,* 2007; Benoit *et al.,* 2010). For further investigation of the thermal stability of RRM12 WT and its mutants, the impact of Cys13 on the homodimer formation needs to be evaluated. Figure 3.5 shows a Sodium Dodecyl Sulfate (SDS) polyacrylamide gel

electrophoresis (PAGE) of RRM12 WT in absence and presence of dithiothreitol (DTT) at 0.5 and 5 mM, as reducing agent. RRM12 WT is clearly a monomer upon DTT addition, although a monomer–dimer equilibrium appears in samples devoid of DTT. These data were recently confirmed by AU experiments on RRM12 WT samples containing 0.5 mM DTT (data not shown). Thus, RRM12 WT construct, which includes Cys13, behaves as a monomer, at least in the experimental conditions used in this work.

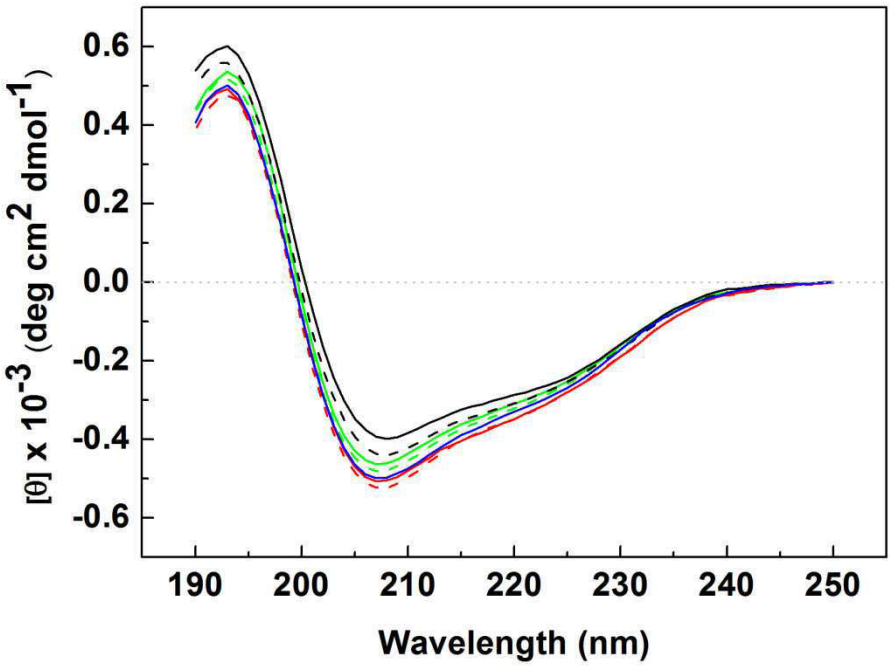

Figure 3.4: Far-UV (190–250 nm) CD spectra of RRM12 WT and its phosphomimetic mutants. RRM12 WT is shown in blue solid line, RRM12 S88A in green solid line, RRM12 S88D in green dashed line, RRM12 S100A in black solid line, RRM12 S100D in black dashed line, RRM12 S158A in red solid line and RRM12 S158D in red dashed line.

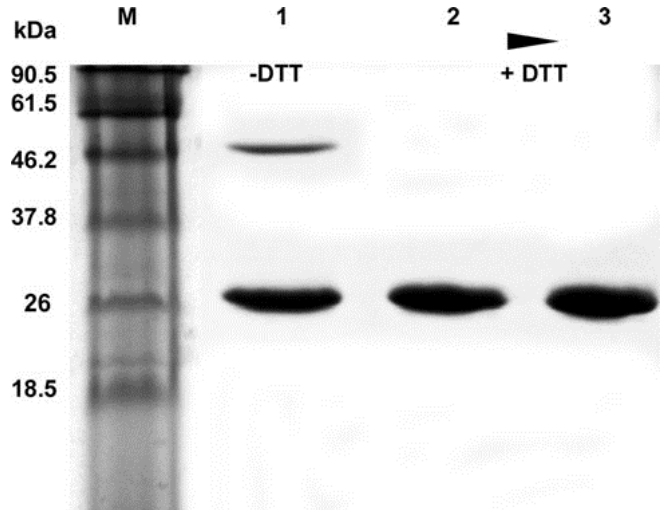

Figure 3.5: PAGE electrophoresis of HuR RRM12 WT. Line 1 HuR RRM12 WT sample devoid of DTT; lines 2 and 3 protein samples previously incubated with 5 and 0.5 mM DTT, respectively, for 90 min before loading into the gel. In each line, 4 µg HuR RRM12 WT was loaded onto an 18% SDS-PAGE gel. M: Pro-stain protein molecular weight marker (Intron Technologies Inc.).

3.2 RRM12 Works as a Functional Unit

Recently, it has been demonstrated that the thermal stability of RBDs reveals interactions between neighboring modules (Aroca *et al.,* 2011; Díaz-Moreno *et al.,* 2010). Thermal unfolding studies on the single N-terminal RRM segments and the two-domain construct from HuR were performed to confirm the assembly between RRM1 and RRM2, as inferred from the homology model of HuR RRM12 and the crystal structure of HuD RRM12 (Wang and Tanaka Hall, 2001). CD spectroscopy shows that the T_m for isolated RRM1 (335 ± 3 K) is slightly lower than that for RRM2 (341 ± 2 K; Table 3.2). Interestingly, RRM12 is as stable as RRM1 (335 ± 2 K), suggesting that interdomain interactions are taking place. Such interaction lowers the T_m of RRM2 by ca. 6 K, as previously reported for other RBPs (Aroca *et al.*, 2011; Díaz-Moreno *et al.,* 2010).

Table 3.2: T_m values of HuR N-terminal RRM domains and their phosphomimetic mutants, as calculated by CD and DSF

Constructs	T_m (K) by CD	T_m (K) by DSF
RRM1	335 ± 3	333 ± 1
RRM2	341 ± 2	339 ± 1
RRM12 WT	335 ± 2	332 ± 1
RRM12 S88D	336 ± 1	336 ± 2
RRM12 S88A	331 ± 1	330 ± 2
RRM12 S100D	334 ± 2	333 ± 1
RRM12 S100A	333 ± 1	330 ± 3
RRM12 S158D	330 ± 2	328 ± 3
RRM12 S158A	335 ± 1	330 ± 2

In addition, the denaturation curve of RRM12 is not the sum of the denaturation curves of the two individual RRM1 and RRM2 domains, revealing that only one transition state is observed instead of two. Indeed, the cooperativity of the RRM12 denaturation is strongly reduced as compared with that of the individual domains. These changes in stability between isolated RRM2 and RRM2 in RRM12 construct are confirmed by DSF, although ΔT_m is slightly higher (7 K; Table 3.2; Figure 3.6 A).

Intriguingly, the T_m values calculated by DSF for HuR species are always equal to or lower than those estimated by CD, although ΔT_m is quite independent of the technique used (Table 3.2) .

3.3 Stability of HuR RRM12 is Regulated by Phosphorylation

To analyze the phosphorylation effect of serine residues on the stability of HuR RRM12 construct, this posttranslational modification was mimicked by Ser-to-Asp substitutions.

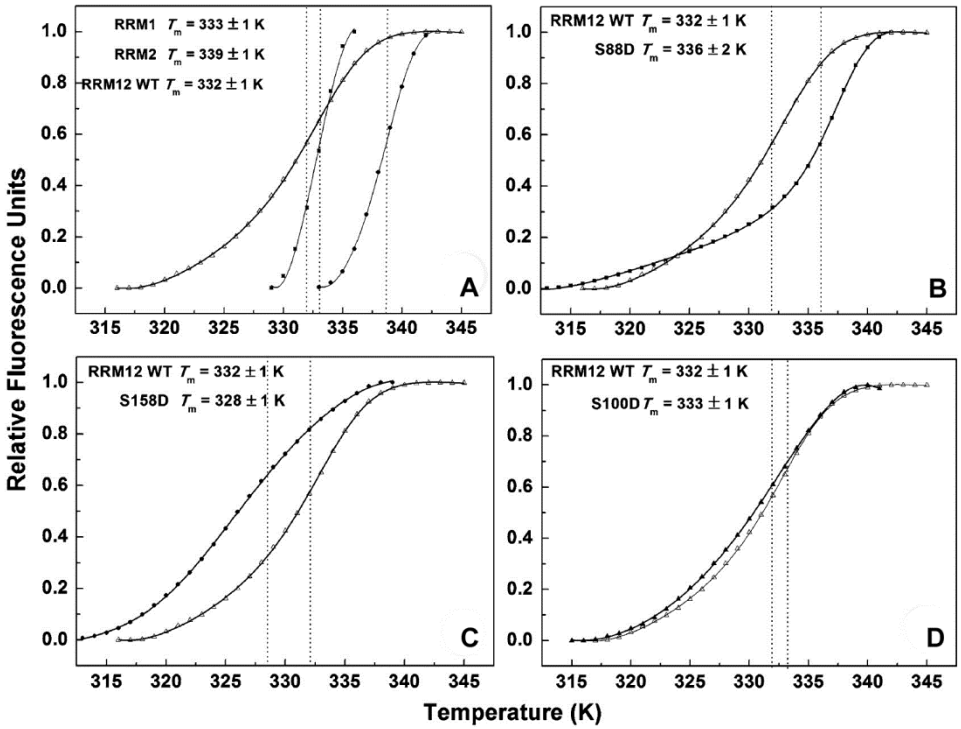

Figure 3.6: Effect of phosphomimetic mutations on the thermal stability of HuR. Unfolding thermal denaturation of HuR N-terminal RRM species and their mutants was determined by DSF by following the fluorescent changes of SYPRO Orange. **A)** RRM1 is represented by filled squares, RRM2 by filled circles and RRM12 WT by open triangles. Ser-by-Asp substitutions are represented as follows: **B)** RRM12 S88D (filled squares), **C)** RRM12 S158D (filled circles), and **D)** RRM12 S100D (filled triangles). Fitted unfolding curves are presented as solid lines, superimposed on experimental data. The melting points (T_m) of the transitions are marked by dashed lines.

Even though the use of Ser/Asp mutations simulates a constitutively phosphorylated protein with only one negative charge, it is herein extensively recommended since two out of three serine residues of RRM12 WT—those at positions 88 and 100—become phosphorylated by the same kinase, Chk2, making *in vitro* kinase assays undesirable.

The nonconserved serine residues, which are localized inside the RRM core, play an essential role in the stability of HuR RRM12. It is worth mentioning that phosphorylation at Ser88 in RRM1 mimicked by the S88D mutant makes the RRM12 construct slightly more stable than its control mutant (S88A) and RRM12 WT. Indeed, T_m of RRM12 S88D is increased by 5 K, using both CD and DSF approaches (Table 3.2; Figure 3.6 B).

In contrast, the addition of a negatively charged group at position 158 (mutation S158D) slightly destabilizes HuR RRM12 with regard to the S158A mutant and RRM12 WT, despite the discrepancies in ΔT_m between CD and DSF. The well-conserved Ser100, which forms part of the short linker between RRM1 and RRM2, displays no significant contributions to the thermal stability of HuR RRM12 upon mutations (ΔT_m < 2.0 K). As expected, the nonphosphorylatable Ser-to-Ala RRM12 mutants behave as RRM12 WT in terms of thermal stability, suggesting that HuR phosphorylation has functional consequences rather than structural effects.

3.4 RNA Binding of HuR RRM12 is Regulated by Phosphorylation

To understand how the interaction of HuR-RRM12 with *c*-fos AU-11-mer RNA may be regulated upon phosphorylation, we assess the affinity of RRM12 WT and its phosphomimetic mutants for the RNA target and explored whether the phosphorylation could modulate recognition *in vitro*, similarly to *in vivo*. We used CD to obtain quantitative data over affinities which lie in the μM range. Our CD data show that the affinity of the two RRM1 and RRM2 domains by the RNA is in the low micromolar range (2.6 ± 0.2 μM; Table 3.3; Figure 3.7). Next, we investigated the effect of phosphorylation at RRM1 and at the RRM12 linker by RRM12 S88D and RRM12 S100D mutants, respectively, which show K_D values comparable to that of RRM12 WT (2.7 ± 0.2 μM for S88D and 2.0 ± 0.1 μM for S100D; Table 3.3). In contrast, RRM12 S158D favors RNA binding (0.6 ± 0.3 μM; Table 3.3), in agreement with previously published data *in vivo* (Doller *et al.,* 2007).

Table 3.3: K_D values of the HuR RRM12 construct and its phosphomimetic mutants, as calculated by CD titration experiments with *c*-fos 11-mer RNA (5´-AUUUUUAUUUU-3´)

Constructs	K_D (μM)
RRM12 WT	2.6 ± 0.2
RRM12 S88D	2.7 ± 0.2
RRM12 S100D	2.0 ± 0.1
RRM12 S158D	0.6 ± 0.3

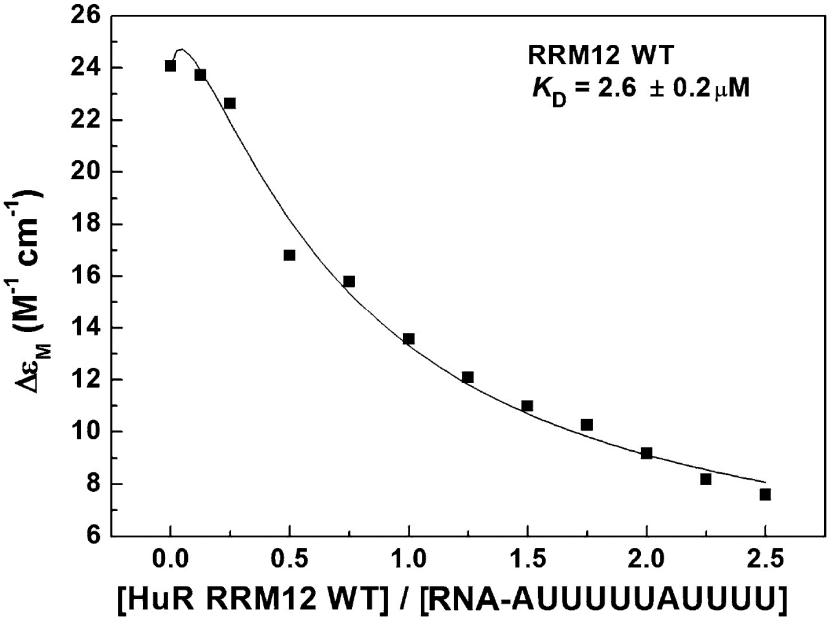

Figure 3.7: RNA binding of HuR RRM12 WT.Changes in the CD signal in the 260–275 nm range of the *c*-fos 11-mer RNA (5´-AUUUUUAUUUU-3´) spectrum during titration with HuR RRM12 WT. Dissociation constant is also shown. Fit corresponds to a quadratic, 1:1 binding model.

3.5 Shedding Light on the HuR C-terminal RRM3 Domain

The most C-terminal HuR-domain RRM3 is of special interest for the working mechanism of the protein, because it is an RRM motif with substantial distinct biophysical properties in comparison to the well-characterized RRM1 and RRM2 domains. In contrast to the other two modules, RRM3 has a very low solubility that hampers its purification. As a consequence, its role in the HuR FL protein is not well-understood (schematically view, see Figure 3.1).

In spite of being the unknown domain, it is reported that RRM3 has adenosyl transferase activity (Meisner *et al.*, 2009) and the capability to interact with other protein partners (Brennan *et al.*, 2000; Gallouzi *et al.*, 2001 b; Rebane *et al.*, 2004; David *et al.*, 2007). Moreover, the RRM3 ELAV protein from *Drosophila melanogaster* – a homologue of human HuR - forms oligomers, in which both the C-end of the first α-helix and the following loop are involved (Toba and White, 2008). Unfortunately, little is known concerning the biophysical properties for this domain, even for the HuR FL protein, due to their low solubility under *in vitro* conditions. In this work, we shed light on the structure of this domain, as well as its role in RNA binding and posttranslational modifications by phosphorylation, for a better understanding of the HuR working mechanisms in the context of mRNA fate.

3.5.1 RRM3 Domain Tumbles Independently in Solution

Taking into account that HuR N-terminal domains - RRM1 and RRM2 - are behaving as a functional unit (see section 3.3), we investigated whether RRM3 is also part of this domain rearrangement, so as to characterize the overall structure of HuR FL. By recording ^{15}N HSQC spectra of ^{15}N RRM12 before and after adding ^{14}N RRM3 (Figure 3.8 A) or *vice versa* (^{15}N RRM3 titrated with ^{14}N RRM12; Figure 3.8 B), any RRM-RRM interaction with an affinity constant K_D in the range from mM to µM would be detected by changes in chemical-shifts or in line widths of resonances. However, both panels of Figure 3.8 reveal that none of the above NMR

parameters changed, so the RRM12 and RRM3 interaction could be excluded. This finding indicates that RRM3 works independently or at least partially independently of RRM12, meaning that the C-terminal RRM3 module of HuR tumbles in solution without a fixed orientation with respect to the N-terminal ones. This domain rearrangement of HuR could explain how RRM3 can be easily isolated from the HuR core by a caspase-mediated cleavage, which has been reported as a regulatory step that contributes to an amplified apoptotic response (Mazroui *et al.*, 2008; von Roretz *et al.*, 2012).

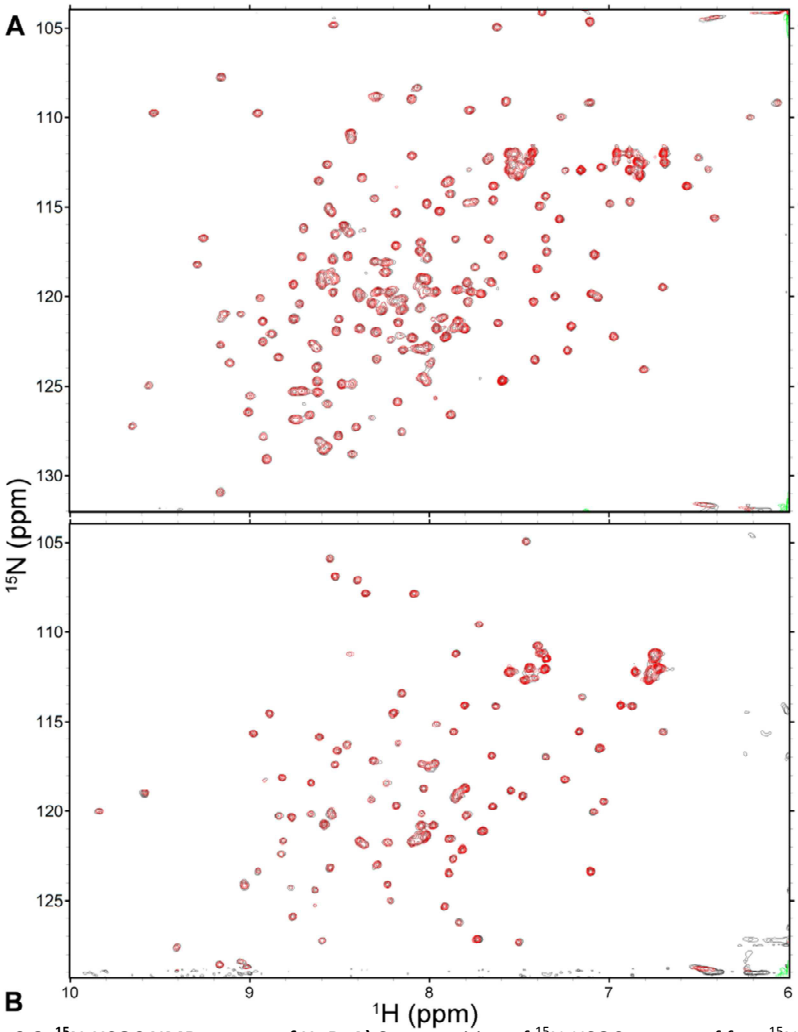

Figure 3.8: ^{15}N-HSQC NMR spectra of HuR. A) Superposition of ^{15}N-HSQC spectra of free ^{15}N HuR RRM12 (black) and after adding ^{14}N HuR RRM3 (red) at a RRM12:RRM3 ratio of 1:4.
B) Superposition of ^{15}N-HSQC spectra of free ^{15}N HuR RRM3 (black) and in complex with ^{14}N HuR RRM12 complex (red) at the same ratio as in A).

3.5.2 NMR Restraint-Based Model of RRM3

We have established a protocol for expression and purification of HuR RRM3 WT and RRM3 S318D. For this purpose we have tested a set of buffer conditions with different amounts of detergents and salts (data not shown). Best results were achieved using the anionic detergent sarkosyl to increase HuR RRM3 solubility. After removing detergent and salt from the protein preparations, concentrations of no more than 200 µM were reached. Due to this low solubility, we could record 3D NMR spectra based on the ^{13}C resonance to assign only backbone atoms, but not those experiments with which obtain Nuclear Overhauser Effect (NOE) signals and distance information to be further implemented in structure calculations. However, automatic assignment worked well using MARS server and most of resonances appearing at the ^{15}N HSQC spectrum of RRM3 WT were successfully assigned (Figure 3.9). Actually, non-labeled resonances mainly correspond to signals from the TEV cleavage site located between the 6×His-tag and the protein sequence. Using NMR chemical-shifts and protein sequences as restraints, both structural models of RRM3 WT and RRM3 S318D were built up with the CS23D server (see Figure 3.10; Wishart *et al.*, 2008).

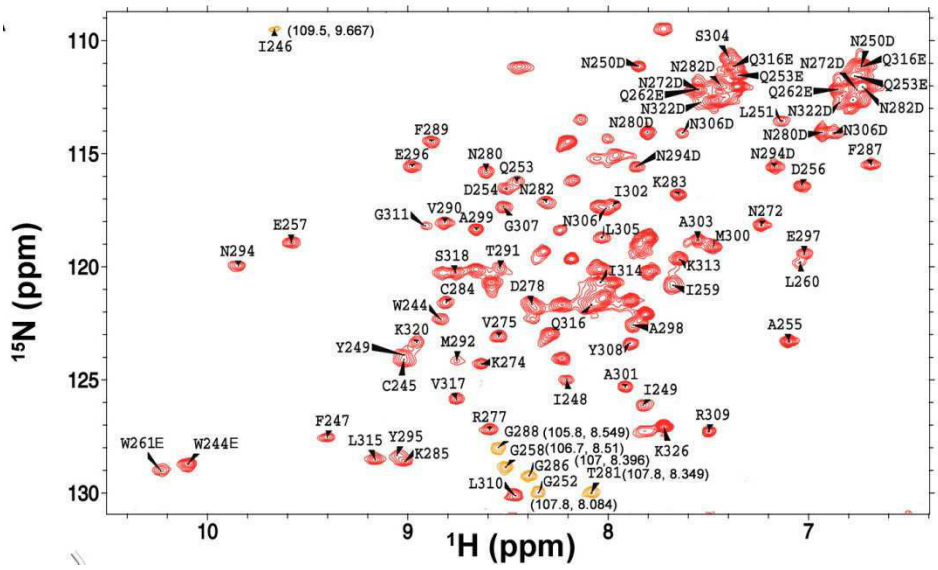

Figure 3.9: HuR RRM3. ^{15}N-HSQC spectrum of HuR-RRM3 WT along with the assignment. Labels stand for the amino acids of RRM3 following the numbers in the HuR -FL protein.

Both models have the conserved structure of two α-helices packed against four anti-parallel β strands with the canonical $\beta_1\alpha_1\beta_2\beta_3\alpha_2\beta_4$ topology characteristic of RRM motifs. Comparison between the RRM3 WT model with that of the phosphomimetic mutant (RRM3 S318D) reveals minor differences mainly found at flexible loop regions. In fact, the RMSD for backbone atoms between both models is ca. 1.14 Å. Figure 3.10 shows how the side-chain of Ser318 at the β_4 strand is well-exposed to solvent in order to be accessible to Protein Kinase C δ (PKCδ) and to become phosphorylated.

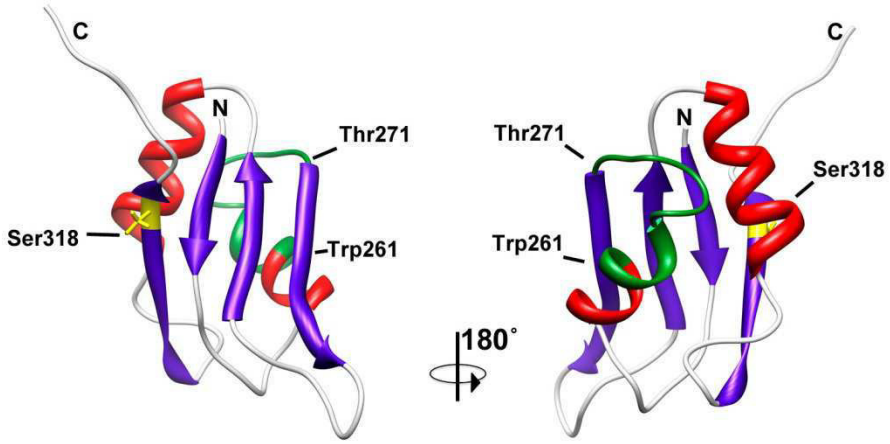

Figure 3.10: Structural model of HuR RRM3 WT domain built using chemical-shifts of backbone atoms as restraints in the CS23D server. The side-chain of Ser318, which becomes phosphorylated, is highlighted in yellow. Those residues of RRM3 WT between Trp261 and Thr271, which are in intermediate exchange on the NMR timescale for chemical-shift perturbations are marked in green.

Intriguingly, the residue stretch ranging between Trp261 and Thr271 was not possible to assign in either RRM3 WT or RRM3 S318D, as indicated in Figure 3.10. This suggests that the helix/coil element is in a conformational intermediate exchange on the NMR time scale. Previously, it has been described the importance of RRM3 for ELAV – a homologue to HuR in *Drosophila* – multimerization (Toba and White, 2008). Indeed, authors concluded that the non-detectable Trp261 by NMR – Trp419 in ELAV sequence - was essential for protein-protein interactions. Thus, we suggest that the Trp261-Thr271 stretch form a dimerization epitope that involves the C-end of helix α_1. Such a case was reported for the interactions between HuR RRM1 motifs through helices α_1 and α_2 (Benoit *et al.*, 2010).

The Hε of Trp261 from RRM3 WT in the ^{15}N HSQC spectrum was easily assigned by comparison with that of RRM3 W261E mutant. It is worth to mention that the resonance of Hε (Trp261) was broader than Hε (Trp244) – (32.9 Hz in ^{15}N / 55.7 Hz in ^{1}H and 27.7 Hz in ^{15}N / 40.8 Hz in ^{1}H, respectively), in agreement with the monomer-dimer exchange proposed for this helix/coil element (Figure 3.10).

3.5.3 Oligomerization of HuR RRM3

To get further insight on HuR oligomerization and the above mentioned low solubility of this protein, the formation of HuR RRM3 multimers was investigated by AU assays and MALDI measurements (Figure 3.11). By AU experiments (Figure 3.12), we could determine that the apparent molecular weight was ca. 19.2 kDa, which differs from the expected one for a monomer (14.2 kDa).

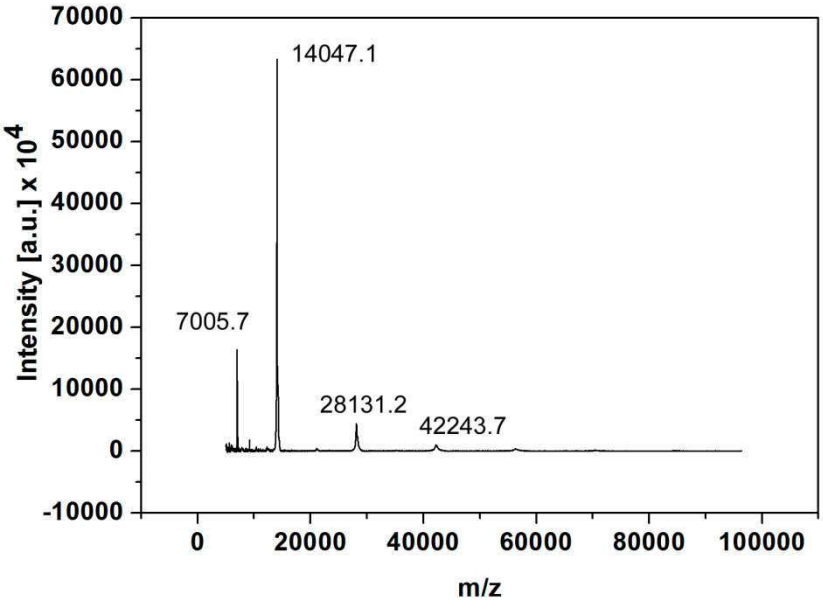

Figure 3.11: Oligomerization of HuR RRM3. MALDI mass spectrometry reveals that RRM3 WT is a mixture of monomers (MW of 14047.1 Da) and dimers (28131.2 kDa) at 150 µM of protein

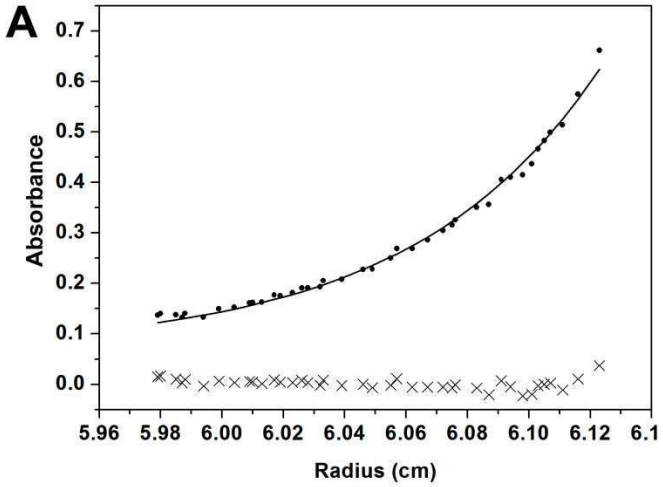

Figure 3.12: AU experiments using HuR RRM3 WT and RRM3 W261A species.

A) AU at sedimentation equilibrium conditions. The apparent molecular weight (MW) is determined as 19033 ± 1425 Da, differing slightly from the estimated one for a monomer (14342.2 Da).

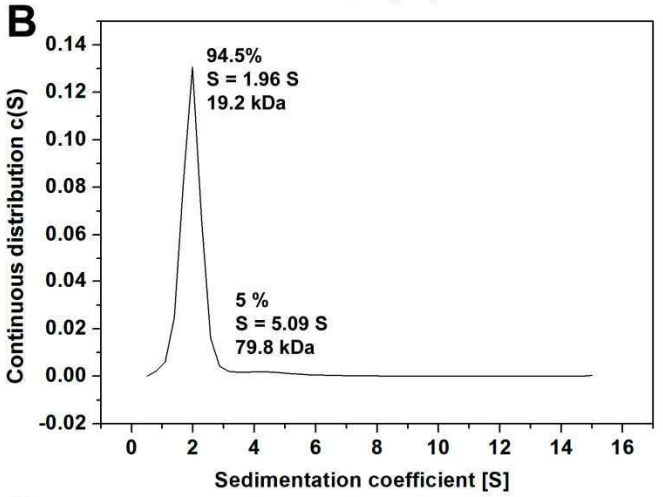

B) The sedimentation coefficient of WT protein calculated by sedimentation velocity at 45.000 rpm results in 1.96 S and 19.2 kDa. A small population (~ 5%) corresponds to 5.08 S and 79.8 kDa

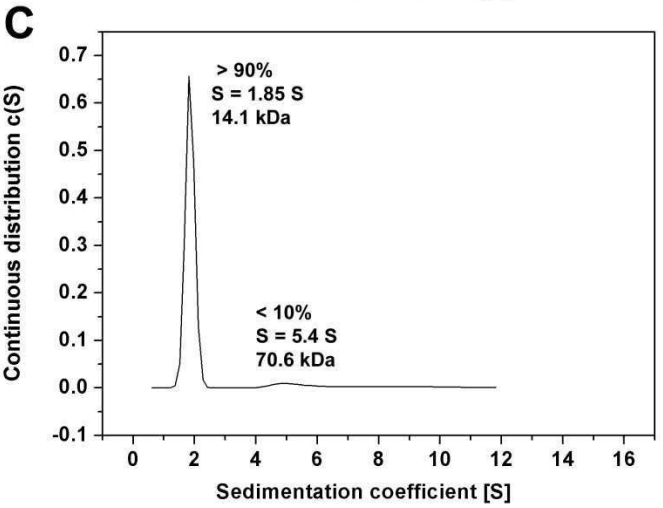

C) The sedimentation coefficient of W261E mutant at the same velocity as the WT construct results in 1.85 S and 14.1 kDa. A small population (~ 5%) corresponds to 5.4 S and 70.6 kDa.

The results fit in the best way to a fast/intermediate exchange model between monomeric and dimeric species, with a K_A of about 1.8 x 10^4 M^{-1}. Then, about 70% of HuR RRM3 WT is already in the monomeric form at protein concentration used in these AU assays. The dimeric population may be substantially increased at NMR experiments which demand larger protein amounts. In addition, a small fraction of the protein (5%) tends to form aggregates with a molecular weight of ca. 79.8 kDa (Figure 3.12 B). MALDI experiments on HuR RRM3 WT confirmed the dimer formation and even trimers, which must be stable (Figure 3.11).

In contrast to HuR RRM3 WT, the RRM3 W261E mutant is mainly monomeric in AU experiments. Under similar conditions in sedimentation velocity experiments, the molecular weight (MW) of this species was 14.1 kDa, which corresponds to the MW of the monomer state (14.2 kDa). Aggregation could be also observed as an additional peak corresponding to the molecular weight of 70.6 kDa, as happens for the WT protein (Figure 3.12 C). Thus, the Trp-261-to-Glu261 mutation impairs dimerization of the RRM3 domain.

3.6 RNA Binding of HuR RRM3

To test the RNA sequence specificity by HuR RRM3 WT domain, its interactions with two short 5-mer RNA oligonucleotides, namely 5´-AUUUA-3´ and 5´-UUUUU-3´, were studied by NMR titrations (Figure 3.13 and 3.14). Average chemical-shift perturbations ($\Delta\delta_{avg}$) inferred from the titrations of ^{15}N-labeled RRM3 with both RNA oligonucleotides revealed that RRM3 binds to 5´-UUUUU-3´ with an apparent higher affinity than 5´-AUUUA-3´ (Figure 3.15, A and C), which indicates a preferential binding for pyrimidine bases than for purine derivates However, as the chemical-shift perturbations were too small, quantification of the binding was not feasible.

The two RNA molecules lie on the RRM3 canonical platform, which comprises aromatic residues mainly localized at the central β strands (β_1 and β_3) from β-sheet (Figure 3.15, panels B and D). In fact, backbone amides for residues ranging from Phe247 and Leu251 at β_1-RNP2 and from Phe287 and Met292 at β_3-RNP1 were all perturbed in titrations with both RNAs, as

previously reported (Query *et al.*, 1989; Shamoo *et al.*, 1997). Interestingly, the protein platform with which HuR RRM3 binds to 5′-UUUUU-3′ RNA is extended to involve the whole β-sheet, including most of β_2 and few signals at β_4 signals (Figure 3.15, panels B and D). In addition to $\Delta\delta_{avg}$, some RRM3 signals at the protein-nucleic acid interface broadened beyond the detection limit independently of the RNA oligonucleotide used. Residues such as Ile248, Leu251, Val275 and Lys320 showed this behavior for both 5′-UUUUU-3′ and 5′-AUUUA-3′ RNAs.

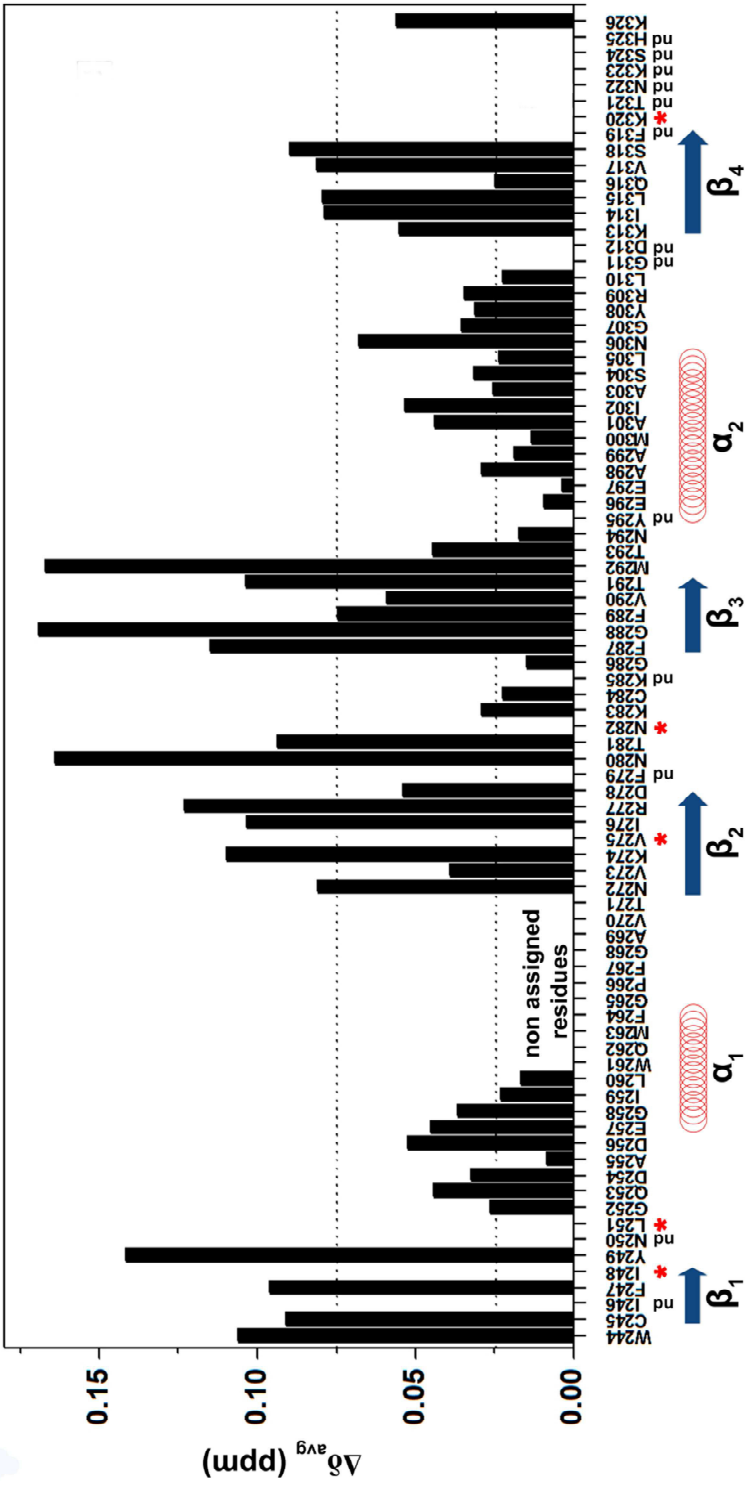

Figure 3.13: RNA binding of HuR RRM3 with the 5´-UUUUU-3´ oligonucleotide. Average chemical-shift differences ($\Delta\delta_{avg}$) between free and RNA-bound HuR RRM3 in a ratio of 4:1. Secondary structure elements of RRM3 are symbolized by blue arrows for β strands and red coil symbols for α-helices. Asterisk symbols (*) stand for residues broadened beyond the detection upon RNA binding.

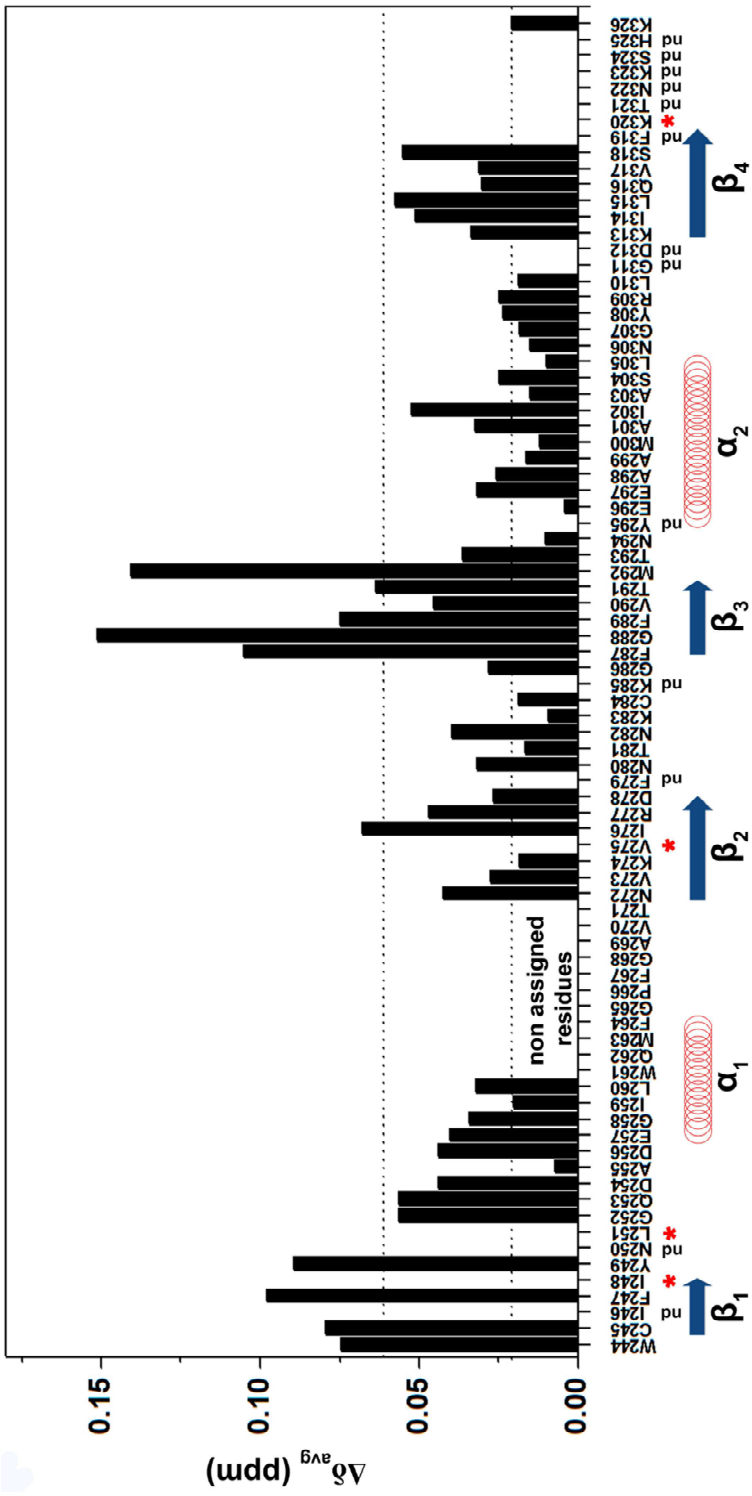

Figure 3.14: RNA binding of HuR RRM3 with the 5´-AUUUA-3´ oligonucleotide. Average chemical-shift differences ($\Delta\delta_{avg}$) between free and RNA-bound HuR RRM3 in a ratio of 4:1. Secondary structure elements of RRM3 are symbolized by blue arrows for β strands and red coil symbols for α-helices. Asterisk symbols (*) stand for residues broadened beyond the detection upon RNA binding.

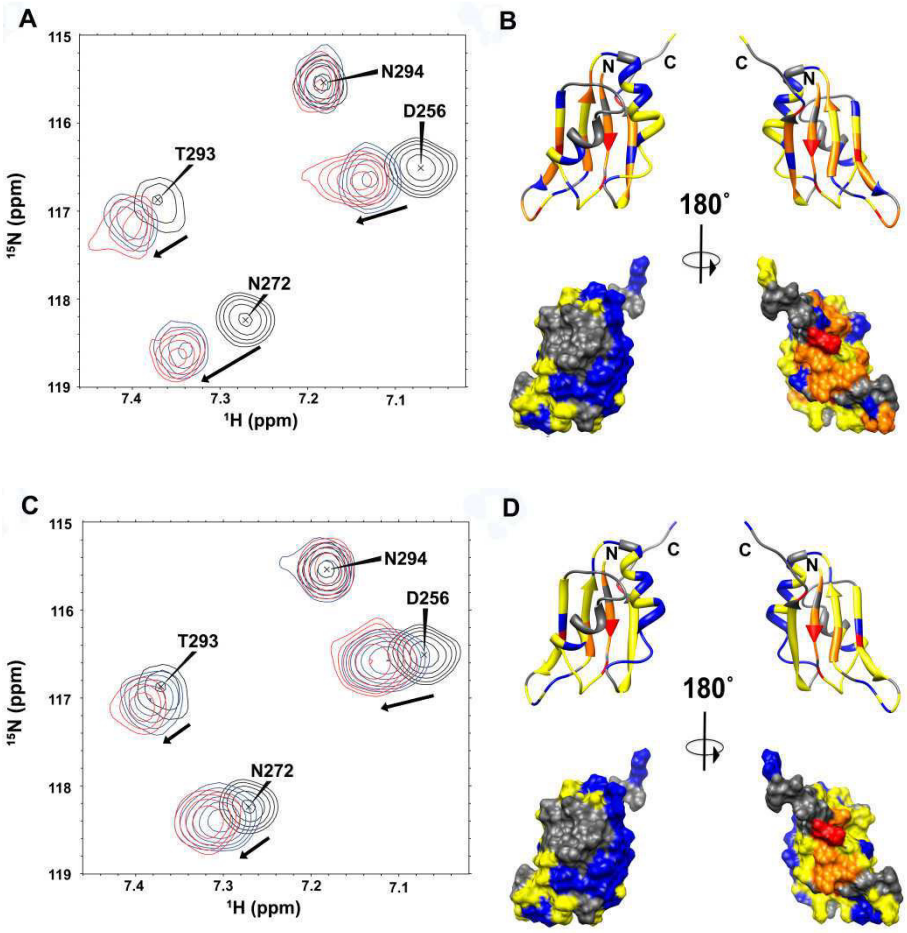

Figure 3.15: RNA binding of HuR RRM3 with the 5´-UUUUU-3´ (A,B) and 5´-AUUUA-3´ (C,D) oligonucleotides. **(A,C)** Superposition of ^{15}N-HSQC spectra of HuR RRM3 WT of free (black) and bound to RNA oligos in an RNA:RRM3 ratio of 2:1 (blue) and 4:1 (red). A subset of four representative resonances is labeled in black. **(B,D)** Map of HuR RRM3 interface upon binding to RNA. RRM3 surface is rotated 180˚ around the vertical axis in each view. Residues are colored, according to $\Delta\delta_{avg}$ (ppm): blue for values < 0.025, yellow for 0.025 ≤ $\Delta\delta_{avg}$ ≤ 0.075 and orange for values > 0.075. Resonances broadened beyond the detection limit are colored in red. Prolines and unassigned resonances are indicated in gray.

3.7 The Phosphomimetic HuR RRM3 S318D Mutant

Phosphorylation at Ser318 residue of HuR RRM3 domain was mimicked by Ser-to-Asp single mutation, which had negligible effects on both the secondary structure (Figure 3.16 A and Table 3.4) and the chemical stability (Figure 3.16 B) of the protein, as inferred from far-UV CD and fluorescence measurements, respectively.

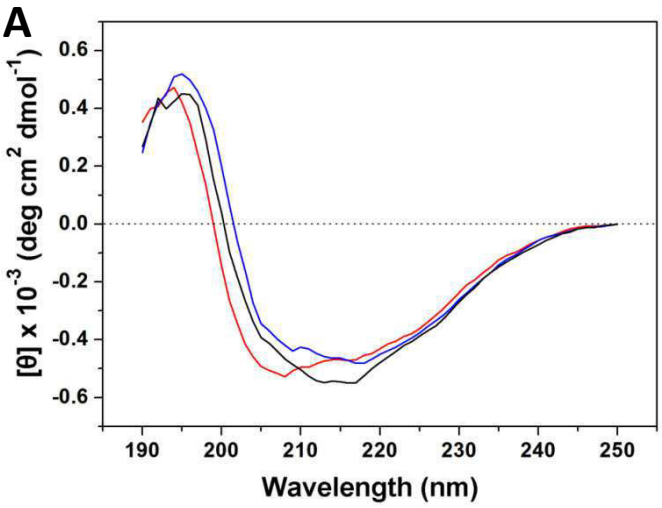

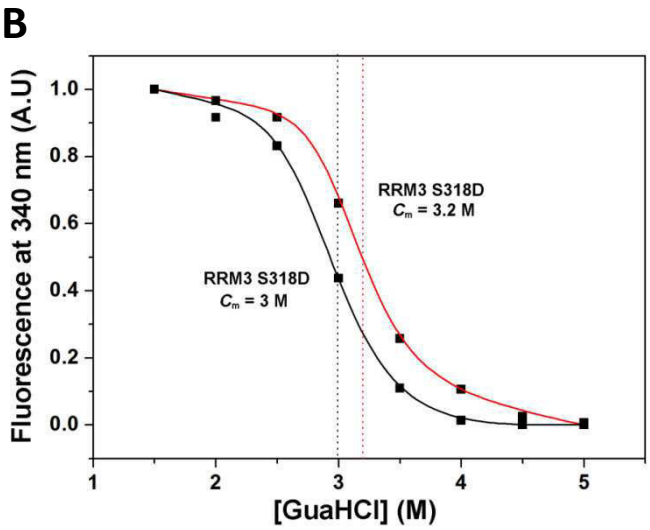

Figure 3.16:
HuR RRM3 S318D: A phosphomimetic mutant.
A) Far-UV (190–250 nm) CD spectra of HuR RRM3 domain constructs. RRM3 WT is presented in blue, RRM3 S318A in red and RRM3 S318D in black.

B) Chemical denaturation with guanidine hydrochloride (GuaHCl) of RRM3 WT (blue) and RRM3 S318D (black). Fitted unfolding curves are presented as solid lines, superimposed on experimental data in squares. The midpoint GuaHCl concentrations (C_m) of the transitions are marked by dashed lines.

HuR RRM3 S318D binding to RNA targets was monitored by NMR in solution (Figure 3.17). Data suggests that the phosphomimetic mutant binds to the 5´-UUUUU-3´ RNA oligonucleotides with slightly less affinity than RRM3 WT (Figure 3.18) opposite to previous reports on AU-bearing mRNA stretches (Doller *et al.*, 2010). Thus, it is likely that the addition of a negatively charged group by site-directed mutagenesis results in electrostatic repulsion with respect to phosphate groups from RNA.

Table 3.4: Percentage of secondary structure for HuR RRM3 WT and mutant species.

Constructs	α-helix (%)	β-strand (%)	Turn (%)	Unstructured (%)*
RRM3 WT	13.18 ± 1.47	31.49 ± 3.22	21.79 ± 1.79	32.04 ± 3.47
RRM3 S318A	12.68 ± 0.58	36.09 ± 0.70	20.74 ± 0.84	29.80 ± 1.71
RRM3 S318D	16.65 ± 0.66	33.73 ± 0.90	20.26 ± 0.86	29.93 ± 2.57

* This section refers to both disordered and flexible and ordered but nonregular structured parts of the protein.

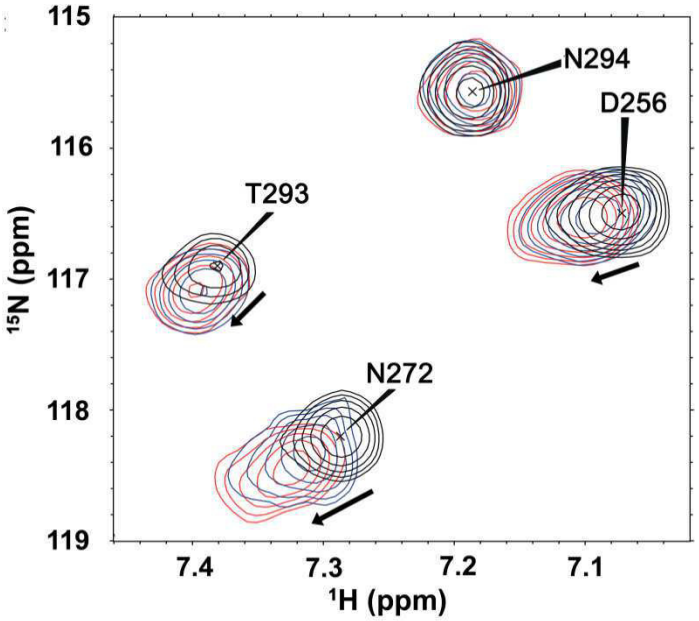

Figure 3.17: HuR RRM3 S318D: A phosphomimetic mutant. Superposition of ^{15}N HSQC spectra of free HuR RRM3 S318D (black) and bound to 5´-UUUUU-3´ RNA in a RNA:RRM3 ratio of 2:1 (blue) and 4:1 (red). A subset of four representative resonances is labeled in black.

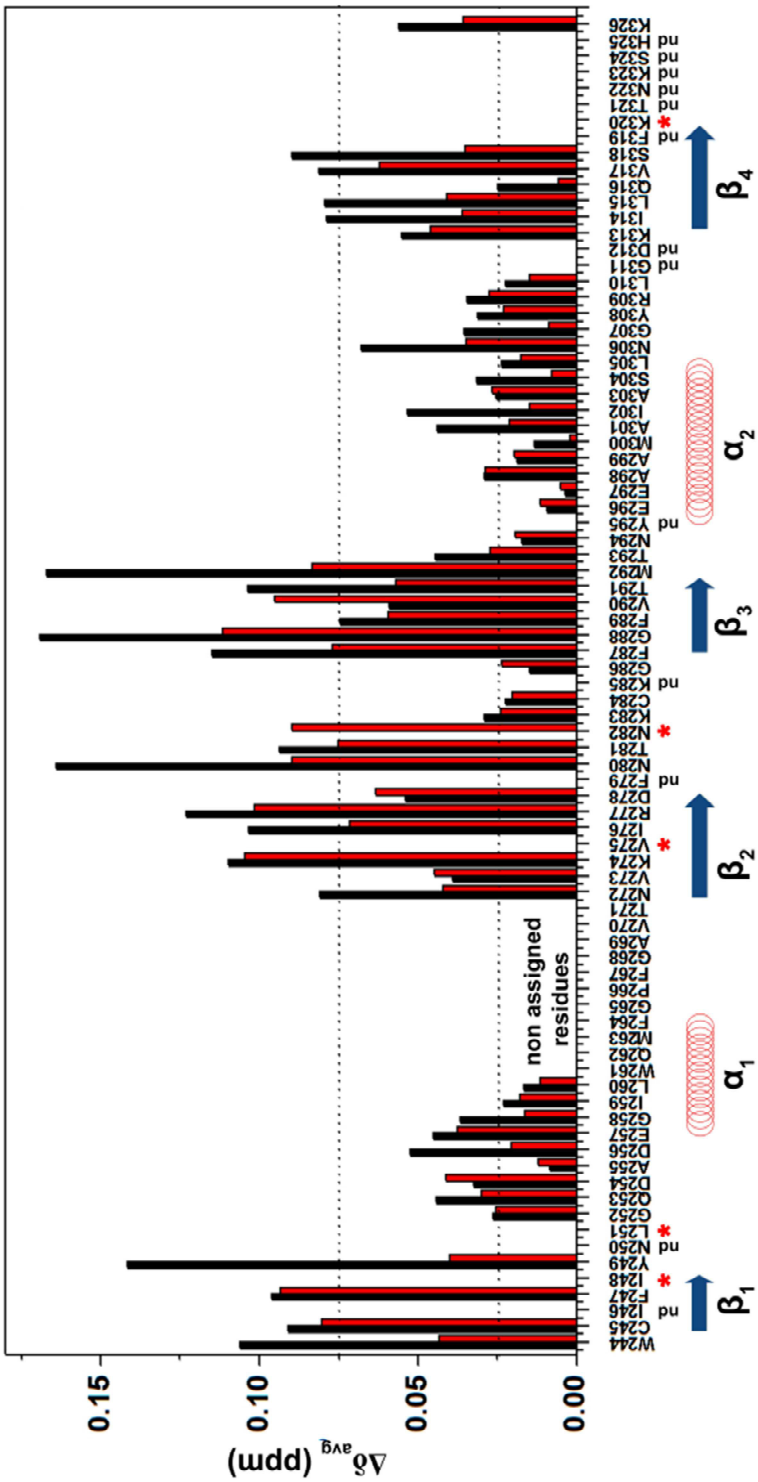

Figure 3.18: Comparison of average chemical-shift differences ($\Delta\delta_{avg}$) between free and RNA-bound HuR RRM3 WT (black) and HuR RRM3 S318D (red) in a ratio of 4:1 for 5´-UUUUU-3´ RNA oligo. Secondary structure elements of RRM3 are symbolized by blue arrows for β-strands and red coil symbols for α-helices. Asterisk symbols (*) stand for residues broadened beyond the detection upon RNA binding for the RRM3 S318D mutant.

Discussion

Discussion

4.1 HuR Modular Assembly

HuR consists of three RRM domains, whose function in RNA binding is well-characterized *in vivo*, despite the global function and working mechanisms of HuR FL protein are still not fully understood.

The most N-terminal RRM1 and RRM2 motifs – only separated by a 3_{10} helix – work as a compact structural unit. This cooperative assembly remains unchanged upon phosphorylation of three Ser residues localized inside RRM motifs and at the interdomain linker (see also sections 4.3 and 4.4, Phosphorylation of HuR).

The C-terminal RRM domain (RRM3) of HuR is separated from RRM12 by a hinge region that includes a sixty residue sequence, called HNS. This linker has a transport function shuttling the protein from the nucleus to the cytoplasm and *vice versa* and also has a cleavage site between the RRM12 and RRM3 domains. The cleavage takes place under apoptotic conditions at residue Asp226 (Mazroui *et al.*, 2008). We demonstrate that RRM3 tumbles *in vitro* independently of RRM12 in conditions and no interaction of the domains can be detected. Combining this result with the cleavage mechanism of the protein, it seems probable that RRM3 could be evolve to play apoptotic functions, although HuR has been traditionally identified as an anti-apoptotic protein. The cleavage could be a trigger to let RRM3 act in different or additional functions than in context with the FL protein. A future working perspective would be to find out whether there are distinct working mechanisms of isolated RRM3 and the domain in context with the HuR FL. Therefore, during evolution, RRM3 could have been adapted to have an apoptotic function, whereas RRM12 is specialized in the mainly anti-apoptotic working mechanism of HuR.

4.2 RRM12 Works as a Unique Functional Unit

Thermal stability studies of HuR species indicate the importance of the cooperation between the two N-terminal RRM domains of HuR, which work as a functional unit. The comparison of T_m values for isolated RRM1 or RRM2 and the two-domain construct RRM12 reveals that RRM12 shows the same thermal stability as RRM1, while RRM2 is substantially more stable. In addition, the fact that the denaturation curve of HuR RRM12 is not the sum of those from the two individual RRM1 and RRM2 domains suggests cooperativity between both modules.

It is tempting to speculate that the RRM12 modular interaction is essential for RNA recognition activity, similarly to what was previously observed for RRM1–RRM2 motifs of the homologous HuD protein upon *c*-fos RNA binding (Wang and Tanaka Hall, 2001). Indeed, the preferred orientation between RNA binding domains helps to establish a high-affinity RNA-binding platform (Vitali *et al.*, 2006; Li *et al.*, 2010) and/or to stabilize a suitable conformation that can adapt to the changes in the direction of the RNA chain inside the highly structured 3´ UTRs, as previously suggested (Díaz-Moreno *et al,.* 2010).

Altogether, the results indicate that HuR RRM12 works as a functional unit, independently of RRM3.

4.3 Phosphorylation of HuR RRM12

To study changes in structure and stability of HuR induced by serine phosphorylation, we designed three Ser-by-Asp mutations. Two of them are localized at the RRM cores, while the third one is in the interdomain linker between RRM1 and RRM2. No significant changes in secondary structure were observed for any of these phosphomimetic mutants, unlike what has been recently published for other RNA binding domains (Díaz-Moreno *et al.*, 2009). Therefore, phosphorylation effects on HuR seem to be essentially related to RNA binding properties and/or intermolecular protein interactions rather than to changes of the HuR structure, as confirmed by our CD RNA binding titrations. CD experiments in the far-UV range

confirmed that the secondary structure is not changed significantly by phosphorylation.

4.3.1 Phosphorylation of HuR RRM12 and Thermal Stability

The thermal stability of HuR constructs is regulated by phosphorylation. The phosphomimetic mutant S88D slightly stabilizes RRM1 in the RRM12 context, which can be explained by the addition of a negative charge to the protein loop mainly governed by two positively charged residues (Benoit *et al.*, 2010). Thus, Asp88 could minimize the electrostatic repulsion between Arg85 and Lys89, which would restrict the loop mobility.

Phosphorylation at the level of the RRM12 linker region at Ser100 residue also has a negligible effect on HuR stability. A plausible explanation is that this solvent-exposed residue does not make many contacts with neighbors. Intriguingly, phosphorylation at Ser100 increases RNA binding *in vivo* (Abdelmohsen *et al.,* 2007b), although the equivalent serine in the homologous HuD Ser126 is facing away from the RNA in the HuD/*c*-fos mRNA crystal structure (Wang and Tanaka Hall, 2001).

Slightly destabilizing phosphorylation of Ser158 could be explained based on electrostatic repulsion with another nearby negative residue Glu162, although the negatively charged Asp158 is added at the N-end of α-helix 2 of HuR RRM2.

4.3.2 Phosphorylation of HuR RRM12 and RNA Binding

In terms of RNA binding, it has been previously reported that *in vivo* HuR phosphorylation at Ser88 increases the docking of RNA targets to the RNA binding sites (Abdelmohsen *et al.*, 2007b). Also it is proposed that the phosphoserine at position 88 exhibits a Mg^{2+}-ion-mediated interaction with a phosphate group from RNA (Benoit *et al.*, 2010).

In this thesis, no substantial differences in binding affinities were observed between RRM12 WT and the phosphomimetic RRM12 S88D mutant by performing *in vitro* CD titrations using *c*-fos RNA.

Posttranslational modification of Ser158 at RRM2 domain mimicked by the RRM12 S158D mutation tightly regulates the binding of HuR RRM12 with *c*-fos RNA *in vitro*. Actually, the RNA binding affinity of RRM12 S158D is four times larger than that of RRM12 WT, in agreement with previous data *in vivo* (Doller *et al,.* 2007).

Additionally, *in vitro* CD RNA-RRM12 titrations reveal no effect of the S100D mutation on RNA recognition with respect to RRM12 WT. Therefore, phosphorylation at this site would influence RRM2– interdomain linker interactions and the rearrangement between RRM domains, rather than directly repulsing RNA (Benoit *et al.,* 2010).

Perturbations in HuR stability upon posttranslational modifications such as phosphorylation may explain the HuR behavior in binding RNA molecules, as well as in determining their lifetime and translation rate.

4.4 HuR RRM3

To shed light on the most C-terminal HuR RRM3 domain, which has been the HuR unknown module up to date from the structural point of view, a novel expression and purification protocol to improve its solubility has been developed.

HuR RRM3 is the domain of HuR that is of special interest due to its differences to the N-terminal RRM domains RRM1 and RRM2. This domain is separated from the N-terminal RRM1 and RRM2 by a sixty residue linker that is cleaved at residue Asp226 to separate the protein under apoptotic conditions (Mazroui *et al.*, 2008). The biophysical properties of the RRM3 are distinct to the N-terminal ones, resulting in low aquaeous solubility.

This thesis reports how HuR RRM3 domain tumbles independently in solution with respect to the RRM12 tandem. This might make the HNS linker accessible — in particular its Ser226 — for caspase-dependent cleavage, as previously reported by Mazroui *et al.*, 2008. Thus, the finding that RRM3 behaves as an autonomous working module within HuR FL can provide the protein with additional functions like adenosyl transferase activity (Meisner *et al.*, 2009) and HuR-protein molecular recognition processes, as was shown for the homolog *Drosophila* protein (Toba and

White, 2008) that enables more alternatives for HuR in RNA binding and processing. In addition, the RRM3-containing cleavage product acquires new functions in triggering apoptosis because it selectively binds to and stabilizes caspase-9 mRNA in an ARE-dependent manner (von Roretz *et al.*, 2012). This agrees with our NMR titrations that demonstrate a binding of cleaved RRM3 to AREs, although previous studies suggested that the HuR RRM3 role — as part of HuR FL — in binding to single-stranded ARE-bearing mRNAs was negligible (Chung *et al.*, 1996; Yeap *et al.*, 2002, Fialcowitz-White *et al.*, 2007, Barker *et al.*, 2012). Actually, HuR RRM3 associates with the poly(A) tails of mRNAs (Ma *et al.*, 1997; Anderson *et al.*, 2000), which is crucial for effective mRNA stabilization by HuR (Fan and Steitz, 1998b).

4.4.1 Multimerization of HuR RRM3

On an intermediate NMR time scale, isolated RRM3 is in a monomer/multimer exchange that makes the resonances belonging to the Trp261-Thr271 stretch at the C-end of helix α_1 non-detectable. Thus, we suggest that RRM3 dimerization involves its α_1-helix placed at the surface opposite to the RNA-binding platform, as previously proposed for homologous proteins such as ELAV in *Drosophila* upon mutating Trp419 (Trp261 in HuR; Toba and White, 2008).

Toba and colleagues reported that multimerization of the homolog ELAV protein from *Drosophila* is dependent on RRM3 and the linker part (Toba and White, 2008). In this work it could be demonstrated that also the isolated domain of the human homolog HuR is able to form such multimers. This is especially interesting due to the cleavage of RRM3 and that it appears isolated within the cell under apoptotic conditions (Mazroui *et al.*, 2008). It could be the case that, despite multimerization, the protein transports distinct Uracile-rich RNA targets and accumulates them by multimerization in form of stress granules (Gallouzi *et al.*, 2000). Furthermore we can speculate that HuR RRM3 may be involved in degradation pathways, as it is already reported that certain RBPs, such as KSRP or AUF1, interact with the exosome (Chen *et al.*, 2001).

Our AU- and MALDI analysis confirm the oligomerization of RRM3, and that RRM3 W261E mutant shifts the monomer/dimer equilibrium towards the monomeric RRM3 form. Therefore, RRM-RRM interactions

often take place through their α-helices. For instance, RRM3 and RRM4 from Polypyrimidine Tract Binding protein (PTB) mainly contact through helix α_2 of RRM4 and helix α_1 and α_2 of RRM3, resulting in the perpendicular positioning of both RRM (Oberstrass *et al.*, 2005). On the other hand, in FBP-Interacting Repressor (FIR) protein, the α-helix face of RRM1 packs onto the β-sheet face of RRM2, creating a stable interface (Crichlow *et al.*, 2008; Cukier *et al.*, 2010). Interestingly enough is the crystallographic structure of HuR RRM1 motif, which reveals a homodimer assembled through helices α_1 and α_2 (Benoit *et al.*, 2010).

Multimerization of Hu protein family is then dependent on RRM3 motif and more especially on its well-conserved Trp261 (Toba and White, 2008). In fact, the whole Trp261-Thr271 stretch is highly conserved among Hu proteins. Our structural studies on HuR RRM3 also demonstrate that the monomer/dimer exchange of HuR RRM3 takes place even in absence of RNA, in contrast to previous reports suggesting that RNA promotes HuR FL multimerization (David *et al.*, 2007; Fialcowitz-White *et al.*, 2007). Importantly, no additional resonances corresponding to the Trp261-Thr271 gap appear on the ^{15}N-HSQC NMR spectra upon binding to short single-stranded 5-mer RNA oligonucleotides, from which it follows that the oligomerization exchange remains unaltered. The fact that HuR FL forms stable oligomeric complexes in presence of long RNA fragments suggests that additional experiments are necessary to explain how far the oligomerization of isolated RRM3 would change by long and highly-structured ARE-bearing RNAs. On the other hand, the multimerization of HuR could be prevented by the W216E mutation, as already showed for the homolog *Drosophila* protein (Toba and White, 2008). For this mutant, the AU experiments demonstrate a unique monomeric protein population, also independent of RNA interactions. For future investigation, it would be of interest what consequences this mutation has at the cellular level.

4.4.2 RNA Binding of HuR RRM3

RRM-comprising RBPs are usually known to bind single-stranded nucleic acids by stacking with aromatic residues placed at the central β-strands (β_1 and β_3) of the β-sheet, although a high variety of RNA binding mechanisms have been described for RRM modules (for a review, see Clery

et al., 2008). By NMR experiments we confirm the RNA binding to these secondary structure elements of RRM3 for both 5´-AUUUA-3´ and 5´-UUUUU-3´ oligonucleotides. In addition, we found out that the HuR RRM3 protein platform to interact with 5´-UUUUU-3´ RNA is extended and involves the whole β-sheet. This agrees with a preferential binding of RRM3 to pyrimidine bases rather than to purine derivates, based on chemical-shift perturbations data.

Preferences by 5-mer U-rich elements over AU-rich motifs were already observed for the heterogeneous nuclear RiboNucleoprotein C protein (hnRNP1; Sokolowski *et al.*, 2001) and HuR FL (Sokolowski *et al.*, 1999; López de Silanes *et al.*, 2004). More recently, it has been also demonstrated that HuR FL recognizes mRNAs containing U-richness and single-strandedness, where a substitution of U by A or C has a moderate effect on HuR binding affinity, whereas an exchange by G has a drastic effect (Barker *et al.*, 2012). The interruption of U-rich sequences with Cs to result UC-rich motifs is also recognized by HuR FL, although its RRM3 module does not bind this RNA probe at all (Yeap *et al.*, 2002). Meriting particular interest, the RRM3-containing cleavage product specifically binds ARE1 of caspase-9 mRNA, which lacks of 5´-AUUUA-3´ sequences but contains a U-rich region (von Roretz *et al.*, 2012). Thus, ARE1 of caspase-9 mRNA is classified as a Class III ARE, according to the categories defined by Chen and coworkers (Chen *et al.*, 1995).

Ongoing experiments would be necessary to find out which sequence specificity and number of nucleotides are preferred for distinct RRM domains not only from HuR protein but also from other RBPs. This observation is a small contribution to the complex field of the interaction between proteins and RNA inside the cell, where we have a sum of many more factors, as competition with other RBPs by RNA sequences and cellular conditions. Indeed, the complex network of elements acting in cis- and trans-factors within the cell makes it difficult to predict those exact working mechanisms for controlling mRNA fate.

4.4.3 Phosphorylation of HuR RRM3

The RBPs which act as *trans*-factors are often upper-regulated by posttranslational modifications, such as

phosphorylation. In HuR, phosphorylation at RRM3 Ser318 residue implies an important mode in its regulation, with consequences in colon carcinoma cells due to HuR dysregulation (Doller *et al.*, 2011). The Ser318 residue of HuR RRM3, which is phosphorylated by PKCδ (Doller *et al.*, 2008a), was mutated by an aspartate to mimic phosphorylation events.

Both RRM3 WT and RRM3 S318D models agree on the secondary structure and the chemical stability. The major difference was found at the level of RNA recognition, since RRM3 S318D binds U-rich stretches with an apparent lower affinity than RRM3 WT, although RNA docks on both RRM3 species using similar platforms. This result can be explained by an electrostatic repulsion effect between Asp318 and the negatively charged RNA (Barker *et al.*, 2012). Indeed, the backbone amide of Asp318 is physically in contact with RNA, as inferred from chemical-shift data.

In contrast to our findings, Doller and coworkers (Doller *et al.*, 2010) reported a higher binding affinity of phosphorylated HuR FL with AU-bearing mRNA stretches (Doller *et al.*, 2010). Plausible explanations arise from: i) differences in length, degree of structure and sequence of AU-containing long mRNAs and 5´-UUUUU-3´ short RNA molecules; ii) differences in number of RRMs making up HuR FL and RRM3 S318D species; iii) differences on how Ser318 residue is modified by PKCδ-dependent phosphorylation of HuR FL or by Ser318-by-Asp318 substitution on isolated HuR RRM3.

Our study underlines the exceptional properties of HuR RRM3 as a multi-functional domain which may lead to HuR oligomerization and binding to U-rich RNA targets at once, using two opposite RRM surfaces.

Conclusions

Conclusions

1. The three RNA Recognitionn Motifs (RRM) of the HuR protein are arranged in two different functional complexes, namely the the N-terminal di-domain RRM12 and the C-terminal domain RRM3. In the absence of RNA, RRM12 and RRM3 tumble independently from each other.

2. When forming the RRM12 di-domain, the thermal stability of RRM1 is not affected but RRM2 is significantly destabilized. This finding suggests that RRM12 forms a tandem unit.

3. Phosphorylation-mimicking mutations have negligible effects on the secondary structure of the HuR RRM domains.

4. Phosphorylation-mimicking mutations of the RRM12 construct have diverse effects on the thermal stability of the protein, depending on the position of the mutated serine. The RRM12 di-domain is slightly destabilized by the S88D mutation in RRM1, significantly destabilized by the S158D mutation in RRM3 and is not affected by the S100D mutation in the linker between RRM1 and RRM2.

5. The binding affinity of the RRM12 S158D phosphorylation-mimicking mutant to the *c*-fos mRNA oligomer 5´-AUUUUAUUUUA-3´ is 4–fold higher than that of RRM12 WT. On the other hand, no differences in the RNA affinities of the RRM12 S88D and S100D species with respect to the WT are observed.

6. A successful detergent-based strategy to get the HuR RRM3 solubilized has been developed for the first time.

7. An NMR restraint-based model of HuR RRM3 has been created using the CS23D server. The model reveals the canonical $\beta_1\alpha_1\beta_2\beta_3\alpha_2\beta_4$ topology of HuR RRM3.

8. A conserved binding surface patch on the β–sheet of HuR RRM3 interacts with both 5´-mer AU-rich and U-rich RNA stretches. Interestingly, the domain seems to bind to 5´-UUUUU-3´ RNA with higher affinity than to 5´-AUUUA-3´ oligonucleotides. Binding to the U-rich stretches involves the whole β–sheet, whereas the interaction of RRM3 with AU-rich oligonucleotides is restricted to β_1 and β_3 strands.

9. Posttranslational modification of HuR RRM3 by phosphorylation has negligible effects on both, the structure and stability, of the protein. However, the RRM3 S318D phosphomimetic mutant binds to the 5´-mer RNA oligomer 5´-UUUUU-3´ with less affinity than the WT protein.

10. HuR RRM3 WT is in a monomer/dimer equilibrium even in absence of RNA. The dimerization epitope spans the residues from Trp261 to Thr271, which are located on the surface of α_1-helix and its C-terminal nearby loop at the opposite site of the RNA binding platform.

References

References

Abdelmohsen K, Lal A, Kim HH, Gorospe M (2007a) Posttranscriptional orchestration of an anti-apoptotic program by HuR. Cell Cycle 6:1288-1292

Abdelmohsen K, Pullmann R, Jr., Lal A, Kim HH, Galban S, Yang X, Blethrow JD, Walker M, Shubert J, Gillespie DA, Furneaux H, Gorospe M (2007b) Phosphorylation of HuR by Chk2 regulates SIRT1 expression. Mol Cell 25:543-557

Abdelmohsen K, Srikantan S, Kuwano Y, Gorospe M (2008) miR-519 reduces cell proliferation by lowering RNA-binding protein HuR levels. Proc Natl Acad Sci U S A 105:20297-20302

Abdelmohsen K, Srikantan S, Yang X, Lal A, Kim HH, Kuwano Y, Galban S, Becker KG, Kamara D, de Cabo R, Gorospe M (2009) Ubiquitin-mediated proteolysis of HuR by heat shock. Embo J 28:1271-1282

Abdelmohsen K, Kim MM, Srikantan S, Mercken EM, Brennan SE, Wilson GM, Cabo R, Gorospe M (2010) miR-519 suppresses tumor growth by reducing HuR levels. Cell Cycle 9:1354-1359

Adam SA, Nakagawa T, Swanson MS, Woodruff TK, Dreyfuss G (1986) mRNA polyadenylate-binding protein: gene isolation and sequencing and identification of a ribonucleoprotein consensus sequence. Mol Cell Biol 6:2932-2943

Al-Ahmadi W, Al-Ghamdi M, Al-Haj L, Al-Saif M, Khabar KS (2009) Alternative polyadenylation variants of the RNA binding protein, HuR: abundance, role of AU-rich elements and auto-Regulation. Nucleic Acids Res 37:3612-3624

Allain FH, Bouvet P, Dieckmann T, Feigon J (2000) Molecular basis of sequence-specific recognition of pre-ribosomal RNA by nucleolin. Embo J 19:6870-6881

Anderson KD, Morin MA, Beckel-Mitchener A, Mobarak CD, Neve RL, Furneaux HM, Burry R, Perrone-Bizzozero NI (2000) Overexpression of HuD, but not of its truncated form HuD I+II, promotes GAP-43 gene expression and neurite outgrowth in PC12 cells in the absence of nerve growth factor. J Neurochem 75:1103-1114

Arnold K, Bordoli L, Kopp J, Schwede T (2006) The SWISS-MODEL workspace: a web-based environment for protein structure homology modelling. Bioinformatics 22:195-201

Aroca A, Díaz-Quintana A, Díaz-Moreno I (2011) A structural insight into the C-terminal RNA recognition motifs of T-cell intracellular antigen-1 protein. FEBS Lett 585:2958-2964

Ashiya M, Grabowski PJ (1997) A neuron-specific splicing switch mediated by an array of pre-mRNA repressor sites: evidence of a regulatory role for the polypyrimidine tract binding protein and a brain-specific PTB counterpart. Rna 3:996-1015

Atasoy U, Watson J, Patel D, Keene JD (1998) ELAV protein HuA (HuR) can redistribute between nucleus and cytoplasm and is upregulated during serum stimulation and T cell activation. J Cell Sci 111 (Pt 21):3145-3156

Atasoy U, Curry SL, Lopez de Silanes I, Shyu AB, Casolaro V, Gorospe M, Stellato C (2003) Regulation of eotaxin gene expression by TNF-alpha and IL-4 through mRNA stabilization: involvement of the RNA-binding protein HuR. J Immunol 171:4369-4378

Backe PH, Messias AC, Ravelli RB, Sattler M, Cusack S (2005) X-ray crystallographic and NMR studies of the third KH domain of hnRNP K in complex with single-stranded nucleic acids. Structure 13:1055-1067

Badis G, Saveanu C, Fromont-Racine M, Jacquier A (2004) Targeted mRNA degradation by deadenylation-independent decapping. Mol Cell 15:5-15

Bagga PS, Arhin GK, Wilusz J (1998) DSEF-1 is a member of the hnRNP H family of RNA-binding proteins and stimulates pre-mRNA cleavage and polyadenylation in vitro. Nucleic Acids Res 26:5343-5350

Bakheet T, Frevel M, Williams BR, Greer W, Khabar KS (2001) ARED: human AU-rich element-containing mRNA database reveals an unexpectedly diverse functional repertoire of encoded proteins. Nucleic Acids Res 29:246-254

Bakheet T, Williams BR, Khabar KS (2003) ARED 2.0: an update of AU-rich element mRNA database. Nucleic Acids Res 31:421-423

Barker A, Epis MR, Porter CJ, Hopkins BR, Wilce MC, Wilce JA, Giles KM, Leedman PJ (2012) Sequence requirements for RNA binding by HuR and AUF1. J Biochem 151:423-437

Barreau C, Paillard L, Osborne HB (2005) AU-rich elements and associated factors: are there unifying principles? Nucleic Acids Res 33:7138-7150

Bartel DP (2004) MicroRNAs: genomics, biogenesis, mechanism, and function. Cell 116:281-297

Bhattacharyya SN, Habermacher R, Martine U, Closs EI, Filipowicz W (2006) Relief of microRNA-mediated translational repression in human cells subjected to stress. Cell 125:1111-1124

Beelman CA, Stevens A, Caponigro G, LaGrandeur TE, Hatfield L, Fortner DM, Parker R (1996) An essential component of the decapping enzyme required for normal rates of mRNA turnover. Nature 382:642-646

Bellavia D, Mecarozzi M, Campese AF, Grazioli P, Talora C, Frati L, Gulino A, Screpanti I (2007) Notch3 and the Notch3-upregulated RNA-binding protein HuD regulate Ikaros alternative splicing. Embo J 26:1670-1680

Benoit RM, Meisner NC, Kallen J, Graff P, Hemmig R, Cebe R, Ostermeier C, Widmer H, Auer M (2010) The x-ray crystal structure of the first RNA recognition motif and site-directed mutagenesis suggest a possible HuR redox sensing mechanism. J Mol Biol 397:1231-1244

Beuth B, Pennell S, Arnvig KB, Martin SR, Taylor IA (2005) Structure of a Mycobacterium tuberculosis NusA-RNA complex. Embo J 24:3576-3587

Birney E, Kumar S, Krainer AR (1993) Analysis of the RNA-recognition motif and RS and RGG domains: conservation in metazoan pre-mRNA splicing factors. Nucleic Acids Res 21:5803-5816

Bleichert F, Baserga SJ (2007) The long unwinding road of RNA helicases. Mol Cell 27:339-352

Bolognani F, Tanner DC, Merhege M, Deschenes-Furry J, Jasmin B, Perrone-Bizzozero NI (2006) In vivo post-transcriptional regulation of GAP-43 mRNA by overexpression of the RNA-binding protein HuD. J Neurochem 96:790-801

Bouvet P, Diaz JJ, Kindbeiter K, Madjar JJ, Amalric F (1998) Nucleolin interacts with several ribosomal proteins through its RGG domain. J Biol Chem 273:19025-19029

Braddock DT, Baber JL, Levens D, Clore GM (2002a) Molecular basis of sequence-specific single-stranded DNA recognition by KH domains: solution structure of a complex between hnRNP K KH3 and single-stranded DNA. Embo J 21:3476-3485

Braddock DT, Louis JM, Baber JL, Levens D, Clore GM (2002b) Structure and dynamics of KH domains from FBP bound to single-stranded DNA. Nature 415:1051-1056

Brennan CM, Gallouzi IE, Steitz JA (2000) Protein ligands to HuR modulate its interaction with target mRNAs in vivo. J Cell Biol 151:1-14

Brennan CM, Steitz JA (2001) HuR and mRNA stability. Cell Mol Life Sci 58:266-277

Brown CE, Tarun SZ, Jr., Boeck R, Sachs AB (1996) PAN3 encodes a subunit of the Pab1p-dependent poly(A) nuclease in Saccharomyces cerevisiae. Mol Cell Biol 16:5744-5753

Bushati N, Cohen SM (2007) MicroRNA functions. Annu Rev Cell Dev Biol 23:175-205

Caceres JF, Stamm S, Helfman DM, Krainer AR (1994) Regulation of alternative splicing in vivo by overexpression of antagonistic splicing factors. Science 265:1706-9

Calnan B, Tidor B, Biancalana S, Hudson D, Frankel A (1991) Arginine-mediated RNA recognition: the arginine fork. Science 252:1167-1171

Carballo E, Lai WS, Blackshear PJ (1998) Feedback inhibition of macrophage tumor necrosis factor-alpha production by tristetraprolin. Science 281:1001-1005

Carson JH, Cui H, Barbarese E (2001) The balance of power in RNA trafficking. Curr Opin Neurobiol 11:558-563

Chabot B, Blanchette M, Lapierre I, La Branche H (1997) An intron element modulating 5' splice site selection in the hnRNP A1 pre-mRNA interacts with hnRNP A1. Mol Cell Biol 17:1776-1786

Chan RC, Black DL (1997) The polypyrimidine tract binding protein binds upstream of neural cell-specific c-src exon N1 to repress the splicing of the intron downstream. Mol Cell Biol 17:4667-4676

Chang TC, Yamashita A, Chen CY, Yamashita Y, Zhu W, Durdan S, Kahvejian A, Sonenberg N, Shyu AB (2004) UNR, a new partner of poly(A)-binding protein, plays a key role in translationally coupled mRNA turnover mediated by the c-fos major coding-region determinant. Genes Dev 18:2010-2023

Chen CD, Kobayashi R, Helfman DM (1999) Binding of hnRNP H to an exonic splicing silencer is involved in the regulation of alternative splicing of the rat beta-tropomyosin gene. Genes Dev 13:593-606

Chen CY, Gherzi R, Ong SE, Chan EL, Raijmakers R, Pruijn GJ, Stoecklin G, Moroni C, Mann M, Karin M (2001) AU binding proteins recruit the exosome to degrade ARE-containing mRNAs. Cell 107:451-464

Chen CY, Shyu AB (1995) AU-rich elements: characterization and importance in mRNA degradation. Trends Biochem Sci 20:465-470

Chen CY, Xu N, Shyu AB (2002) Highly selective actions of HuR in antagonizing AU-rich element-mediated mRNA destabilization. Mol Cell Biol 22:7268-7278

Cherry J, Karschner V, Jones H, Pekala PH (2006) HuR, an RNA-binding protein, involved in the control of cellular differentiation. In Vivo 20:17-23

Chiba Y, Johnson MA, Lidder P, Vogel JT, van Erp H, Green PJ (2004) AtPARN is an essential poly(A) ribonuclease in Arabidopsis. Gene 328:95-102

Chkheidze AN, Lyakhov DL, Makeyev AV, Morales J, Kong J, Liebhaber SA (1999) Assembly of the alpha-globin mRNA stability complex reflects binary interaction between the pyrimidine-rich 3' untranslated region determinant and poly(C) binding protein alphaCP. Mol Cell Biol 19:4572-4581

Cho SJ, Zhang J, Chen X (2010) RNPC1 modulates the RNA-binding activity of, and cooperates with, HuR to regulate p21 mRNA stability. Nucleic Acids Res 38:2256-2267

Chou MY, Rooke N, Turck CW, Black DL (1999) hnRNP H is a component of a splicing enhancer complex that activates a c-src alternative exon in neuronal cells. Mol Cell Biol 19:69-77

Chung S, Jiang L, Cheng S, Furneaux H (1996) Purification and properties of HuD, a neuronal RNA-binding protein. J Biol Chem 271:11518-11524

Clemens KR, Wolf V, McBryant SJ, Zhang P, Liao X, Wright PE, Gottesfeld JM (1993) Molecular basis for specific recognition of both RNA and DNA by a zinc finger protein. Science 260:530-533

Clery A, Blatter M, Allain FH (2008) RNA recognition motifs: boring? Not quite. Curr Opin Struct Biol 18:290-298

Collier B, Goobar-Larsson L, Sokolowski M, Schwartz S (1998) Translational inhibition in vitro of human papillomavirus type 16 L2 mRNA mediated through interaction with heterogenous ribonucleoprotein K and poly(rC)-binding proteins 1 and 2. J Biol Chem 273:22648-22656

Cote CA, Gautreau D, Denegre JM, Kress TL, Terry NA, Mowry KL (1999) A Xenopus protein related to hnRNP I has a role in cytoplasmic RNA localization. Mol Cell 4:431-437

Crichlow GV, Zhou H, Hsiao HH, Frederick KB, Debrosse M, Yang Y, Folta-Stogniew EJ, Chung HJ, Fan C, De la Cruz EM, Levens D, Lolis E, Braddock D (2008) Dimerization of FIR upon FUSE DNA binding suggests a mechanism of c-myc inhibition. Embo J 27:277-289

Crick F (1970) Central dogma of molecular biology. Nature 227:561-563

Crick FH (1958) On protein synthesis. Symp Soc Exp Biol 12:138-163

Cukier CD, Hollingworth D, Martin SR, Kelly G, Díaz-Moreno I, Ramos A (2010) Molecular basis of FIR-mediated c-myc transcriptional control. Nat Struct Mol Biol 17:1058-1064

Cukier CD, Ramos A (2011) Modular protein-RNA interactions regulating mRNA metabolism: a role for NMR. Eur Biophys J 40:1317-1325

Daubner GM, Clery A, Allain FH (2013) RRM-RNA recognition: NMR or crystallography...and new findings. Curr Opin Struct Biol 23:100-108

David PS, Tanveer R, Port JD (2007) FRET-detectable interactions between the ARE binding proteins, HuR and p37AUF1. Rna 13:1453-1468

Dean JL, Wait R, Mahtani KR, Sully G, Clark AR, Saklatvala J (2001) The 3' untranslated region of tumor necrosis factor alpha mRNA is a target of the mRNA-stabilizing factor HuR. Mol Cell Biol 21:721-730

Deana A, Celesnik H, Belasco JG (2008) The bacterial enzyme RppH triggers messenger RNA degradation by 5' pyrophosphate removal. Nature 451:355-358

De Guzman RN, Wu ZR, Stalling CC, Pappalardo L, Borer PN, Summers MF (1998) Structure of the HIV-1 nucleocapsid protein bound to the SL3 psi-RNA recognition element. Science 279:384-388

Dehlin E, Wormington M, Korner CG, Wahle E (2000) Cap-dependent deadenylation of mRNA. Embo J 19:1079-1086

Del Gatto-Konczak F, Olive M, Gesnel MC, Breathnach R (1999) hnRNP A1 recruited to an exon in vivo can function as an exon splicing silencer. Mol Cell Biol 19:251-260

Dempsey LA, Sun H, Hanakahi LA, Maizels N (1999) G4 DNA binding by LR1 and its subunits, nucleolin and hnRNP D, A role for G-G pairing in immunoglobulin switch recombination. J Biol Chem 274:1066-1071

Díaz-Moreno I, Hollingworth D, Frenkiel TA, Kelly G, Martin S, Howell S, Garcia-Mayoral M, Gherzi R, Briata P, Ramos A (2009) Phosphorylation-mediated unfolding of a KH domain regulates KSRP localization via 14-3-3 binding. Nat Struct Mol Biol 16:238-246

Díaz-Moreno I, Hollingworth D, Kelly G, Martin S, Garcia-Mayoral M, Briata P, Gherzi R, Ramos A (2010) Orientation of the central domains of KSRP and its implications for the interaction with the RNA targets. Nucleic Acids Res 38:5193-5205

Dickson AM, Anderson JR, Barnhart MD, Sokoloski KJ, Oko L, Opyrchal M, Galanis E, Wilusz CJ, Morrison TE, Wilusz J (2012) Dephosphorylation of HuR protein during alphavirus infection is associated with HuR relocalization to the cytoplasm. J Biol Chem 287:36229-36238

Ding J, Hayashi MK, Zhang Y, Manche L, Krainer AR, Xu RM (1999) Crystal structure of the two-RRM domain of hnRNP A1 (UP1) complexed with single-stranded telomeric DNA. Genes Dev 13:1102-1115

Dingwall C, Ernberg I, Gait MJ, Green SM, Heaphy S, Karn J, Lowe AD, Singh M, Skinner MA, Valerio R (1989) Human immunodeficiency virus 1 tat protein binds trans-activation-responsive region (TAR) RNA in vitro. Proc Natl Acad Sci U S A 86:6925-6929

Doller A, Huwiler A, Muller R, Radeke HH, Pfeilschifter J, Eberhardt W (2007) Protein kinase C alpha-dependent phosphorylation of the mRNA-stabilizing factor HuR: implications for posttranscriptional regulation of cyclooxygenase-2. Mol Biol Cell 18:2137-2148

Doller A, Akool el S, Huwiler A, Muller R, Radeke HH, Pfeilschifter J, Eberhardt W (2008a) Posttranslational modification of the AU-rich element binding protein HuR by protein kinase Cdelta elicits angiotensin II-induced stabilization and nuclear export of cyclooxygenase 2 mRNA. Mol Cell Biol 28:2608-2625

Doller A, Pfeilschifter J, Eberhardt W (2008b) Signalling pathways regulating nucleo-cytoplasmic shuttling of the mRNA-binding protein HuR. Cell Signal 20:2165-2173

Doller A, Schlepckow K, Schwalbe H, Pfeilschifter J, Eberhardt W (2010) Tandem phosphorylation of serines 221 and 318 by protein kinase Cdelta coordinates mRNA binding and nucleocytoplasmic shuttling of HuR. Mol Cell Biol 30:1397-1410. Epub 2010 Jan 19.

Doller A, Winkler C, Azrilian I, Schulz S, Hartmann S, Pfeilschifter J, Eberhardt W (2011) High-constitutive HuR phosphorylation at Ser 318 by PKCdelta propagates tumor relevant functions in colon carcinoma cells. Carcinogenesis 32:676-685

Dominguez C, Fisette JF, Chabot B, Allain FH (2010) Structural basis of G-tract recognition and encaging by hnRNP F quasi-RRMs. Nat Struct Mol Biol 17:853-861

Dreyfuss G, Swanson MS, Pinol-Roma S (1988) Heterogeneous nuclear ribonucleoprotein particles and the pathway of mRNA formation. Trends Biochem Sci 13:86-91

Dreyfuss G, Kim VN, Kataoka N (2002) Messenger-RNA-binding proteins and the messages they carry. Nat Rev Mol Cell Biol 3:195-205

D´Souza V, Summers MF (2004) Structural basis for packaging the dimeric genome of Moloney murine leukaemia virus. Nature 431:586-590

Du Q, Melnikova IN, Gardner PD (1998) Differential effects of heterogeneous nuclear ribonucleoprotein K on Sp1- and Sp3-mediated transcriptional activation of a neuronal nicotinic acetylcholine receptor promoter. J Biol Chem 273:19877-19883

Du Z, Lee JK, Tjhen R, Li S, Pan H, Stroud RM, James TL (2005) Crystal structure of the first KH domain of human poly(C)-binding protein-2 in complex with a C-rich strand of human telomeric DNA at 1.7 A. J Biol Chem 280:38823-38830

Elliott D, Ladomery M (2011) 4 The RNA-binding proteins. In: Molecular Biology of RNA, First Edition. New York, NY: Oxford University Press, 65-84. Print.

Embade N, Fernandez-Ramos D, Varela-Rey M, Beraza N, Sini M, Gutierrez de Juan V, Woodhoo A, Martinez-Lopez N, Rodriguez-Iruretagoyena B, Bustamante FJ, de la Hoz AB, Carracedo A, Xirodimas DP, Rodriguez MS, Lu SC, Mato JM, Martinez-Chantar ML (2012) Murine double minute 2 regulates Hu antigen R stability in human liver and colon cancer through NEDDylation. Hepatology 55:1237-1248

Eversole A, Maizels N (2000) In vitro properties of the conserved mammalian protein hnRNP D suggest a role in telomere maintenance. Mol Cell Biol 20:5425-5432

Fan XC, Steitz JA (1998a) HNS, a nuclear-cytoplasmic shuttling sequence in HuR. Proc Natl Acad Sci U S A 95:15293-15298

Fan XC, Steitz JA (1998b) Overexpression of HuR, a nuclear-cytoplasmic shuttling protein, increases the in vivo stability of ARE-containing mRNAs. Embo J 17:3448-3460

Fialcowitz-White EJ, Brewer BY, Ballin JD, Willis CD, Toth EA, Wilson GM (2007) Specific protein domains mediate cooperative assembly of HuR oligomers on AU-rich mRNA-destabilizing sequences. J Biol Chem 282:20948-20959

Figueroa A, Cuadrado A, Fan J, Atasoy U, Muscat GE, Munoz-Canoves P, Gorospe M, Munoz A (2003) Role of HuR in skeletal myogenesis through coordinate regulation of muscle differentiation genes. Mol Cell Biol 23:4991-5004

Filippova N, Yang X, King P, Nabors LB (2012) Phosphoregulation of the RNA-binding Protein Hu Antigen R (HuR) by Cdk5 Affects Centrosome Function. J Biol Chem 287:32277-32287

Finger LD, Johansson C, Rinaldi B, Bouvet P, Feigon J (2004) Contributions of the RNA-binding and linker domains and RNA structure to the specificity and affinity of the nucleolin RBD12/NRE interaction. Biochemistry 43:6937-6947

Fiset S, Chabot B (2001) hnRNP A1 may interact simultaneously with telomeric DNA and the human telomerase RNA in vitro. Nucleic Acids Res 29:2268-2275

Forch P, Valcarcel J (2001) Molecular mechanisms of gene expression regulation by the apoptosis-promoting protein TIA-1. Apoptosis 6:463-468

Frankel AD, Biancalana S, Hudson D (1989) Activity of synthetic peptides from the Tat protein of human immunodeficiency virus type 1. Proc Natl Acad Sci U S A 86:7397-7401

Fu XD (1995) The superfamily of arginine/serine-rich splicing factors. Rna 1:663-680

Gallouzi IE, Brennan CM, Stenberg MG, Swanson MS, Eversole A, Maizels N, Steitz JA (2000) HuR binding to cytoplasmic mRNA is perturbed by heat shock. Proc Natl Acad Sci U S A 97:3073-3078

Gallouzi IE, Steitz JA (2001a) Delineation of mRNA export pathways by the use of cell-permeable peptides. Science 294:1895-1901

Gallouzi IE, Brennan CM, Steitz JA (2001b) Protein ligands mediate the CRM1-dependent export of HuR in response to heat shock. Rna 7:1348-1361

Gao M, Fritz DT, Ford LP, Wilusz J (2000) Interaction between a poly(A)-specific ribonuclease and the 5' cap influences mRNA deadenylation rates in vitro. Mol Cell 5:479-488

Garcia JA, Harrich D, Pearson L, Mitsuyasu R, Gaynor RB (1988) Functional domains required for tat-induced transcriptional activation of the HIV-1 long terminal repeat. Embo J 7:3143-3147

Garneau NL, Wilusz J, Wilusz CJ (2007) The highways and byways of mRNA decay. Nat Rev Mol Cell Biol 8:113-126

Ghosh M, Aguila HL, Michaud J, Ai Y, Wu MT, Hemmes A, Ristimaki A, Guo C, Furneaux H, Hla T (2009) Essential role of the RNA-binding protein HuR in progenitor cell survival in mice. J Clin Invest 119:3530-3543

Glisovic T, Bachorik JL, Yong J, Dreyfuss G (2008) RNA-binding proteins and post-transcriptional gene regulation. FEBS Lett 582:1977-1986

Good PJ (1995) A conserved family of elav-like genes in vertebrates. Proc Natl Acad Sci U S A 92:4557-4561

Gorbalenya AE, Koonin EV (1993) Helicases: amino acid sequence comparisons and structure–function relationships. Curr Opin Struct Biol 3: 419–429

Guttinger S, Muhlhausser P, Koller-Eichhorn R, Brennecke J, Kutay U (2004) Transportin2 functions as importin and mediates nuclear import of HuR. Proc Natl Acad Sci U S A 101:2918-2923

Gruber AR, Fallmann J, Kratochvill F, Kovarik P, Hofacker IL (2011) AREsite: a database for the comprehensive investigation of AU-rich elements. Nucleic Acids Res 39:D66-69

Habelhah H, Shah K, Huang L, Ostareck-Lederer A, Burlingame AL, Shokat KM, Hentze MW, Ronai Z (2001) ERK phosphorylation drives cytoplasmic accumulation of hnRNP-K and inhibition of mRNA translation. Nat Cell Biol 3:325-330

Hammond SM, Bernstein E, Beach D, Hannon GJ (2000) An RNA-directed nuclease mediates post-transcriptional gene silencing in Drosophila cells. Nature 404:293-296

Handa N, Nureki O, Kurimoto K, Kim I, Sakamoto H, Shimura Y, Muto Y, Yokoyama S (1999) Structural basis for recognition of the tra mRNA precursor by the Sex-lethal protein. Nature 398:579-585

Heaphy S, Dingwall C, Ernberg I, Gait MJ, Green SM, Karn J, Lowe AD, Singh M, Skinner MA (1990) HIV-1 regulator of virion expression (Rev) protein binds to an RNA stem-loop structure located within the Rev response element region. Cell 60:685-693

Hinman MN, Lou H (2008) Diverse molecular functions of Hu proteins. Cell Mol Life Sci 65:3168-3181

Hirose Y, Manley JL (2000) RNA polymerase II and the integration of nuclear events. Genes Dev 14:1415-1429

Hoek KS, Kidd GJ, Carson JH, Smith R (1998) hnRNP A2 selectively binds the cytoplasmic transport sequence of myelin basic protein mRNA. Biochemistry 37:7021-7029

Houseley J, Tollervey D (2009) The many pathways of RNA degradation. Cell 136:763-776

Hudson BP, Martinez-Yamout MA, Dyson HJ, Wright PE (2004) Recognition of the mRNA AU-rich element by the zinc finger domain of TIS11d. Nat Struct Mol Biol 11:257-264

Iyaguchi D, Yao M, Tanaka I, Toyota E (2009) Cloning, expression, purification and preliminary crystallographic studies of the adenylate/uridylate-rich element-binding protein HuR complexed with its target RNA. Acta Crystallogr Sect F Struct Biol Cryst Commun 65:285-287

Inoue M, Muto Y, Sakamoto H, Yokoyama S (2000) NMR studies on functional structures of the AU-rich element-binding domains of Hu antigen C. Nucleic Acids Res 28:1743-1750

Ishikawa F, Matunis MJ, Dreyfuss G, Cech TR (1993) Nuclear proteins that bind the pre-mRNA 3' splice site sequence r(UUAG/G) and the human telomeric DNA sequence d(TTAGGG)n. Mol Cell Biol 13:4301-4310

Izaurralde E, Jarmolowski A, Beisel C, Mattaj IW, Dreyfuss G, Fischer U (1997) A role for the M9 transport signal of hnRNP A1 in mRNA nuclear export. J Cell Biol 137:27-35

Jain RG, Andrews LG, McGowan KM, Pekala PH, Keene JD (1997) Ectopic expression of Hel-N1, an RNA-binding protein, increases glucose transporter (GLUT1) expression in 3T3-L1 adipocytes. Mol Cell Biol 17:954-962

Janga SC, Mittal N (2011) Construction, structure and dynamics of post-transcriptional regulatory network directed by RNA-binding proteins. Adv Exp Med Biol 722:103-117

Johansson C, Finger LD, Trantirek L, Mueller TD, Kim S, Laird-Offringa IA, Feigon J (2004) Solution structure of the complex formed by the two N-terminal RNA-binding domains of nucleolin and a pre-rRNA target. J Mol Biol 337:799-816

Jones PG, VanBogelen RA, Neidhardt FC (1987) Induction of proteins in response to low temperature in Escherichia coli. J Bacteriol 169:2092-2095

Jung YS, Zweckstetter M (2004) Mars - robust automatic backbone assignment of proteins. J Biomol NMR 30:11-23

Kang MJ, Ryu BK, Lee MG, Han J, Lee JH, Ha TK, Byun DS, Chae KS, Lee BH, Chun HS, Lee KY, Kim HJ, Chi SG (2008) NF-kappaB activates transcription of the RNA-binding factor HuR, via PI3K-AKT signaling, to promote gastric tumorigenesis. Gastroenterology 135:2030-2042

Kannt A, Lancaster CR, Michel H (1998) The role of electrostatic interactions for cytochrome c oxidase function. J Bioenerg Biomembr 30:81-87

Katsanou V, Papadaki O, Milatos S, Blackshear PJ, Anderson P, Kollias G, Kontoyiannis DL (2005) HuR as a negative posttranscriptional modulator in inflammation. Mol Cell 19:777-789

Kawai T, Lal A, Yang X, Galban S, Mazan-Mamczarz K, Gorospe M (2006) Translational control of cytochrome c by RNA-binding proteins TIA-1 and HuR. Mol Cell Biol 26:3295-3307

Kedde M, Agami R (2008) Interplay between microRNAs and RNA-binding proteins determines developmental processes. Cell Cycle 7:899-903

Keene JD (1999) Why is Hu where? Shuttling of early-response-gene messenger RNA subsets. Proc Natl Acad Sci U S A 96:5-7

Kessler MM, Henry MF, Shen E, Zhao J, Gross S, Silver PA, Moore CL (1997) Hrp1, a sequence-specific RNA-binding protein that shuttles between the nucleus and the cytoplasm, is required for mRNA 3'-end formation in yeast. Genes Dev 11:2545-2556

Kiefer F, Arnold K, Kunzli M, Bordoli L, Schwede T (2009) The SWISS-MODEL Repository and associated resources. Nucleic Acids Res 37:D387-392

Kiledjian M, Dreyfuss G (1992) Primary structure and binding activity of the hnRNP U protein: binding RNA through RGG box. Embo J 11:2655-2664

Kiledjian M, Wang X, Liebhaber SA (1995) Identification of two KH domain proteins in the alpha-globin mRNP stability complex. Embo J 14:4357-4364

Kiledjian M, DeMaria CT, Brewer G, Novick K (1997) Identification of AUF1 (heterogeneous nuclear ribonucleoprotein D) as a component of the alpha-globin mRNA stability complex. Mol Cell Biol 17:4870-4876

Kim HH, Yang X, Kuwano Y, Gorospe M (2008) Modification at HuR (S242) alters HuR localization and proliferative influence. Cell Cycle 7:3371-3377

Kim HS, Wilce MC, Yoga YM, Pendini NR, Gunzburg MJ, Cowieson NP, Wilson GM, Williams BR, Gorospe M, Wilce JA (2011) Different modes of interaction by TIAR and HuR with target RNA and DNA. Nucleic Acids Res 39:1117-1130

Korner CG, Wormington M, Muckenthaler M, Schneider S, Dehlin E, Wahle E (1998) The deadenylating nuclease (DAN) is involved in poly(A) tail removal during the meiotic maturation of Xenopus oocytes. Embo J 17:5427-5437

Kshirsagar M, Parker R (2004) Identification of Edc3p as an enhancer of mRNA decapping in Saccharomyces cerevisiae. Genetics 166:729-739

Kundu P, Fabian MR, Sonenberg N, Bhattacharyya SN, Filipowicz W (2012) HuR protein attenuates miRNA-mediated repression by promoting miRISC dissociation from the target RNA. Nucleic Acids Res 40:5088-5100

LaBranche H, Dupuis S, Ben-David Y, Bani MR, Wellinger RJ, Chabot B (1998) Telomere elongation by hnRNP A1 and a derivative that interacts with telomeric repeats and telomerase. Nat Genet 19:199-202

LaCava J, Houseley J, Saveanu C, Petfalski E, Thompson E, Jacquier A, Tollervey D (2005) RNA degradation by the exosome is promoted by a nuclear polyadenylation complex. Cell 121:713-724

Lal A, Mazan-Mamczarz K, Kawai T, Yang X, Martindale JL, Gorospe M (2004) Concurrent versus individual binding of HuR and AUF1 to common labile target mRNAs. Embo J 23:3092-3102

Lal A, Kawai T, Yang X, Mazan-Mamczarz K, Gorospe M (2005) Antiapoptotic function of RNA-binding protein HuR effected through prothymosin alpha. Embo J 24:1852-1862

Laue T M, Shah B D, Ridgeway T M & Pelletier S L (1992) Computer-aided interpretation of analytical sedimentation data for proteins in Analytical Ultracentrifugation in Biochemistry and Polymer Science (Eds Harding, S. E., Rowe, A.J. & Horton, J.C.) 90−125 (Royal Society of Chemistry, Cambridge, 1992).

Lee MS, Henry M, Silver PA (1996) A protein that shuttles between the nucleus and the cytoplasm is an important mediator of RNA export. Genes Dev 10:1233-1246

Lee Y, Ahn C, Han J, Choi H, Kim J, Yim J, Lee J, Provost P, Radmark O, Kim S, Kim VN (2003) The nuclear RNase III Drosha initiates microRNA processing. Nature 425:415-419

Levine TD, Gao F, King PH, Andrews LG, Keene JD (1993) Hel-N1: an autoimmune RNA-binding protein with specificity for 3' uridylate-rich untranslated regions of growth factor mRNAs. Mol Cell Biol 13:3494-3350

Lewis HA, Musunuru K, Jensen KB, Edo C, Chen H, Darnell RB, Burley SK (2000) Sequence-specific RNA binding by a Nova KH domain: implications for paraneoplastic disease and the fragile X syndrome. Cell 100:323-332

Li H, Park S, Kilburn B, Jelinek MA, Henschen-Edman A, Aswad DW, Stallcup MR, Laird-Offringa IA (2002) Lipopolysaccharide-induced methylation of HuR, an mRNA-stabilizing protein, by CARM1. Coactivator-associated arginine methyltransferase. J Biol Chem 277:44623-44630

Li H, Shi H, Wang H, Zhu Z, Li X, Gao Y, Cui Y, Niu L, Teng M (2010) Crystal structure of the two N-terminal RRM domains of Pub1 and the poly(U)-binding properties of Pub1. J Struct Biol 171:291-297

Liu X, Mertz JE (1995) HnRNP L binds a cis-acting RNA sequence element that enables intron-dependent gene expression. Genes Dev 9:1766-1780

Liu Z, Luyten I, Bottomley MJ, Messias AC, Houngninou-Molango S, Sprangers R, Zanier K, Kramer A, Sattler M (2001) Structural basis for recognition of the intron branch site RNA by splicing factor 1. Science 294:1098-1102

Liu H, Rodgers ND, Jiao X, Kiledjian M (2002) The scavenger mRNA decapping enzyme DcpS is a member of the HIT family of pyrophosphatases. Embo J 21:4699-4708

Liu Q, Greimann JC, Lima CD (2006) Reconstitution, activities, and structure of the eukaryotic RNA exosome. Cell 127:1223-1237

Loflin P, Chen CY, Shyu AB (1999) Unraveling a cytoplasmic role for hnRNP D in the in vivo mRNA destabilization directed by the AU-rich element. Genes Dev 13:1884-1897

Lopez de Silanes I, Zhan M, Lal A, Yang X, Gorospe M (2004) Identification of a target RNA motif for RNA-binding protein HuR. Proc Natl Acad Sci U S A 101:2987-2992

Lorentzen E, Walter P, Fribourg S, Evguenieva-Hackenberg E, Klug G, Conti E (2005) The archaeal exosome core is a hexameric ring structure with three catalytic subunits. Nat Struct Mol Biol 12:575-581

Lund E, Guttinger S, Calado A, Dahlberg JE, Kutay U (2004) Nuclear export of microRNA precursors. Science 303:95-98

Lunde BM, Moore C, Varani G (2007) RNA-binding proteins: modular design for efficient function. Nat Rev Mol Cell Biol 8:479-490

Lykke-Andersen J (2002) Identification of a human decapping complex associated with hUpf proteins in nonsense-mediated decay. Mol Cell Biol 22:8114-8121

Ma WJ, Cheng S, Campbell C, Wright A, Furneaux H (1996) Cloning and characterization of HuR, a ubiquitously expressed Elav-like protein. J Biol Chem 271:8144-8151

Ma WJ, Chung S, Furneaux H (1997) The Elav-like proteins bind to AU-rich elements and to the poly(A) tail of mRNA. Nucleic Acids Res 25:3564-3569

Ma JB, Ye K, Patel DJ (2004) Structural basis for overhang-specific small interfering RNA recognition by the PAZ domain. Nature 429:318-322

Ma JB, Yuan YR, Meister G, Pei Y, Tuschl T, Patel DJ (2005) Structural basis for 5'-end-specific recognition of guide RNA by the A. fulgidus Piwi protein. Nature 434:666-670

Macrae IJ, Zhou K, Li F, Repic A, Brooks AN, Cande WZ, Adams PD, Doudna JA (2006) Structural basis for double-stranded RNA processing by Dicer. Science 311:195-198

Marasa BS, Srikantan S, Martindale JL, Kim MM, Lee EK, Gorospe M, Abdelmohsen K (2010) MicroRNA profiling in human diploid fibroblasts uncovers miR-519 role in replicative senescence. Aging 2:333-343

Maris C, Dominguez C, Allain FH (2005) The RNA recognition motif, a plastic RNA-binding platform to regulate post-transcriptional gene expression. Febs J 272:2118-2131

Matsumoto K, Wolffe AP (1998) Gene regulation by Y-box proteins: coupling control of transcription and translation. Trends Cell Biol 8:318-823

Matunis EL, Kelley R, Dreyfuss G (1994) Essential role for a heterogeneous nuclear ribonucleoprotein (hnRNP) in oogenesis: hrp40 is absent from the germ line in the dorsoventral mutant squid. Proc Natl Acad Sci U S A 91:2781-2784

Mayeda A, Krainer AR (1992) Regulation of alternative pre-mRNA splicing by hnRNP A1 and splicing factor SF2. Cell 68:365-375

Mazan-Mamczarz K, Galban S, Lopez de Silanes I, Martindale JL, Atasoy U, Keene JD, Gorospe M (2003) RNA-binding protein HuR enhances p53 translation in response to ultraviolet light irradiation. Proc Natl Acad Sci U S A 100:8354-8359

Mazroui R, Di Marco S, Clair E, von Roretz C, Tenenbaum SA, Keene JD, Saleh M, Gallouzi IE (2008) Caspase-mediated cleavage of HuR in the cytoplasm contributes to pp32/PHAP-I regulation of apoptosis. J Cell Biol 180:113-127

McMullen MR, Cocuzzi E, Hatzoglou M, Nagy LE (2003) Chronic ethanol exposure increases the binding of HuR to the TNFalpha 3'-untranslated region in macrophages. J Biol Chem 278:38333-38341

Meisner NC, Hintersteiner M, Mueller K, Bauer R, Seifert JM, Naegeli HU, Ottl J, Oberer L, Guenat C, Moss S, Harrer N, Woisetschlaeger M, Buehler C, Uhl V, Auer M (2007) Identification and mechanistic characterization of low-molecular-weight inhibitors for HuR. Nat Chem Biol 3:508-515

Meisner NC, Hintersteiner M, Seifert JM, Bauer R, Benoit RM, Widmer A, Schindler T, Uhl V, Lang M, Gstach H, Auer M (2009) Terminal adenosyl transferase activity of posttranscriptional regulator HuR revealed by confocal on-bead screening. J Mol Biol 386:435-450

Miau LH, Chang CJ, Shen BJ, Tsai WH, Lee SC (1998) Identification of heterogeneous nuclear ribonucleoprotein K (hnRNP K) as a repressor of C/EBPbeta-mediated gene activation. J Biol Chem 273:10784-10791

Michelotti EF, Michelotti GA, Aronsohn AI, Levens D (1996) Heterogeneous nuclear ribonucleoprotein K is a transcription factor. Mol Cell Biol 16:2350-2360

Min H, Chan RC, Black DL (1995) The generally expressed hnRNP F is involved in a neural-specific pre-mRNA splicing event. Genes Dev 9:2659-2671

Michelotti EF, Michelotti GA, Aronsohn AI, Levens D (1996) Heterogeneous nuclear ribonucleoprotein K is a transcription factor. Mol Cell Biol 16:2350-2360

Milone J, Wilusz J, Bellofatto V (2004) Characterization of deadenylation in trypanosome extracts and its inhibition by poly(A)-binding protein Pab1p. Rna 10:448-457

Min H, Chan RC, Black DL (1995) The generally expressed hnRNP F is involved in a neural-specific pre-mRNA splicing event. Genes Dev 9:2659-2671

Minvielle-Sebastia L, Beyer K, Krecic AM, Hector RE, Swanson MS, Keller W (1998) Control of cleavage site selection during mRNA 3' end formation by a yeast hnRNP. Embo J 17:7454-7468

Moore MJ, Proudfoot NJ (2009) Pre-mRNA processing reaches back to transcription and ahead to translation. Cell 136:688-700

Moreira A, Takagaki Y, Brackenridge S, Wollerton M, Manley JL, Proudfoot NJ (1998) The upstream sequence element of the C2 complement poly(A) signal activates mRNA 3' end formation by two distinct mechanisms. Genes Dev 12:2522-2534

Mouland AJ, Xu H, Cui H, Krueger W, Munro TP, Prasol M, Mercier J, Rekosh D, Smith R, Barbarese E, Cohen EA, Carson JH (2001) RNA trafficking signals in human immunodeficiency virus type 1. Mol Cell Biol 21:2133-2143

Mourelatos Z, Abel L, Yong J, Kataoka N, Dreyfuss G (2001) SMN interacts with a novel family of hnRNP and spliceosomal proteins. Embo J 20:5443-5452

Muhlrad D, Parker R (2005) The yeast EDC1 mRNA undergoes deadenylation-independent decapping stimulated by Not2p, Not4p, and Not5p. Embo J 24:1033-1045

Muto Y, Yokoyama S (2012) Structural insight into RNA recognition motifs: versatile molecular Lego building blocks for biological systems. WIREs RNA 2012, 3:229–246. doi: 10.1002/wrna.1107 3:229-246

Myer VE, Fan XC, Steitz JA (1997) Identification of HuR as a protein implicated in AUUUA-mediated mRNA decay. Embo J 16:2130-2139

Nagai K, Oubridge C, Jessen TH, Li J, Evans PR (1990) Crystal structure of the RNA-binding domain of the U1 small nuclear ribonucleoprotein A. Nature 348:515-520

Oberstrass FC, Auweter SD, Erat M, Hargous Y, Henning A, Wenter P, Reymond L, Amir-Ahmady B, Pitsch S, Black DL, Allain FH (2005) Structure of PTB bound to RNA: specific binding and implications for splicing regulation. Science 309:2054-2057

Okano HJ, Darnell RB (1997) A hierarchy of Hu RNA binding proteins in developing and adult neurons. J Neurosci 17:3024-3037

Opyrchal M, Anderson JR, Sokoloski KJ, Wilusz CJ, Wilusz J (2005) A cell-free mRNA stability assay reveals conservation of the enzymes and mechanisms of mRNA decay between mosquito and mammalian cell lines. Insect Biochem Mol Biol 35:1321-1334

Ostareck DH, Ostareck-Lederer A, Wilm M, Thiele BJ, Mann M, Hentze MW (1997) mRNA silencing in erythroid differentiation: hnRNP K and hnRNP E1 regulate 15-lipoxygenase translation from the 3' end. Cell 89:597-606

Ostareck DH, Ostareck-Lederer A, Shatsky IN, Hentze MW (2001) Lipoxygenase mRNA silencing in erythroid differentiation: The 3'UTR regulatory complex controls 60S ribosomal subunit joining. Cell 104:281-290

Oubridge C, Ito N, Evans PR, Teo CH, Nagai K (1994) Crystal structure at 1.92 A resolution of the RNA-binding domain of the U1A spliceosomal protein complexed with an RNA hairpin. Nature 372:432-438

Parker JS, Roe SM, Barford D (2004) Crystal structure of a PIWI protein suggests mechanisms for siRNA recognition and slicer activity. Embo J 23:4727-4737

Parker JS, Roe SM, Barford D (2005) Structural insights into mRNA recognition from a PIWI domain-siRNA guide complex. Nature 434:663-666

Pavletich NP, Pabo CO (1991) Zinc finger-DNA recognition: crystal structure of a Zif268-DNA complex at 2.1 A. Science 252:809-817

Peitsch MC, (1995) Protein modeling by E-mail. Bio/Technology 13:658-660.

Perez-Cañadillas JM (2006) Grabbing the message: structural basis of mRNA 3'UTR recognition by Hrp1. Embo J 25:3167-3178

Pettersen EF, Goddard TD, Huang CC, Couch GS, Greenblatt DM, Meng EC, Ferrin TE (2004) UCSF Chimera - a visualization system for exploratory research and analysis. J Comput Chem 25:1605-1612

Picard B, Wegnez M (1979) Isolation of a 7S particle from Xenopus laevis oocytes: a 5S RNA-protein complex. Proc Natl Acad Sci U S A 76:241-245

Popper KR (1971) The open society and its enemies. 1, The spell of Plato. Fifth edition, revised. Princeton: Princeton University Press. Print.

Price SR, Evans PR, Nagai K (1998) Crystal structure of the spliceosomal U2B"-U2A' protein complex bound to a fragment of U2 small nuclear RNA. Nature 394:645-650

Privalov PL (1979) Stability of proteins: small globular proteins. Adv Protein Chem 33:167-241

Query CC, Bentley RC, Keene JD (1989) A common RNA recognition motif identified within a defined U1 RNA binding domain of the 70K U1 snRNP protein. Cell 57:89-101

Rajagopalan LE, Westmark CJ, Jarzembowski JA, Malter JS (1998) hnRNP C increases amyloid precursor protein (APP) production by stabilizing APP mRNA. Nucleic Acids Res 26:3418-3423

Rebane A, Aab A, Steitz JA (2004) Transportins 1 and 2 are redundant nuclear import factors for hnRNP A1 and HuR. Rna 10:590-599

Reverdatto SV, Dutko JA, Chekanova JA, Hamilton DA, Belostotsky DA (2004) mRNA deadenylation by PARN is essential for embryogenesis in higher plants. Rna 10:1200-1214

Russell ID, Tollervey D (1992) NOP3 is an essential yeast protein which is required for pre-rRNA processing. J Cell Biol 119:737-747

Ryter JM, Schultz SC (1998) Molecular basis of double-stranded RNA-protein interactions: structure of a dsRNA-binding domain complexed with dsRNA. Embo J 17:7505-7513

Sachs AB, Bond MW, Kornberg RD (1986) A single gene from yeast for both nuclear and cytoplasmic polyadenylate-binding proteins: domain structure and expression. Cell 45:827-835

Santoro MM, Bolen DW (1988) Unfolding free energy changes determined by the linear extrapolation method. 1. Unfolding of phenylmethanesulfonyl alpha-chymotrypsin using different denaturants. Biochemistry 27:8063-8068

Scheiba RM, Aroca A, Díaz-Moreno I (2012) HuR thermal stability is dependent on domain binding and upon phosphorylation. Eur Biophys J 41:597-605

Schuck P (2000) Size-distribution analysis of macromolecules by sedimentation velocity ultracentrifugation and lamm equation modeling. Biophys J 78:1606-1619

Searles MA, Lu D, Klug A (2000) The role of the central zinc fingers of transcription factor IIIA in binding to 5 S RNA. J Mol Biol 301:47-60

Shamoo Y, Abdul-Manan N, Williams KR (1995) Multiple RNA binding domains (RBDs) just don't add up. Nucleic Acids Res 23:725-728

Shamoo Y, Krueger U, Rice LM, Williams KR, Steitz TA (1997) Crystal structure of the two RNA binding domains of human hnRNP A1 at 1.75 A resolution. Nat Struct Biol 4:215-222

Shih SC, Claffey KP (1999) Regulation of human vascular endothelial growth factor mRNA stability in hypoxia by heterogeneous nuclear ribonucleoprotein L. J Biol Chem 274:1359-1365

Silvera D, Gamarnik AV, Andino R (1999) The N-terminal K homology domain of the poly(rC)-binding protein is a major determinant for binding to the poliovirus 5'-untranslated region and acts as an inhibitor of viral translation. J Biol Chem 274:38163-38170

Singh M, Choi CP, Feigon J (2013) xRRM: A new class of RRM found in the telomerase La family protein p65. RNA Biol 10:353-359

Siomi H, Matunis MJ, Michael WM, Dreyfuss G (1993) The pre-mRNA binding K protein contains a novel evolutionarily conserved motif. Nucleic Acids Res 21:1193-1198

Sokolowski M, Furneaux H, Schwartz S (1999) The inhibitory activity of the AU-rich RNA element in the human papillomavirus type 1 late 3' untranslated region correlates with its affinity for the elav-like HuR protein. J Virol 73:1080-1091

Sokolowski M, Schwartz S (2001) Heterogeneous nuclear ribonucleoprotein C binds exclusively to the functionally important UUUUU-motifs in the human papillomavirus type-1 AU-rich inhibitory element. Virus Res 73:163-175

Sommerville J, Ladomery M (1996 a) Masking of mRNA by Y-box proteins. Faseb J 10:435-443

Sommerville J, Ladomery M (1996 b) Transcription and masking of mRNA in germ cells: involvement of Y-box proteins. Chromosoma 104:469-478

Song JJ, Smith SK, Hannon GJ, Joshua-Tor L (2004) Crystal structure of Argonaute and its implications for RISC slicer activity. Science 305:1434-1437

Sreerama N, Woody RW (2000) Estimation of protein secondary structure from circular dichroism spectra: comparison of CONTIN, SELCON, and CDSSTR methods with an expanded reference set. Anal Biochem 287:252-260

Srikantan S, Gorospe M (2012) HuR function in disease. Front Biosci 17:189-205

Stefl R, Xu M, Skrisovska L, Emeson RB, Allain FH (2006) Structure and specific RNA binding of ADAR2 double-stranded RNA binding motifs. Structure 14:345-355

Steiger M, Carr-Schmid A, Schwartz DC, Kiledjian M, Parker R (2003) Analysis of recombinant yeast decapping enzyme. Rna 9:231-238

Stevens A, Maupin MK (1987) A 5'→3' exoribonuclease of Saccharomyces cerevisiae: size and novel substrate specificity. Arch Biochem Biophys 252:339-347

Subramanian T, Govindarajan R, Chinnadurai G (1991) Heterologous basic domain substitutions in the HIV-1 Tat protein reveal an arginine-rich motif required for transactivation. Embo J 10:2311-2318

Swanson MS, Nakagawa TY, LeVan K, Dreyfuss G (1987) Primary structure of human nuclear ribonucleoprotein particle C proteins: conservation of sequence and domain structures in heterogeneous nuclear RNA, mRNA, and pre-rRNA-binding proteins. Mol Cell Biol 7:1731-1739

Symmons MF, Williams MG, Luisi BF, Jones GH, Carpousis AJ (2002) Running rings around RNA: a superfamily of phosphate-dependent RNases. Trends Biochem Sci 27:11-18

Szabo A, Dalmau J, Manley G, Rosenfeld M, Wong E, Henson J, Posner JB, Furneaux HM (1991) HuD, a paraneoplastic encephalomyelitis antigen, contains RNA-binding domains and is homologous to Elav and Sex-lethal. Cell 67:325-333

Tharun S, He W, Mayes AE, Lennertz P, Beggs JD, Parker R (2000) Yeast Sm-like proteins function in mRNA decapping and decay. Nature 404:515-518

Toba G, White K (2008) The third RNA recognition motif of Drosophila ELAV protein has a role in multimerization. Nucleic Acids Res 36:1390-1399

Tomonaga T, Levens D (1995) Heterogeneous nuclear ribonucleoprotein K is a DNA-binding transactivator. J Biol Chem 270:4875-4881

Tran H, Maurer F, Nagamine Y (2003) Stabilization of urokinase and urokinase receptor mRNAs by HuR is linked to its cytoplasmic accumulation induced by activated mitogen-activated protein kinase-activated protein kinase 2. Mol Cell Biol 23:7177-7188

Tucker M, Valencia-Sanchez MA, Staples RR, Chen J, Denis CL, Parker R (2001) The transcription factor associated Ccr4 and Caf1 proteins are components of the major cytoplasmic mRNA deadenylase in Saccharomyces cerevisiae. Cell 104:377-386

Van der Houven van Oordt W, Diaz-Meco MT, Lozano J, Krainer AR, Moscat J, Caceres JF (2000) The MKK(3/6)-p38-signaling cascade alters the subcellular distribution of hnRNP A1 and modulates alternative splicing regulation. J Cell Biol 149:307-316

Van Dijk E, Cougot N, Meyer S, Babajko S, Wahle E, Seraphin B (2002) Human Dcp2: a catalytically active mRNA decapping enzyme located in specific cytoplasmic structures. Embo J 21:6915-6924

Vargason JM, Szittya G, Burgyan J, Hall TM (2003) Size selective recognition of siRNA by an RNA silencing suppressor. Cell 115:799-811

Venter JC, Adams MD, Myers EW, Li PW, Mural RJ, Sutton GG, Smith HO, Yandell M, Evans CA, Holt RA, Gocayne JD, Amanatides P, Ballew RM, Huson DH, Wortman JR, Zhang Q, Kodira CD, Zheng XH, Chen L, Skupski M, Subramanian G, Thomas PD, Zhang J, Gabor Miklos GL, Nelson C, Broder S, Clark AG, Nadeau J, McKusick VA, Zinder N, Levine AJ, Roberts RJ, Simon M, Slayman C, Hunkapiller M, Bolanos R, Delcher A, Dew I, Fasulo D, Flanigan M, Florea L, Halpern A, Hannenhalli S, Kravitz S, Levy S, Mobarry C, Reinert K, Remington K, Abu-Threideh J, Beasley E, Biddick K, Bonazzi V, Brandon R, Cargill M, Chandramouliswaran I, Charlab R, Chaturvedi K, Deng Z, Di Francesco V, Dunn P, Eilbeck K, Evangelista C, Gabrielian AE, Gan W, Ge W, Gong F, Gu Z, Guan P, Heiman TJ, Higgins ME, Ji RR, Ke Z, Ketchum KA, Lai Z, Lei Y, Li Z, Li J, Liang Y, Lin X, Lu F, Merkulov GV, Milshina N, Moore HM, Naik AK, Narayan VA, Neelam B, Nusskern D, Rusch DB, Salzberg S, Shao W, Shue B, Sun J, Wang Z, Wang A, Wang X, Wang J, Wei M, Wides R, Xiao C, Yan C, *et al.* (2001) The sequence of the human genome. Science 291:1304-1351

Vitali F, Henning A, Oberstrass FC, Hargous Y, Auweter SD, Erat M, Allain FH (2006) Structure of the two most C-terminal RNA recognition motifs of PTB using segmental isotope labeling. Embo J 25:150-162

Von Roretz C, Beauchamp P, Di Marco S, Gallouzi IE (2011) HuR and myogenesis: being in the right place at the right time. Biochim Biophys Acta 1813:1663-1667

Von Roretz C, Jin Lian X, Macri AM, Punjani N, Clair E, Drouin O, Dormoy-Raclet V, Ma JF, Gallouzi IE (2012) Apoptotic-induced cleavage shifts HuR from being a promoter of survival to an activator of caspase-mediated apoptosis. Cell Death Differ 20:154-168

Wang H, Zeng F, Liu Q, Liu H, Liu Z, Niu L, Teng M, Li X (2013) The structure of the ARE-binding domains of Hu antigen R (HuR) undergoes conformational changes during RNA binding. Acta Crystallogr D Biol Crystallogr 69:373-380

Wang S, Hu Y, Overgaard MT, Karginov FV, Uhlenbeck OC, McKay DB (2006) The domain of the Bacillus subtilis DEAD-box helicase YxiN that is responsible for specific binding of 23S rRNA has an RNA recognition motif fold. Rna 12:959-967

Wang W, Caldwell MC, Lin S, Furneaux H, Gorospe M (2000a) HuR regulates cyclin A and cyclin B1 mRNA stability during cell proliferation. Embo J 19:2340-2350

Wang W, Furneaux H, Cheng H, Caldwell MC, Hutter D, Liu Y, Holbrook N, Gorospe M (2000b) HuR regulates p21 mRNA stabilization by UV light. Mol Cell Biol 20:760-769

Wang W, Yang X, Cristofalo VJ, Holbrook NJ, Gorospe M (2001) Loss of HuR is linked to reduced expression of proliferative genes during replicative senescence. Mol Cell Biol 21:5889-5898

Wang W, Yang X, Kawai T, Lopez de Silanes I, Mazan-Mamczarz K, Chen P, Chook YM, Quensel C, Kohler M, Gorospe M (2004) AMP-activated protein kinase-regulated phosphorylation and acetylation of importin alpha1: involvement in the nuclear import of RNA-binding protein HuR. J Biol Chem 279:48376-48388

Wang X, McLachlan J, Zamore PD, Hall TM (2002) Modular recognition of RNA by a human pumilio-homology domain. Cell 110:501-512

Wang X, Tanaka Hall TM (2001) Structural basis for recognition of AU-rich element RNA by the HuD protein. Nat Struct Biol 8:141-145

Weeks KM, Ampe C, Schultz SC, Steitz TA, Crothers DM (1990) Fragments of the HIV-1 Tat protein specifically bind TAR RNA. Science 249:1281-1285

Wishart DS, Arndt D, Berjanskii M, Tang P, Zhou J, Lin G (2008) CS23D: a web server for rapid protein structure generation using NMR chemical shifts and sequence data. Nucleic Acids Res 36:W496-W502

Wolfe SA, Nekludova L, Pabo CO (2000) DNA recognition by Cys2His2 zinc finger proteins. Annu Rev Biophys Biomol Struct 29:183-212

Xu N, Chen CY, Shyu AB (2001) Versatile role for hnRNP D isoforms in the differential regulation of cytoplasmic mRNA turnover. Mol Cell Biol 21:6960-6971

Yeap BB, Voon DC, Vivian JP, McCulloch RK, Thomson AM, Giles KM, Czyzyk-Krzeska MF, Furneaux H, Wilce MC, Wilce JA, Leedman PJ (2002) Novel binding of HuR and poly(C)-binding protein to a conserved UC-rich motif within the 3'-

untranslated region of the androgen receptor messenger RNA. J Biol Chem 277:27183-27192

Ye K, Malinina L, Patel DJ (2003) Recognition of small interfering RNA by a viral suppressor of RNA silencing. Nature 426:874-878

Yamashita A, Chang TC, Yamashita Y, Zhu W, Zhong Z, Chen CY, Shyu AB (2005) Concerted action of poly(A) nucleases and decapping enzyme in mammalian mRNA turnover. Nat Struct Mol Biol 12:1054-1063

Yang X, Bani MR, Lu SJ, Rowan S, Ben-David Y, Chabot B (1994) The A1 and A1B proteins of heterogeneous nuclear ribonucleoparticles modulate 5' splice site selection in vivo. Proc Natl Acad Sci U S A 91:6924-6928

Yang WH, Yu JH, Gulick T, Bloch KD, Bloch DB (2006) RNA-associated protein 55 (RAP55) localizes to mRNA processing bodies and stress granules. Rna 12:547-554

Yi R, Qin Y, Macara IG, Cullen BR (2003) Exportin-5 mediates the nuclear export of pre-microRNAs and short hairpin RNAs. Genes Dev 17:3011-3016

Yi J, Chang N, Liu X, Guo G, Xue L, Tong T, Gorospe M, Wang W (2010) Reduced nuclear export of HuR mRNA by HuR is linked to the loss of HuR in replicative senescence. Nucleic Acids Res 38:1547-1558

Yuan YR, Pei Y, Ma JB, Kuryavyi V, Zhadina M, Meister G, Chen HY, Dauter Z, Tuschl T, Patel DJ (2005) Crystal structure of A. aeolicus argonaute, a site-specific DNA-guided endoribonuclease, provides insights into RISC-mediated mRNA cleavage. Mol Cell 19:405-419

Zhu H, Hasman RA, Young KM, Kedersha NL, Lou H (2003) U1 snRNP-dependent function of TIAR in the regulation of alternative RNA processing of the human calcitonin/CGRP pre-mRNA. Mol Cell Biol 23:5959-5971

Zhu H, Hasman RA, Barron VA, Luo G, Lou H (2006) A nuclear function of Hu proteins as neuron-specific alternative RNA processing regulators. Mol Biol Cell 17:5105-5114

Zhu H, Zhou HL, Hasman RA, Lou H (2007) Hu proteins regulate polyadenylation by blocking sites containing U-rich sequences. J Biol Chem 282:2203-2210

Zhu H, Hinman MN, Hasman RA, Mehta P, Lou H (2008) Regulation of neuron-specific alternative splicing of neurofibromatosis type 1 pre-mRNA. Mol Cell Biol 28:1240-1251

UNIVERSIDAD DE SEVILLA

CSIC
CONSEJO SUPERIOR DE INVESTIGACIONES CIENTÍFICAS

JUNTA DE ANDALUCIA

cicCartuja

centro de
investigaciones científicas
isla de la cartuja

Consejo Superior de Investigaciones Científi
Junta de Andalucía
Universidad de Sevilla